Norwegian University of Life Sciences
Faculty of Science and Technology

Philosophiae Doctor (PhD)
Thesis 2019:30

Laser-based survey of building objects and buildings

Laserbasert oppmåling av bygningsobjekter og bygninger

Ivar Oveland

Laser-based survey of building objects and buildings

Laserbasert oppmåling av bygningsobjekter og bygninger

Philosophiae Doctor (PhD) Thesis

Ivar Oveland

Norwegian University of Life Sciences
Faculty of Science and Technology

Ås (2019)

Thesis number 2019:30

ISSN 1894-6402

ISBN 978-82-575-1589-8

A doctoral thesis at the Norwegian University of Life Sciences consists of either a monograph or a compendium of papers in published or manuscript form. In the latter case, the introductory part, from an overall perspective, summarizes and collates the research objectives, theoretical fundamentals, results, and conclusions presented in the separate papers, and documents the coherence of the thesis.

Evaluation committee

First opponent
Senior University Lecturer Petri Niiles Rönnholm
Department of Built Environment
Aalto University
Aalto, Finland

Second opponent
Associate Prof. Erling Onstein
Department of Manufacturing and Civil Engineering,
Norwegian University of Science and Technology (NTNU)
Gjøvik, Norway

Committee coordinator
Prof. Nils Bjugstad
Faculty of Science and Technology,
Norwegian University of Life Sciences (NMBU)
Ås, Norway

Supervisors

Prof. Thomas Kringlebotn Thiis (Main supervisor)
Faculty of Science and Technology,
Norwegian University of Life Sciences (NMBU)
Ås, Norway

Assistant Prof. Ivar Maalen-Johansen (Co-supervisor)
Faculty of Science and Technology,
Norwegian University of Life Sciences (NMBU)
Ås, Norway

Prof. Eilif Hjelseth (Co-supervisor)
Department of Civil and Environmental Engineering
Norwegian University of Science and Technology (NTNU)
Trondheim, Norway

Acknowledgments

First and foremost, I would like to thank my supervisors prof. Thomas Kringlebotn Thiis, assistant prof. Ivar Maalen Johansen and prof. Eilif Hjelseth who excellently guided me through this research study experience. You have all made this into an amazing journey.

Secondly, I would like to thank senior lecturer dr. Grzegorz Cielniak who made our great visit to Lincoln possible. He is an inspiration and a source of knowledge that never runs out.

Prof. Jon Glenn Omholt Gjevestad at NMBU has given me tremendous support and helped me every time the backpack hardware failed to work. I would also like to thank Linda Bystrøm and the Property department at NMBU who made it possible to use the Realtek building in my research. I am grateful to prof. Terje Gobakken and dr. Marius Hauglin who was a tremendous inspiration during the forest related research.

Special thanks go to dr. Narve Schipper Kjørsvik and Terratec AS for developing special software tools in Terrapos to support my research questions. TerraTec AS and Cautus Geo AS have free of charge provided support and high-quality instrumentation and made my fieldwork possible. Special thanks also go to Jürgen Spindler and the collaboration with Sørum municipality and Ullensaker municipality.

The Norwegian Building Authority, Cautus Geo AS and Geomatikk survey have kindly founded parts of the studies.

I would also like to thanks all my colleagues and fellow Ph.D. students at the division of geomatics at NMBU, the robotic group at NMBU and the LCAS group in Lincoln. These relations have given me lots of knowledge and many great laughs.

Finally, I would like to thank my family and friends for their understanding and support, and most of all to my wife Elin and children Oda and Olivia.

Ivar Oveland

Såbulia, 2018-10-27

Abstract

Building information models (BIMs) for facility management is gaining interest. Different technologies for collecting the raw material to extract such model are in rapid development. The most common technologies are based on images, structure light, laser or a combination of these. The new technologies have the potential to provide efficient data collection, but not necessarily at the same accuracy compared to the traditional methods. This thesis has explored how to rapidly establish a BIM for an existing building. This was done by investigating two different aspects related to this task. The first aspect was related to product specification and provide a framework for ordering and controlling a laser-based survey of a building. The second aspect explores how a laser-based system could be used to rapidly survey an existing building.

Through the thesis and the first aspect, it is shown that the Norwegian survey community is lacking an unambiguous product specification for building surveys performed for BIM extraction and that the survey seldomly is adequately controlled. Based on these findings a product specification has been developed in cooperation with building owners. This cooperation made it possible to test the product specification in real projects. The product specification was developed through three different versions. The zero version was presented at the World Building Congress in 2016 and was tested in a renovation project at the Norwegian University of Life Sciences. The evaluation of the project led to the first version that was used in a framework competition arranged by Ullensaker municipality in the south-east of Norway. The result led to the second and final version of the product specification. The proposed product specification follows a simplified transaction pattern between the customer and the producer. The focus has been on the customer's request for a building survey suitable for BIM extraction and the customer's acceptance actions when the building survey is delivered. The acceptance actions are based on well–known standards created by the Norwegian Mapping Authority. The customer request is based on the acceptance actions. This ensures that every requirements can be verified in the accepting stage. The main purposes of the product specification were to ensure reliable results and to minimize the difference between the customer request and the producer’s delivery. Additionally, an unambiguous product specification can ensure a fair competition situation between the producers and give the producers the possibility to select the best-suited technology.

The second aspect is related to how a building can be efficiently surveyed and explores how this could be done with a laser-based system. A human carried survey system was developed through three stages. The first and second stages focused on circle shaped objects and were realized in cooperation with the Faculty of Environmental Sciences and Natural Resource Management at the Norwegian University of Life Sciences. The system surveyed tree diameter at breast height within sample plots in size 250-500 m^2. The system was able to detect 87.5% of the trees with a mean difference of 0.1 cm, and a root mean square of 2.2 cm. The novel aspect is related to how the trees are segmented and how the diameters are estimated without losing precision due to degraded pose solution. The result can be used in forestry inventory projects together with airborne laser surveys. The third stage was made for indoor measurements. The main focus was on how to aid the navigation solution in the absence of Global Navigation Satellite System signals. The method divides the laser point measurements into small time frames. For each time frame, the laser points were automatically classified into column, walls, floor, and ceiling. This information was used to support a scan matching method called semantic-assisted normal distributions transform. The result from the scan matching was used to create a trajectory of the walking path followed during data capture. This result was fed back into the inertial navigation processing to aid the solution when the system was located inside the building. This gives the inertial navigation process the ability to reject scan matching failures. The novel method was able to improve the survey accuracy from a maximum deviation of 12.6 m to 1.1 m. The third stage had two different Inertial Measurement Units (IMU) installed. The most accurate system was a tactical graded IMU, and the lowest accurate system was an automotive graded IMU. With the proposed method, the automotive graded system was able to perform at a higher level than a standalone tactical graded solution.

Sammendrag

Interessen for å bruke BygningsInformasjonsModeller (BIMer) i forvaltning, drift og vedlikehold av bygninger er økende. Ulike teknologier for innsamling av data for å etablere slike modeller er i rask utvikling. De vanligste teknologiene er basert på bilder, strukturert lys, laser eller en kombinasjon av disse. Nye teknologi utfører målingene veldig effektivt, men ikke med samme nøyaktighet som tradisjonelle metoder. Denne studien har undersøkt hvordan en raskt kan etablere en BIM i et eksisterende bygg. Dette ble gjort ved å utforske to ulike aspekter av problemstillingen. Det første aspektet ser på produktspesifikasjon og foreslår et rammeverk til bruk ved bestilling og kontroll av laser- basert innmåling av eksisterende bygning. Det andre aspektet utforsker hvordan et laser- basert system raskt kan måle opp eksisterende bygg.

Studiet viser at det mangler en entydig produktspesifikasjon for oppmåling av eksisterende bygg med det formål å ekstrahere en BIM. Et annet moment er at slike måleoppdrag sjelden blir grundig kontrollert. Basert på dette ble det utviklet en produktspesifikasjon i samarbeid med ulike bygningseiere. Dette samarbeidet gjorde det mulig å teste produktspesifikasjonen på virkelige prosjekter. Produktspesifikasjonen ble utviklet gjennom tre ulike versjoner. Versjon null ble presentert på «the World Building Congress» i 2016 og ble testet på et renoveringsprosjekt ved Norges Miljø- og Biovitenskapelige Universitet. Resultatet av dette gav en ny versjon av produktspesifikasjonen, som deretter ble benyttet i en rammeavtalekonkurranse arrangert av Ullensaker kommune i Norge. Evalueringen av dette prosjekter resulterte i versjon to, og dermed den siste versjon av produktspesifikasjonen i dette studiet. Den foreslåtte produktspesifikasjonen følger et forenklet samhandlingsmønster mellom kunden og produsenten. Fokuset har vært på de kravene kunden bør stille til en bygningsoppmåling som er tiltenkt en ekstrahering av en BIM. Studiet fokuserer også på hvordan oppmålingen bør kontrolleres. Kontrollmetodene som er benyttet baserer seg på standarder utgitt av Kartverket i Norge, og danner også fundamentet for hvilke krav som bør stilles i tilbudsforespørselen. Målsetningen har vært at alle krav som stilles skal kunne etterprøves i mottakskontrollen. Hensikten med produktspesifikasjonen har vært å sikre pålitelig oppmåling og minimere forskjellen mellom kundens forventning og leverandørens leveranse. I tillegg kan en entydig produktspesifikasjon sikre en rettferdig konkurransesituasjon mellom leverandørene, og gi leverandørene muligheten til å velge den mest tjenlige teknologien.

Det andre aspektet i studiet undersøker hvordan en mest effektivt kan måle opp en bygning, og hvordan dette kan gjøres med et laserbasert system. I løpet av studiet ble et bærbart lasersystem utviklet gjennom tre ulike steg. Fokuset på det første og andre steget var å måle objekter med sirkulært tverrsnitt, og ble gjennomført i samarbeid med Fakultet for miljøvitenskap og naturforvaltning, Norges Miljø- og Biovitenskapelige Universitet. Lasersystemet ble brukt til å måle tre diameter i brysthøyde innenfor prøveflater med en størrelse fra 250 til 500 m^2. Slike prøveflater blir brukt til å kalibrere flybårne lasermålinger for skogtaksering. Det bærbare lasersystemet fant 87.5% av trærne, med et midlere avvik på 0.1 cm og en RMSE på 2.2 cm. Det unike med løsningen er knyttet til hvordan trærne blir segmentert og hvordan trærnes diameter blir estimert uten å miste presisjon som en følge av svak posisjons- og orienteringsløsning. Det tredje steget ble utviklet for innendørs datafangst. Hovedfokuset var å undersøke hvordan treghetsløsningen kunne bli støttet av lasermålingene når signalet fra navigasjonssatellittene uteble. Metoden deler lasermålingene opp i små tidsepoker. Hver tidsepoke gir en laserpunktsky som automatisk ble klassifisert til punktklassene stolpe, vegg, tak og gulv. Denne informasjonen ble brukt til å støtte skannmatchingsmetoden kalt "semantic-assisted normal distributions transform". Resultatet fra skannmatchingen ble brukt til å lage en navigasjonsløsning. Denne løsningen ble ført tilbake til treghetsnavigasjonsberegningen for å støtte løsningen i de periodene systemet var uten signaler fra navigasjonssatellittene. Metoden var i stand til å forbedre navigasjons-løsningen inne i bygget fra et maksimalt avvik på 12.6 m til 1.1 m. Det bærbare lasersystemet utviklet i steg tre hadde to ulike treghetsplattformer. Det mest nøyaktige treghetssystemet var klassifisert som "tactical grade" og det minst nøyaktige system var klassifisert som "automotive grade". Ved hjelp av skannmatching oppnådde navigasjonsløsningen med "automotive grade" treghetssystemet en høyere nøyaktighet enn navigasjonsløsningen hvor en benyttet treghetsplattformen klassifisert som "tactical grade" uten støtte fra skannmatching.

Appended Papers

This thesis is based on the following papers:

Paper I:

"Framework for enabling scan to BIM services for multiple purposes – Purpose BIM"

Hjelseth, Eilif; Oveland, Ivar; and Maalen-Johansen, Ivar; (2016). Framework for enabling scan to BIM services for multiple purposes – Purpose BIM, Proceedings of the CIB World Building Congress 2016: Volume V - Advancing Products and Services. Tampere University of Technology. Department of Civil Engineering, ISBN 978-952-15-3745-5, page 868- 879.

Paper II:

"Automatic Estimation of Tree Position and Stem Diameter Using a Moving Terrestrial Laser Scanner."

Oveland, Ivar; Hauglin, Marius; Gobakken, Terje; Næsset, Erik; Maalen-Johansen, Ivar, (2017), Automatic estimation of tree position and stem diameter using a moving terrestrial laser scanner, Remote Sensing, Volume 9 issue 4, 350.

Paper III:

"Comparing Three Different Ground Based Laser Scanning Methods for Tree Stem Detection"

Oveland, Ivar; Hauglin, Marius; Giannetti, Francesca; Schipper Kjørsvik, Narve; Gobakken, Terje, (2018), Comparing Three Different Ground Based Laser Scanning Methods for Tree Stem Detection, Remote Sensing, Volume 10 issue 4, 538.

Paper IV: (in final revision)

"Laser scanning, product specification and Level of Accuracy evaluation"

Oveland, Ivar; Revhaug, Inge; Maalen- Johansen, Ivar, (2018), Laser scanning, product specification and Level of Accuracy evaluation, KART OG PLAN, POB 5003, NO-1432 Ås, ISSN 0047-3278

Paper V: (To be submitted)

"Evaluation of product specification for terrestrial laser scanning to extract a building information model"

Oveland, Ivar, (2019)

Figures

Tables

List of abbreviations

AiA	American Institute of Architects
AEC	Architecture, Engineering, and Construction
EBA	Entreprenørforeningen Bygg og Anlegg
DBH	Tree Diameter at Breast Height
DIN18710	Deutsches Institut für Normung, Engineering survey
FOG	Fiber Optic Gyro
FOV	Field Of View
GeodataProduction	Produksjon av basis geodata
GeodataQuality	Geodatakvalitet
GNSS	Global Navigation Satellite System
HLS	Handheld Laser Scanner
ICP	Iterative Closest Point
IDDS	Integrated Design and Delivery Solutions
IMU	Inertial Measurement Unit
LoA	Level of Accuracy
LoD	Level of Development
MEMS	Micro Electro Mechanical System
MMI	Model Modenhets Indeks
NMBU	Norwegian University of Life Sciences
MSAC	M-estimator SAmple Consensus
pose	Position and orientation
RANSAC	RANdom SAmple Consensus
RIF	Rådgivende Ingeniørers Forening
RMS	Root Mean Square
RMSE	Root Mean Square Error
SE-NDT	Semantic-assisted Normal Distributions Transform
TLS	Terrestrial Laser Scanner
UAV	Unmanned Aerial Vehicle
USIBD	USIBD Level of accuracy specification guide

Table of Contents

1. Introduction

1.1 Introduction to the main research question

For large building projects, it has become common to use a Building Information Model (BIM) to make the planning and construction process more efficient, but also to use BIM to support the building owner throughout the building´s entire life cycle. Most existing buildings are built without a BIM. It has therefore become more popular to create a BIM for existing buildings to ensure efficient facility management [1]. Nevertheless, some building owners might be reluctant to do this. One reason is the cost to establish the model compared to the benefits. However, the data capture technology is in rapid development. New technology has become easier to use where the manufactures offer cloud processing of the captured data [2, 3]. To improve the cost-benefit ratio, studies have introduced multiple purposes BIM [4]. The idea is to use the BIM not just for one purpose, but for multiple purposes.

The main research question in this thesis is how to rapidly establish a BIM for an existing building. The thesis has focused on two main aspects of this question. The first is how to build up a product specification for the survey of an existing building. This research question will be referred to as product specification development. This question covers both the description of the product and how to control the result. The product specification is fitted into well-known and open access standards in the Norwegian land surveying community. The idea is that a land surveyor in a regular Norwegian municipality should be able to understand the product specification and to perform the necessary control measurements of the scan. With the proposed product specification, it is possible to distinguish between different accuracy levels. This is an important option that can introduce new technology. The new building scanning technologies have in common that the data capture time and the accuracy is low compared to traditional terrestrial laser scanning surveys. In situations where the building owner does not need the highest accuracy, they have the opportunity to benefit from the new scanning technology and reduce the cost. Another motivation for the product specification developed in this study was to propose a framework to evaluate the achieved result. In this study, 11 different building surveys were evaluated with the proposed framework. The result showed that few of the delivered products achieved the requirements specified in the tendering process through the product specification. The reason for this could be a combination of building owners who do not control the delivered product and building scanning suppliers that are not used to being evaluated based on the proposed framework. The hypothesis within this research question is that a product specification could ensure a multiple purpose BIM, increase the model reliability and open up for new technologies.

The second part of the study explores how a laser-based system could rapidly survey a building to support the extraction of a BIM. An operative laser-based backpack scanner system was developed and built through three different stages. This research question will be referred to as laser-based system. The processing tools were made by combining methods from the robotics and the geomatics. The different disciplines are summarized in Figure 1.

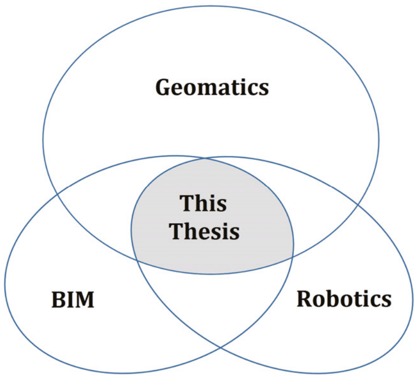

Figure 1. The study combines elements from the disciplines Geomatics, Robotics and Building information model (BIM), with the main focus on the Geomatics discipline.

One of the key element from the robotics used in this study is Random sample consensus (RANSAC) [5]. This method has been used to find laser measurements belonging to a straight line or flat surface. Another important method is scan matching [6] used to fit two different point clouds collected from different locations. A method called loop closure [7] has the possibility to detect that the robot is back at a location where it has been before. This is an observation with the potential to improve the position and orientation (pose) accuracy dramatically. Loop closure detects potential drift in the pose estimate and is often used to distribute the error over time using the covariance. The geomatics discipline includes mapping, object recognition, land surveying, laser scanning, Global Navigation Satellite System (GNSS), and inertial navigation. The different disciplines in this study are used to extract objects with cylinder shape (paper II and III), and identify building objects like walls, floors, and ceilings. The final discipline is BIM, which is the application area.

1.2 Structure of the thesis

The structure of this thesis is built around the two research questions called "Product specification development" and "Laser-based system." The questions are treated separately within each main chapter. The main chapters point out the relations between each research question and the different papers, presented in Table 1.

Table 1. Relations between research questions and papers

Paper	Title	Research question	
		Product specification development	Laser-based system
I	"Framework for enabling scan to BIM services for multiple purposes – Purpose BIM"	Version 0	
II	"Automatic Estimation of Tree Position and Stem Diameter Using a Moving Terrestrial Laser Scanner."		Stage 1
III	"Comparing Three Different Ground Based Laser Scanning Methods for Tree Stem Detection"		Stage 2
IV	"Laser scanning, product specification and Level of Accuracy evaluation"	Version 1	
V	"Evaluation of product specification for terrestrial laser scanning to extract a building information model"	Version 2	

The topics described in the papers will not be deeply presented in this thesis. There will nevertheless be given a short overview of the highlights. Topics that are not described in the papers will be described more deeply. The research question regarding the laser-based system contains a third stage which is not yet published in a paper, but described in this thesis.

1.3 Product specification development

Extraction of a BIM for an existing building will in most cases require a certain business process. The process at the simplest requires a customer and a producer. The consumer orders the model and the producer realize the product. An important part of the business process is the communication actions between the two parties. The communication follows a certain transaction pattern. A simple form of transaction pattern is presented by Dietz [8] and shown in Figure 2.

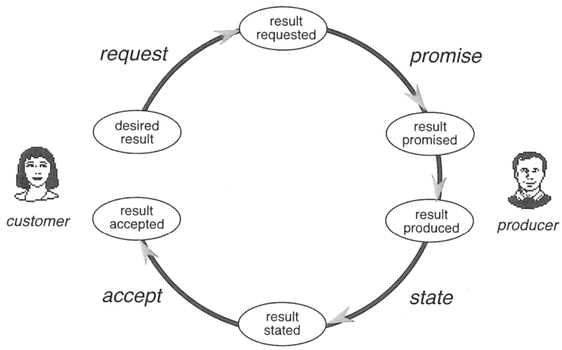

Figure 2. Transaction pattern from Dietz [8]

The simplified transaction pattern is divided into four different stages. The different stages are "request", "promise", "state" and "accept". The first stage "request" involves a process where the customer has a "desired result". This is formalized into a "result requested". The producer is the acting part in the next stages and responds to the request with a "result promised". When the producer has promised to produce a certain product the next stages begin, and the producer starts to produce the "result promised". At the end of the stage, the producer states that the promised result is achieved. In the final stage, the customer evaluates and accepts the "result produced". A successful transaction is achieved when the "desired result" corresponds with the "result accepted". This simplified transaction pattern is also used in the ISO standard 29481 [9, 10]. The standard points out the importance of a common understanding of the used transaction pattern. This study uses the principal from the ISO standard 29481 [9, 10] and the simplified transaction pattern from Dietz[8] in the development of the product specification. The intention of the proposed product specification is that the customer presented in Figure 2 should have a good tool to specify the desired result and a good framework to perform the acceptance.

In front of a BIM realization for an existing building, it is a standard procedure to run some sort of tender process. This process involves a product specification. The specification describes the requirements and expectations for the product. This process has the potential to reduce the risk for both the buyer and the supplier. The buyer risks getting a product with reduced usability. The supplier can risk lost reputation due to an unsatisfied customer or higher expenses than the budget allows. An unambiguous product specification has the potential to remove unwritten expectations and misunderstandings due to different understanding of words like “accuracy”, “point density”, etc. Without a specification, it is easy to get into a situation where the different producers have a different understanding of the requirements. A result of this can be an unfair competition situation. This can occur if a producer calculates the tender based on a certain density while another producer might base their tender on another point density. The point density is one of many factors that increase the data capture cost. With a high density, the producer needs to adjust the scanner settings to a high resolution or to increase the number of scanning locations. Both will have an influence on the data capture time that is directly related to the data capture cost. Typically, the producer with the lowest density is in a position to deliver the best price compared to the competitors with higher point density. Other parameters that directly affect the data capture cost are accuracy, colorized point cloud and reference coordinate frame. In the evaluation process the product specification plays a key role and makes the communication with the producer much easier especially when the expectation is not fulfilled.

The building stock at the Norwegian University of Life Sciences (NMBU) is in a continuous renovation process. In 2016 the renovation of the REALTEK building was initiated. This project was used as a case study in paper IV [11]. It was decided to run a full terrestrial scanning of the building. An offer request was given to five different suppliers. The request specifically asked for achieved accuracy level and a description of how to achieve the objective. When the tenders where analyzed only two of the suppliers had described the accuracy level, and only one had a reliable description to achieve the objective. In another project at Ullensaker municipality in Norway, it was possible to analyze the documentation in the final product. This project was a framework agreement competition and was used in paper V [12]. In total ten different suppliers attended from different Nordic countries. Only one of the suppliers specified the accuracy level in the delivered product, and four suppliers described the reference coordinate frame used in the delivery. These two examples illustrate the importance of an unambiguous product specification and are the motivation to explore the product specification aspect.

There are some essential standards regarding product specification for establishing a BIM for an existing building. The first standard is made by the "Deutsches Institut für Normung," and the topic is Engineering survey [13, 14]. The standard will in the following be referred to as DIN18710. The standard describes requirements regarding surveying activities at construction site works and standardizes the quality and verification of such work. The accuracy requirements are divided into a horizontal and a vertical component, where both are divided into five different levels ranging from low to high accuracy. The horizontal accuracy classes with very low accuracy are called L1, and the very high accuracy class is called L5. DIN18710 also distinct the accuracy between correctness and precision. The correctness describes the distance between the average measured value and the true value, while precision is an expression of the measurements variation, as illustrated in Figure 3.

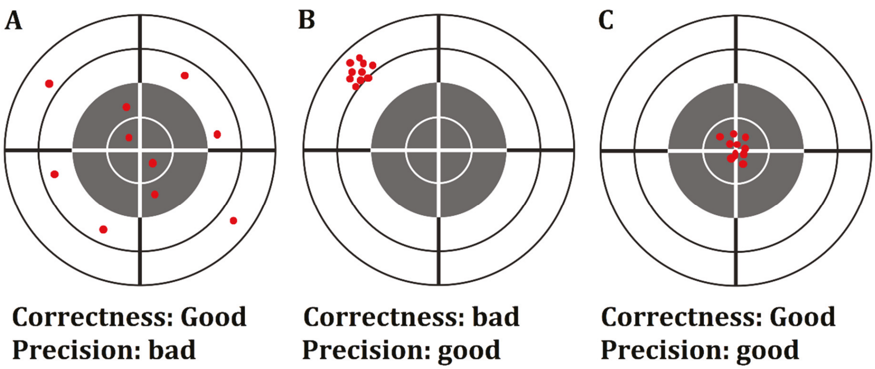

Figure 3. Relation between correctness and precision

Another standard is developed by the U.S. Institute of building documentation. The standard is called "USIBD Level of accuracy specification guide" [15] and will in the following be referred to as USIBD. DIN18710 was used as inspiration when the USIBD was developed. A major difference to DIN18710 is that USIBD also separates into different Level of Accuracy (LoA). This makes it very flexible and makes it possible to set different LoA for different objects categories. Different building objects like doors, walls, windows may then have different accuracy requirement. The USIDB separates the accuracy levels into five different classes. The accuracy level with low accuracy is called LOA10 and the accuracy level with high accuracy is called LOA50. Both DIN18710 and the USIDB seems to have the same accuracy limits. The numbers are identical, but DIN18710 operates with standard deviation while USIBD operates with a 95% confidence level. When a normal distribution is assumed the USIBD accuracy limits need to be divided by 1.96 to correspond with the accuracy limits in DIN18710.

An important aspect of a Product specification development is how to control the delivered result. The product specification sets the criteria to fulfilled, but also gives an indication of how the control should be done. The USIBD and the DIN18710 evaluate the standard deviation. The standard deviation could be evaluated by measuring relative distances inside the building between different building objects. It is also possible to measure the distances within a building object [16]. Another approach is to use targets in the field. The targets have to be placed out in the field before the scanning is performed. Typical targets are reflective tape, April tags, checkerboards and similar. The airborne laser industry uses mostly natural targets in the field. This makes the control procedure very flexible. A procedure using natural targets is described in the norwegian standard "Produksjon av basis geodata"[17]. The standard describes a procedure to control an airborne laser project. In the following, this standard will be referred to as GeodataProduction. Another option is to measure the position of selected building objects. This is typically done in large-scale mapping projects where objects like manholes, houses, fences, etc. are measured with land surveying equipment and compared with the delivered map. The control method is described in the norwegian standard "Geodatakvalitet" [18] which use a quality model based on EN ISO19157:2013 [19]. The Norwegian standard will in the following be referred to as GeodataQuality. The standard describes a method to estimate and evaluate the standard deviation, systematic deviation and the number of gross errors.

Another method to control a laser survey is to evaluate the potential deviation between data captured from different locations that covers the same area [16, 20, 21]. The deviation between data collected from a different location is an expression of the error in the data set. Typically, such error is caused by an error in the instrument's position and orientation [16], mixed pixels due to spatial discontinuity edges, range errors due to specular reflectance (multipath) and instrument calibration issues [21] . The airborne laser mapping industry has used this deviation method since early 2000 [22]. It requires a proper overlap between the scan locations. The airborne laser industry solves this need by ensuring that all scan lines have a perpendicular scan line, called cross line. This cross line ensures a sufficient overlap and is a good starting point for the deviation method. Without a sufficient overlap, it is possible for small errors to accumulate between the different scan lines or scan locations. A typical situation in a terrestrial laser scanning project is a long corridor where a large number of scan locations is needed. Without a sufficient overlap or additional support, the error might propagate down the corridor. In the airborne laser industry, the deviation method is used to perform a daily calibration of the laser equipment. The equipment from early 2000 was especially vulnerable for scale effect. The scale effect is correlated with the scan angle, describing the pointing direction for the flipping mirror inside the laser system. At nadir, the error is zero and increased symmetrically to the edges of the scan. Other parameters like systematic orientation errors are also possible to detect with the deviation method. Due to the high altitude and long ranges, the airborne laser data is sensitive for orientation error. Finally, the deviation method can be used to correct for minor random errors that occur in orientation and position between different flight lines. A deviation map is made by colorizing the height difference between all scan lines. Each of the mentioned errors have a distinct error pattern. The method, therefore, makes it possible to identify the cause of the problem and to correct the error. This method can be used to improve the data quality, but also to evaluate the achieved relative accuracy. The product specification in this study has been developed to fit the evaluation method described in GeodataQuality. In addition, a requirement to evaluate the result using a simplified deviation method was included. This was done by adding requirement to the maximum point cloud thickness.

1.4 Laser-based system

There are many different types of equipment suitable for establishing a BIM for an existing building. Most of the different equipment can be categorized into laser measurements, projection of structured light and image-based measurements. All categories range from high accuracy to low accuracy, and some instruments combine different categories. This study has focused on the laser-based categories to realize the "promise" / "state" illustrated in Figure 2, while the product specification development is the foundation for the "request", and "accept" as shown in Figure 4.

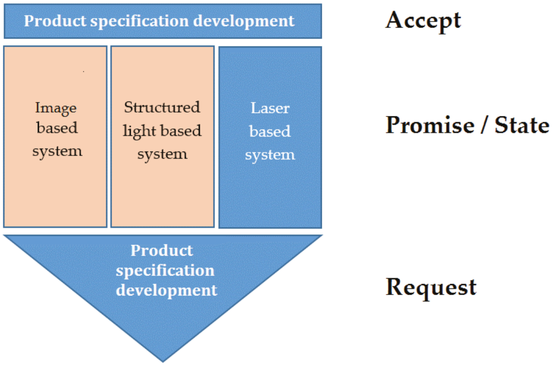

Figure 4. The figure illustrates how the two research questions product specification development and laser-based system are related.

Laser instruments can be divided by the platform that carries the equipment. Typically platforms are aircraft, Unmanned Aerial Vehicle (UAV), car, trolley, tripod, and human. Table 2 gives an overview of each platforms general characteristics. The characteristics are divided into the categories inertial measurement unit (IMU), GNSS, Laser, odometer, visual odometer, and scan matching. The IMU is an essential part of an inertial system. Brown and Hwang [23] has categorized inertial systems into navigation grade, tactical grade, and automotive grade systems. They defined a high-quality system or navigation grade system to standalone keep an excellent pose for some hours. A medium or tactical grade system can in a standalone situation keep an excellent pose for a short time. Low quality or Automotive grade system requires external aiding to maintain an excellent pose. A GNSS system can be categorized into low accuracy which is based on code observation only and provides a 200-1000 cm accuracy. A medium accuracy GNSS phase observation from multiple frequencies and has the potential to provide a 1-3 cm accuracy. A high GNSS accuracy use phase observation from multiple frequencies with long observation series from the same location and has the potential to achieve an accuracy in the 0.2-1.0 cm interval. The laser technology can also be categorized based on the accuracy performance. A low accurate system can achieve a 2-5 cm accuracy on single shots. A medium laser system is in the range of 0.5 to 2 cm while high accuracy laser systems range from 0.01 to 0.5 cm.

Table 2. General characteristics for different carries platform.

Platform	IMU	GNSS	Laser	Odometer	Visual odometer	Scan matching
Aircraft	high	medium	low			yes
UAV	low-medium	medium	low-medium			yes
Vehicle	high	medium	medium-high	yes		
Trolley	low-medium	medium	low–high	yes	yes	yes
Tripod	no-low	no-low	high			yes
Human	medium	no-medium	Low-medium		yes	yes

To improve the accuracy achieved by the different measurements platforms, you can improve the quality of each individual categories IMU, GNSS, Laser, odometer, visual odometer, and scan matching. Another option is to add categories that could provide better aiding opportunities for the inertial navigation system. This aiding can typically be done sequentially or in a loop closure approach. For example, a vehicle carrier system can improve the characteristics by adding visual odometer or scan matching capabilities. A system with multiple categories will in some cases be sensitive to how the observations from the different categories are integrated.

Aircraft, UAV, and vehicle will in most cases be unpractical to use for indoor mapping. These carriers require a certain level of space to be used. A trolley, a tripod, and a human make well suitable platforms for indoor scanning. In general, trollies have a wide range of instrumentation like odometer observations from the wheels. This provides good observations to support the navigation solution. It is also common to use a camera system to extract visual odometer data. A trolley collects data in a short time, but stairs are a challenge. Stairs will in some cases delay the data capture or even make it unpractical. A tripod carrier is commonly used and the most used carrier for BIM extraction. In the Ullensaker project, all of the participants used a tripod carrier. The Tripod carrier provides the highest accuracy level within the laser-based categories[24]. The biggest advantage is that data from a wide Field of View (FOV) is collected. The terrestrial laser scanner Faro focus 3D x130[25] collects data within 360 x 300 degrees from one scan location. If the data is collected with sufficient overlap it is a perfect situation for scan matching, also called cloud-to-cloud registration [26]. With the tripod carrier, it is common to use targets. The wide FOV also ensures that all possible targets are measured. There is a long range of different targets from natural targets, scanner spheres, checker boards to April tags. The different targets have different characteristics. Some targets have the same pattern, while others provide a unique pattern so that they appear as unique objects. In most cases, it is necessary to capture images to get the full capacity of targets with unique patterns. When this is not an option, it is common to scan with maximum resolution within a small section just covering the targets. This reduces the need for images. A common method is also to place a reflecting sheet just under the targets. The benefit is that the position of the target can be measured with a total station and used to improve the registration of the different scan locations. To perform the scanning from a fixed scan position gives a great advantage. Since the scanner is fixed, it is possible to perform multiple measurements on the same spot. This gives the possibility of averaging the distance measurements. This has the potential to increase the accuracy of each individual laser point. Laser data collected from a tripod will in the most cases rely on additional known points to be realized in a global reference frame.

A human is a flexible carrier and can easily move inside a building. When a laser system is carried around the scanner location continuously changes. This gives two large advantages. The first is the fast data acquisition. In theory, it takes the same amount of time to survey a building as it takes to walk through the building. The second advantage is that the scanner never measures the building objects from the same position. If a table is blocking a wall from one location, it might be visible from another location. Since the scanner location is continuously changing the probability to successfully survey the wall increases. This makes the data acquisition really flexible and minimizes the need to prepare the scan location to ensure a complete scan and minimizes the occluded areas. The main disadvantage of a human carried-based system is the accuracy. It is difficult to calculate an accurate pose estimate inside the building. Some of the human carried systems rely on an IMU to calculate the system pose. The quality of the IMU ranges from low graded to medium graded IMUs. Common for the medium graded IMU system is that the initialization process needs to be done in the open air with the support of good GNSS conditions. Most laser scanners carried by humans are not made for the traditional land survey community. They often used so-called low-cost scanners. The main market for their scanners are the robotics community and autonomous vehicles. The scanners are used to discover pedestrians, obstacle detection and in general map the surroundings. It is most common to use laser scanners with multiple beams. However, there are few producers of low-cost laser scanners with multiple beams. Two examples are Velodyne Inc. [27](San Jose, USA) and Ouster, Inc. [28] (San Francisco, USA).

This study explores how a laser-based system can be used to rapidly survey a building and create a BIM. The fastest data capture with a laser-based system is a human carried system. The main reason is that it is easy to pass obstacles like stairs and others. Based on this assumption this study has focused on the human carried systems. Today there are many different commercial versions of human carried systems. Geoslam [2] had one of the first solutions. The company started in 2012 as a joint venture between 3D Laser Mapping [29] and CSIRO [30], Australia's National Science Agency. The concept started as a rotating 2D laser scanner in 2009 [31]. In 2012 Bosse et al. [32] published a version where the scanner system was mounted on a spring. The SLAM methodic was developed from a rotating system [32] and was further developed to handle the new challenges that the spring mounting introduced. This system was called Zebedee and is a lightweight system without GNSS and maintain the pose with a low graded IMU, a two-dimensional laser scanner, and SLAM. The walking motion ensures enough force in the spring to ensure a pendulation on the laser scanner. This ensures a wide distribution of the laser measurements and provides good coverage, but also sufficient overlap between each individual time frame. This is important to ensure a good scan matching and SLAM result. The system has been further developed and goes under the name ZEB1. Today they have a new version called ZEB Revo [29, 33] and ZEB Horizon. In the latest versions, the spring mounted scanner has been replaced by a rotating scanner. Another commercial human carried system is available from the company Kaarta, Inc.[34]. They have two different handheld platforms where one is based on VLP16 laser scanner from Velodyne [27] and the second platform is based on a rotating two dimensional scanner. Both platforms are delivered with IMU and camera. Geoslam and Karrta, Inc provide cloud processing services to ensure an accurate pose estimation and laser point cloud extraction. Additionally Kaarta, inc. also has a cloud processing service that makes it possible for the customer to upload laser data capture with any Velodyne laser scanner to their processing algorithm. The laser data can be captured using your own built laser system, but also with commercial laser systems. The algorithm uses the laser data to perform scan matching between different time frames. This gives an accurate pose estimate during data capture which is used to transform the capture laser data into a common coordinate frame. The service also supports IMU data, which is recommended if large motions are present during data capture.

Other versions have the laser scanner mounted on a backpack. They are normally heavier and come with a higher price tag. Leica Pegasus is a typical example of such equipment [33] . The system has two VLP16 laser scanners from Velodyne, five cameras, GNSS and a fiber optic gyro (FOG) IMU. Vexcel has a commercial backpack system called UltraCam Panther [35, 36] where the main instrument is a spherical camera. Additional instruments are a stereo camera for visual odometry [37], GNSS, IMU and a VLP16 scanner from Velodyne. The GNSS observation is processed together with the IMU data. This result is merged with the result from the visual odometer using bundle adjustment. The accuracy is typical in the 5-10 cm level in an outdoor environment.

There are also more simple instruments based on backpack mount. Good examples are the Heron series from Gexcel [38, 39]. These backpack systems are mainly based on laser scanners from Velodyne. They are mounted in such a way that they reach above the operators head. This ensures a full 360˚ FOV. 3D Laser Mapping also has a backpack system called Robin[40] which is based on a VUX-1HA laser scanner manufactured by Riegl [41]. This scanner has a minimum range of 1.2 m [42] which makes it suitable for the outdoor application and provides an accuracy of 0.005 m up to 30 m range. The system has an IMU and a dual GNSS system that allows the heading orientation to be calculated from the GNSS observation.

A laser-based system is able to measure all visible details in a building and has the potential to measure all visible building objects at the same level of accuracy. An exception is transparent surfaces and mirrors. Laser measurements can be used to extract a BIM. An important aspect is how much can be extracted from the measurement and at which Level Of Development (LoD). There is an ongoing development in the Architecture, Engineering, and Construction (AEC) industry regarding LoD. From the American Institute of Architects (AiA) we have the G202-2013 Project BIM Protocol [43]. This document sets five different LoDs with authorized use and model content. A short overview is presented in Table 3.

Table 3. Short overview of the G202-2013 Project BIM Protocol From AIA

Level of Development	Representation of building objects			Quantities, size, shape, location and orientation		Fabrication, assembly and installation information	Field verificated
	Symbolic or generic representa tion	Generic system, object or assembly	Specific system, object or assembly	Roughly	Correct		
LoD 100	x			x			
LoD 200		x		x			
LoD 300			x		x		
LoD 400			x		x	x	
LoD 500			x		x		x

A Norwegian version is developed in collaboration between "Entreprenørforeningen Bygg og Anlegg" (EBA), "Rådgivende Ingeniørers Forening" (RIF), and "Arkitektbedriftene". All together, they represent approximately 42000 people in the Norwegian AEC community. The result is called Model Modenhets Indeks (MMI) [44] , and the different levels seem to be inspired by the G202-2013 Project BIM Protocol, but have interpreted the levels with respect to practical implementation. BIMFORUM has made a comprehensive document called LOD Specification 2018 Part I [45] and use the same step as the G202-2013 Project BIM Protocol, but with their own interpretations. Common for the mentioned protocols and framework is that the lowest level denominated as "100" does not have any requirements regarding geometric representations. The next level “200” should have individual building objects with an approximate position, orientation, size, and shape. The level denominated as “300” requires exact position, orientation, size, and shape.

2. Materials and Methods

2.1 Product specification development

2.1.1 Introduction to the product specification development

The product specification was developed to provide a good tool to perform the “result requested”, but also for the “result accepted” action. For a realization of a BIM for an existing building, the customer and producer should as a minimum follow the basic step of the transaction pattern presented in Figure 2. In the first stage, the customer should define the desired result. To help the customer, the product specification divides a “result requested” into different accuracy levels. When the accuracy level is selected, the requirements are predefined in the product specification. This makes standardized “result requested” easily available. The next stage is for the different producers to promise to deliver based on the “result requested”. A tendering process is normally used to select a producer. This starts the third stage where the producer captures the necessary data and completes the promised result. When the work is finished, the producer states that the work has been done. The final stage is to test and accept the result. In the final stage, the product specification defines the processes that should be involved prior to accepting the result. Important elements to evaluate are:

- Documentation, metadata, selected accuracy level, and product report
- Definition of used coordinate and height systems
- Transformation parameters to local and global coordinate frame
- Accuracy analysis, description, and availability of the local network
- Point density requirement
- Point cloud thickness requirement
- Accuracy requirement (gross error, standard deviation and average deviation)

2.1.2 Desired result

The first task in the transaction pattern shown in Figure 2 is called the “desired result”. A product specification is a good tool to formalize the “desired result” into a “requested result”. The product specification development in this study was developed through three different steps. The starting point was a product specification framework presented by Hjelseth et al. [4] and called version 0. The specification was divided into three different accuracy levels. The specification was developed based on the accuracy levels achievable for the different laser-based scanning systems. Additionally, the accuracy levels were set to be able to fulfill the necessary accuracy for different purposes. The different purposes were divided into rehabilitation, area information and facility management.

The next step was a part of a renovation project at the Norwegian University of Life Sciences. The building was built in 1960 and was constructed so it could be converted to a hospital if needed. Figure 5 shows the BIM used in the renovation project.

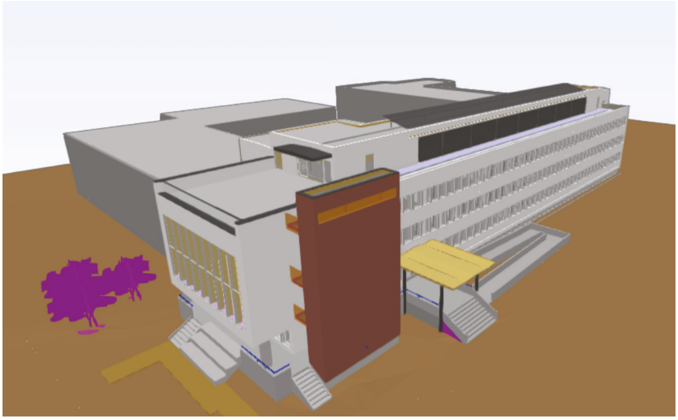

Figure 5. The building information model for the renovation project at the Norwegian University of Life Sciences.

To help with the planning process, it was decided to perform a full survey of the building with the laser-based method. Five different companies were invited to deliver a tender for the job. The product specification presented by Hjelseth et al. [4], version 0 was used in the tendering process. A specific requirement in the tendering process was that the producer should state which accuracy level they would deliver. Two out of five producers specified the accuracy level according to the product specification, and one out of five gave a proper description of how they should achieve the result. After an evaluation process of the project, a new updated product specification was established. The result is called version 1 and is described in paper IV [11].

The product specification version 2 was developed in collaboration with the Ullensaker municipality in Norway and described in paper V [12]. The municipality arranged a framework competition in 2017. Ullensaker municipality has a purchase agreement with the municipality Nannestad, Gjerdrum, Eidsvoll, Hurdal, and Nes. Together they cover an area of 2034 km^2, and the purchase agreement is constructed in such a way that the framework agreement arranged by Ullensaker can be used by all six municipalities. The main purpose of the competition was to get agreements with producers for building surveys and BIM extraction for existing buildings. The product should be used for facility and operation management. The evaluation group was divided into three different teams:

1. Legal requirement and price, Ullensaker municipality, Norway
2. Data acquisition and accuracy, Norwegian University of Life Sciences, Norway
3. Building information modeling, Areo, Norway

This study has focused on data acquisition and accuracy. Ten different companies signed up for the competition. Each company was asked to perform a test scan of a limited area of the town hall at Ullensaker municipality and was given one day to perform the data acquisition. The town hall is shown in Figure 6. The product specification used was based on version 1, but some changes were done, and new elements were added. The evaluation of the project formed the basis for the product specification version 2.

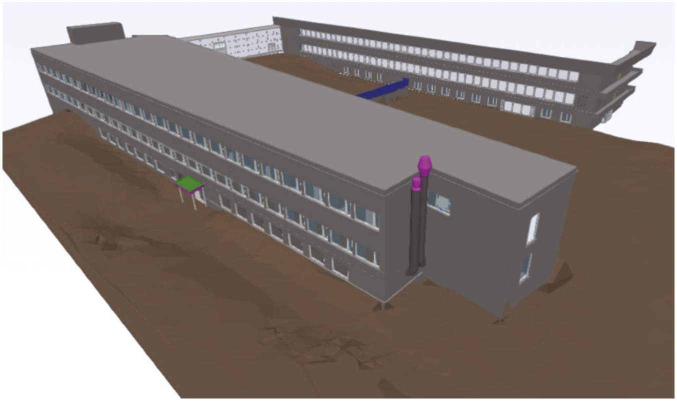

Figure 6. The building information model of the town hall at Ullensaker. The model was created by Geoplan 3D.

2.1.3 Result Accepted

The final step in the transaction pattern is the “result accepted”, see Figure 2. One part of the acceptance analysis is the data acquisition accuracy. The accuracy analysis was done using the Norwegian standards GeodataProduction[17] and GeodataQuality [18]. The standard GeodataProduction describes a method to control the achieved height accuracy for an airborne laser scanning project. This study proposes a method to scale up the procedure to work in a three-dimensional environment. The method uses measured control surfaces to evaluate accuracy. The number of measured points within a control surface varies with the laser point density. When the method was adjusted to indoor scanning, it was assumed that a control surface containing just one control point was sufficient. This was due to the high point density achieved by the terrestrial scanners. A set of control points were measured in each of the three dimensions. The Norwegian standard GeodataQuality [18] includes a lookup table to decide how many objects to measure based on the total amount of objects. This was used to decide how many control points were needed to statistically verify the findings. It was assumed that terrestrial scanning within a limited sized room is relatively homogeneous and each room can be considered as one single object. This assumption was used to find the total amount of rooms to include in the control.

The control measurements were done with a reflectorless total station. The total station was placed on top of each known point and orientated using the remaining know points. The instrument height was measured twice since this manual measurement directly affects the height accuracy. With the reflectorless function, all visible surfaces inside the building were surveyed. A control point can be placed on a flat surface with a minimum size of 0.2 m x 0.2 m, called the control area. The measurements were performed through openings in the buildings like windows and doors. The measurements were then compared to the delivered point cloud. Figure 7 illustrates how a surveyed control point could be located in relation to the laser point cloud and how the deviation was measured. The deviation is the distance along a perpendicular line to a surface that best fit to the laser points within a 0.2 m x 0.2 m control area. The deviation distance was measured manually in Terrascan from Terrasolid [46].

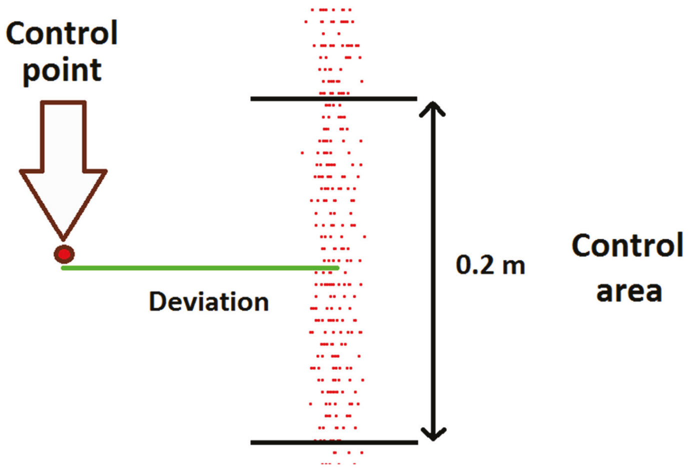

Figure 7. The deviation between the measured control point and the laser point cloud.

The point thickness is the distance between two edge points along a perpendicular line to a surface described by the points inside the control area. The analysis express how a flat surface appears in the laser point cloud. The point cloud thickness was measured by drawing the laser point within a maximum 0.2 m wide profile perpendicular to the surface defined by the point cloud and was measured manually in Terrascan from Terrasolid [46]. A small point cloud thickness is an indication of a good estimation of the pose and a low noise level for the individual laser measurements. Figure 8 shows an example where the scanner position and orientation could have been improved. The perpendicular distance between the extremes was measured to be 6 mm, which is defined to be the point cloud thickness.

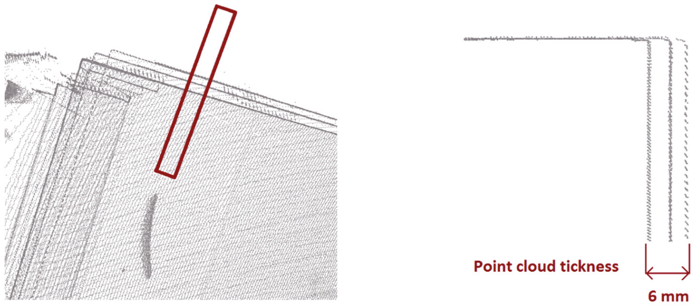

(a) (b)

Figure 8. (a) Top view of a room measured from different scan locations with degraded pose estimate. The rectangle in (a) shows the location of a vertical profile shown in (b).

The laser point density was defined as the maximum distance between two neighbor points in the laser point cloud and was measured manually in Terrascan from Terrasolid [46]. The measurements were done on flat and hard surfaces inside the project area. Occluded areas and surfaces with difficult reflectance like windows were not taken into account.

2.2 Laser-based system

2.2.1 The SensorLab

In 2014 it was decided to establish an interdisciplinary sensor laboratory at NMBU, called the SensorLab. The goal was to collocate knowledge and a large variety of instruments to be used in research projects at NMBU. Typical instrumentation should be GNSS, IMU, cameras, drones, lidar, and typical infrastructure to efficiently build a great variety of proof of concepts.

The application for funding was approved by the research committee at NMBU in May 2015, and the SensorLab was officially established. This study needed different types of laser equipment with different characteristics. Therefore three laser scanners were bought to the SensorLab. This was Faro Focus x130 3D and two Velodyne VLP16. The idea was that the different laser scanners could deliver point clouds with different accuracy levels and be used on different platforms. The Faro scanner could deliver a point cloud project with a standard deviation down to 0.5 cm, while the Velodyne scanners could achieve a standard deviation down to 5 cm depending on the additional instrumentation and procedures. The Faro Scanner [25] is a terrestrial scanner with a built-in GNSS equipment made for code observation only. There is also a tilt sensor, magnetometer and a camera. The specifications for both scanner types are listed in Table 4. The Velodyne VLP16 is in some settings called a low–cost scanner. Since the scanners were purchased, Velodyne has built a new factory where they intend to produce 1 million lasers in 2018 [47]. This high production rate has resulted in a price reduction of 50%.

Table 4. Laser scanner specification

Specification	VLP 16 [27]	Focus 3D x130 [25]
Laser	Class 1	Class 1
Number of beams	16	1
Wavelength	903 nm	1550 nm
Beam divergence	3 mrad	0.19 mrad
Weight	830 g	5200 g
Field of View	30° x 360°	300° x 360°
Accuracy	0.03 m	0.002 m
Range	100 m	130 m
Measurements per second	300 000	976 000

The second research question, called laser-based system, explores new technologies and how a laser-based system could be used to survey an existing building. To test different methods, it was decided to use the newly established Sensorlab and build a laser-based scanner system. Commercial versions like Leica Pegasus [48] were available, but these solutions were outside our budget. Another important reason to make the in-house build was to get full access to all instruments and to all collected data. This was important to ensure that new technology could be tested without any limitation due to proprietary instrument settings or data output restriction. The in-house build was done in different stages, where each stage was used to fulfill the target for the given stage. The overall goal was that each stage should lead towards a fully functioning scanner system for an indoor environment. An overview of the different stages is illustrated in Figure 9 and in the following comes a presentation of each stage.

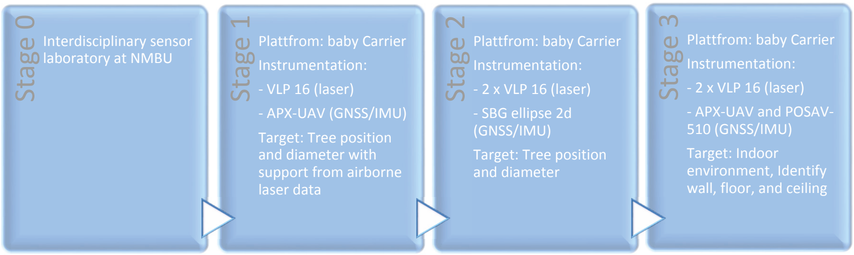

Figure 9. Overview of the different stages for the in-house build laser-based scanner system.

2.2.2 The first stage (paper II)

The first stage was a project together with the Faculty of Environmental Sciences and Natural Resource Management at the Norwegian university of life sciences (NMBU). The goal was to measure the tree diameter at breast height (DBH) and was described in paper II [49]. The tree measurements were performed in sample plots of 250 m^2 for all trees with a DBH > 4 cm. DBH measurements are used in forestry inventory projects to calibrate airborne laser measurements. The study area was located in the southeast of Norway in Gran municipality. The instrumentation consist of three main component; Velodyne VLP16 scanner, GNSS, and IMU. The integrated inertial navigation system Applanix APX-15 UAV[50] was used and mounted under the laser scanner. The IMU center was aligned with the laser scanners origin, x, and z-axis. The GNSS antenna was mounted on top of the scanner and aligned with the IMU origin and z-axis. Figure 10. shows the first stage instrumentation.

Figure 10. The first stage instrumentation used for tree measurements.

The instrument configuration made the system less vulnerable to inaccurate calibration. The main calibration component was a lever arm with approximately just a component in the z-direction. Additional small boresight angles could be expected between the laser and IMU coordinate system. In this study, there was no loop closure and just one single walkthrough. It was therefore assumed that a comprehensive and accurate calibration would not be necessary.

2.2.3 The second stage (paper III)

The second stage was built for forestry application and described in paper III [51]. The inertial navigation system was changed from the Applanix APX-15 UAV to the SBG Ellipse 2D system [52]. The sensor has the capability to use two GNSS antennas. The purpose of the second antenna, called the slave GNSS antenna, was to instantly calculate the heading direction. The sensor has a built-in system capable of processing the real-time heading using the signals from both GNSS antennas. The product specification promises a heading orientation accuracy down to 0.2° where the distance between the two GNSS antennas is longer than 1 m [52]. In the second stage, the distance between the antennas was 0.8 m. The main antenna was called master GNSS antenna, and the location of the different GNSS antennas is shown in Figure 11. To be able to take full advantage of the instant heading capability it was necessary to calibrate the system. Three parameters needed special attention. The first parameter was the distance from the master antenna to the slave antenna realized in the IMU frame. The distance was measured in the plane described by the x and y-axis in the IMU frame and was called the slave lever arm. The second parameter was the angle between the slave lever arm and the x-axis in the IMU frame. This was the angle needed to rotate the slave lever arm around the z-axis in the IMU frame to align with the x-axis in the IMU frame. The angle was found in an iteration process where the angle was adjusted slightly until the bias for the instant heading observation was minimized. The third parameter to calculate was the distance from the IMU frame origo to the antenna reference point for the master GNSS antenna. The distance was measured with a folding ruler and verified in a post-processing procedure in Terrapos v 2.5.90 [53].

In the first build, there was only one horizontal laser scanner. This made it difficult to detect the forest floor, also called the ground level. The forest floor was important to ensure that the DBH measurements were related to the breast height that was defined to be 1.3 m above the forest floor. By adding a vertical scanner, this problem was solved. The scanner was tilted approximately 10° from a vertical mount to avoid the scanner to survey the operator and the backpack. The second laser scanner increased the calibration needs significantly. To be able to use both scanners it was important to transform the measurements into the same coordinate frame. The necessary parameters were the distance from the IMU frame to each of the laser frames, realized in the IMU fame. The distance was measured using a total station. This also gave a rough estimate of the angles in between the same systems also called borsight. To verify all calibration parameters, a calibration field was established. The calibration field consists of a road intersection, surrounding buildings, trees, and poles. The environment was measured with a terrestrial laser scanner as a reference.

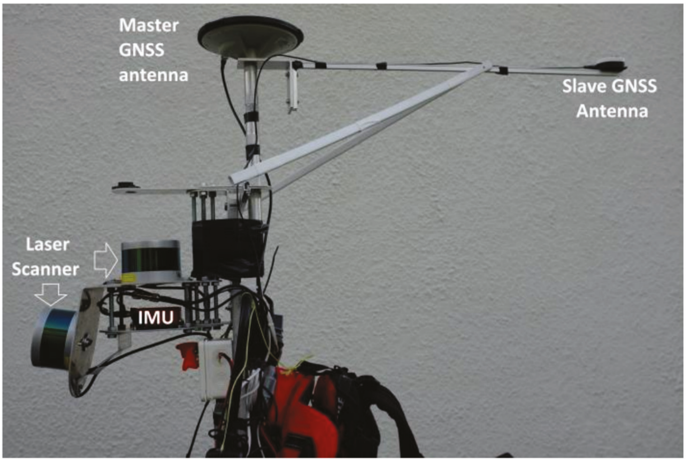

Figure 11. The second stage instrumentation used for tree measurements.

2.2.4 The third stage

The third stage was built for indoor mapping only. The main frame and baby carrier were the same as the second build. The difference was that two different inertial navigation systems were mounted. This was the Applanix APX-15 UAV, and the Applanix POSAV 510 with an IMU called LN200 from the Northrop Grumman [54]. The LN200 IMU has fiber-optics gyros to measure angle rates and silicon Micro Electro Mechanical System (MEMS) accelerometers. The APX-15 UAV is a full MEMS sensor. The LN200 is a medium quality system also called tactical grade in Brown and Hwang [23] inertial sensors categories. Both the APX-15 UAV and the SBG Ellipse 2-D shown in Table 5 are categorized as a low-quality inertial system or automotive grade system. The purpose of the two IMU systems was to evaluate the benefit of a tactical graded IMU.

Table 5. Inertial navigation system performance with normal GNSS satellite configuration, atmospheric conditions, and no significant obstacles.

Specification	Stage 2 SBG Ellipse 2-D [52]	Stage 1, 3 APX-15 UAV [50]	Stage 3 POSAV 510 [55]
Position accuracy (RMS* meter)	0.02-0.05	0.02-0.05	0.02-0.05
Roll and pitch(RMS* degrees)	0.1	0.025	0.005
Heading (RMS* degrees)	0.2	0.080	0.008

* Root mean square

Due to the heavy load and slippery conditions, the baby carrier was placed in a stroller during outdoor transportation as shown in Figure 12. The system was carried as a backpack inside the building.

Figure 12. The third stage used for building surveys.

The main question for the third stage was to test different IMU categories and to analyze the effect on the result. An additional question was to explore how Semantic-assisted Normal Distributions Transform (SE-NDT) scan matching could be used to aid the inertial navigation where the GNSS signals were absent.

2.3 Laser-based system, selected challenges

2.3.1 Point cloud classification

To be able to use the point cloud in further processing it was essential to classify the collected point cloud into different classes. In stage one and two the point classification was used to identify the trees. Additionally, the tree stem diameter should be estimated at the breast height which is defined to be 1.3 m above the forest floor. It was, therefore, necessary to identify the laser points reflected on the forest floor. The classification was based on distance increment and each point's relation to their neighboring points. The detailed description of the methods is presented in paper II and III.

In stage three the point classification was used to improve the scan matching and to prepare for building objects extraction. There are two main approaches used for classifying point clouds. These are a rule-based approach and a machine/deep learning approach. In stage three, a rule-based approached was used. The rule-based approach was built up by sequential rule-based steps, shown in Figure 13. The first step excluded measurements with low intensity and long range. The indoor environment had limited space, so the maximum range was set to 15 m. Both test locations had long corridors, but mostly limited space with single and double seated offices. Therefore, the shorter ranges were more likely to be a building object than the longer ranges. Another reason to exclude the longer ranges was that longer ranges are more vulnerable to inaccuracy in the pose. Finally, longer ranges are more likely to be laser measurements with multipath. A multipath measurement will reflect on more than one surfaces before the beam is returning to the scanner and the result appears as a false point. A laser beam that has reflected on multi-surfaces will typically have a lower intensity compared to a single reflected shot. Based on this assumption all points with lower intensity than a given threshold were excluded.

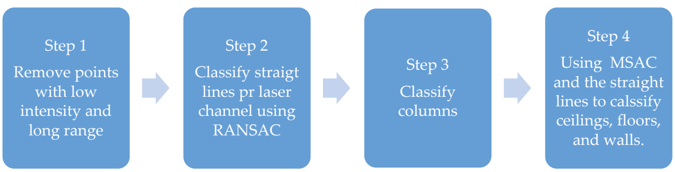

Figure 13. The flowchart describes each step in the proposed rule based classification method.

In stage one and two, the observed distance increment was used for tree classification. In a building environment, the same method was used to classify columns inside the building. This is the third classification step. The increment can also be used to classify walls inside a building. This method worked best when the distance increment was small and stable. The distance increment observed on a straight wall was smallest when the angle between the laser beam and the wall's perpendicular line was small. When the incoming light diverged too much from the perpendicular line, the distance increment became too large. It was difficult to get a correct classification when the distance from the point where the walls perpendicular line coincided with the laser beam. Figure 14 illustrates how the distance increment changes on a straight wall.

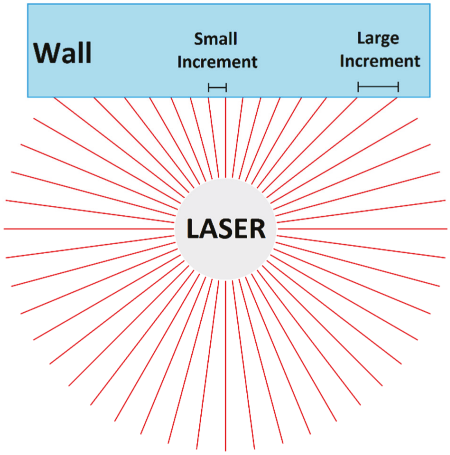

Figure 14. Distance increment related to the incoming light angle. The laser scanner is shown in the center, and the rectangle illustrates a wall. The distance increment is the smallest where the laser beam hits the wall perpendicular to the wall.

It is possible to build in slope to the distance increment evaluation, but this was not tested in this study. Instead, another method was used. This method uses RANSAC [56] to find inlier points located on a straight line, illustrated as step two in Figure 13. This was done separately for each laser channel. Points above a given distance from the straight line were classified as outliers. It was assumed that points on a straight line were parts of a building object like walls, ceilings, and floors. Points classified as outliers was typically furniture, people and similar, but could also be false measurements like multipath points. The inliers from the RANSAC search was then used to find flat surfaces, step four in Figure 13. This was done using a Matlab function called pcfitplane [57]. The function uses a method called M-estimator SAmple Consensus (MSAC) [58]. This is a variant of the RANSAC algorithm and classifies points as inliers and outliers to a best-fit surface. The inlier points were used to create a geometrical model that describes the plane with a corresponding normal vector. The laser scanners pose, and the normal vector was used to decide if the surface was a wall, ceiling or floor. The result classified the point cloud into these classes. The geometrical models could be used to establish a rough BIM with limited information.

To visualize the classification method, data collected in the entrance hall of the Realtek building was used as an example. The area is shown in Figure 15.

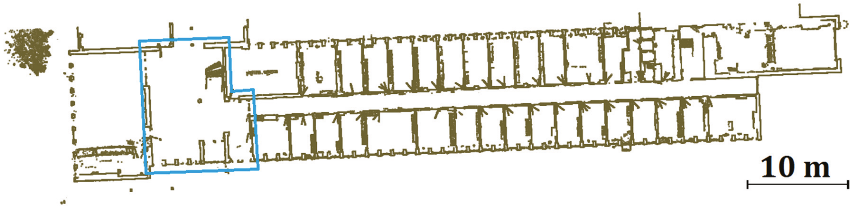

Figure 15. The selected area in the Realtek building used in the classification example shown in blue color.

The selected data is defined as one point cloud and is the measurement collected during one scan rotation for the horizontal scanner. This takes 0.1 seconds. The classification method described in Figure 13 is used, and the result is shown in Figure 16.

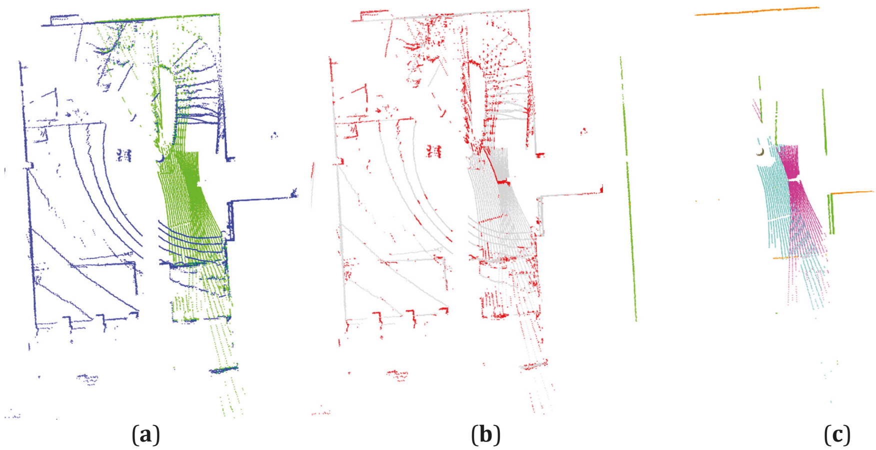

Figure 16. (a) Shows the result from step 1 in Figure 12. The blue color points are measured by the horizontal scanner and the green points from the vertical scanner. (b) Shows the result from step 2 where the grey points are the inlier points from the RANSAC method. (c) shows the result from step 3 and 4 where the points automatically are classified into column walls, floor, and ceiling.

2.3.2 Scan matching and aided inertial navigation

Scan matching is a method to align two different point clouds. The method requires a certain overlap. A scan matching provides transformation parameters that could transform one of the point clouds to fit the reference point cloud. The transformation parameters describe the position and orientation increment between these two point clouds scan locations. The increment was used to aid an inertial navigation system and acted as a velocity update. This was useful where the GNSS signals are interrupted due to obstacles like tall buildings or situations where the data acquisition was inside a building. In this study, two different scan matching methods has been used. The first method is called Iterative Closest Point (ICP)[59] and was used in the first and second stage. The usage of the ICP method is described in paper II and III and not described further in this thesis. The second method was SE-NDT [60] and was used in the third stage. Two laser scanners were used, one horizontal and one vertical. The rotating mirror inside the scanner was turning around the scanner's z-axis. A point cloud was created for each full rotation around the z-axis for the horizontal scanner. This time interval was used to select the corresponding laser data from the vertical scanner. This common point cloud contains data for 1/10 of a second from both horizontal and vertical scanner. Each point in the sequential point cloud was automatically classified into columns, walls, ceiling, and floors. This additional information was used by the SE-NDT method in such a way that points classified as walls were only matched with wall points and similar for the ceiling and the floor points. The column attribute was not used in the SE-NDT. The idea was that this could increase the scan matching reliability. The SE-NDT result was used to find the position increment between these sequential point clouds. This information was then fed back into the pose calculation in Terrapos v 2.5.90[53]. The processing procedure is shown in Figure 17.

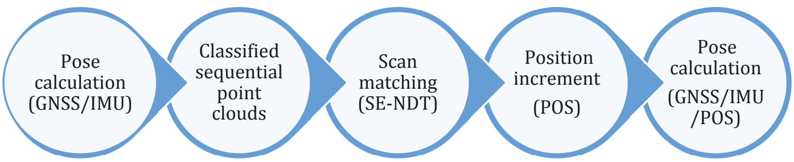

Figure 17. Procedure for SE-NDT aided pose calculation

The processing in Terrapos v 2.5.90 [53] was performed with a tightly coupled extended Kalman filter with backward smoother recursion (Rauch-Tung-Striebel algorithm)

[23] (chapter 6). The software producer extended the functionality to handle the position increments from the SE-NDT scan matching. The observation from the SE-NDT acted as position increment, which in limiting case have similar error characteristics as velocity updates. The standard deviation for the velocity σ_v can be expressed as a function of standard deviation for the distance $\sigma_{\Delta x}$ and time increment Δt, shown in Equation 1.

$$\sigma_v = \frac{\sigma_{\Delta x}}{\Delta t} \tag{1}$$

When $\sigma_{\Delta x}$ is constant σ_v can be reduced by increasing the time interval between the observations Δt. To ensure that $\sigma_{\Delta x}$ is relatively stable it was important to keep a certain overlap between the observations. A theoretical overlap was calculated on the basis of criteria given from the data collection. The maximum speed during data collection was 1.1 m/s, minimum observation distance was approximately 1m, and the laser scanner's field of view was 30°. The result from the overlap analysis is shown in Figure 18. The scanner system in stage three deliver individual point clouds with a rate of 10 Hz. By removing every second point cloud the rate was reduced to 5 Hz. This procedure was used to calculate a theoretical overlap between point clouds at different sample rates and observed ranges. The result showed that a 10 Hz sample rate gives an 80% overlap at a 1 m distance from the laser scanners. A 2 Hz sample rate provides approximately no overlap at 1 m range. Based on these extremes, it was chosen to use a 3.3 Hz rate which provides a 38% overlap at 1 m range.

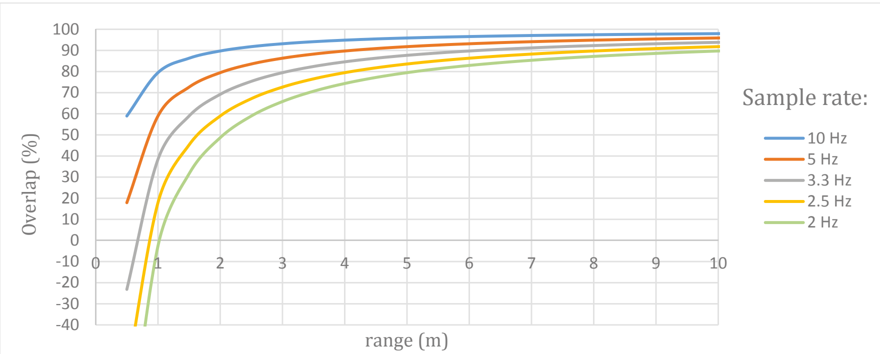

Figure 18. The overlap between observations as a function of sample rates and range

The result from the SE-NDT provides homogeneous transformation matrices for each time "t". These matrices can be used to extract the position x_t^a given in the SE-NDT frame indexed as "a" and the direction cosine matrix C_o^a used to transform from the object (laser) frame indexed as "o" to "a" frame. This information is fed back into Terrapos v 2.5.90. Terrapos use the earth frame "e" as the main frame. The a-frame may have an arbitrary offset and orientation with respect to the "e" frame. To be able to transform from the "e" frame to the "a" frame it is necessary to go through the IMU frame indexed as "s", the platform frame indexed as "p" frame and the laser frame. The position increment observation Δx_t^a is fed back into Terrapos is given by Equation 2-5, where ε^a represents noise and unmodelled effects:

$$\Delta x_t^a = x_t^a - x_{t-1}^a + \varepsilon^a \tag{2}$$

The computed perturbed increment observation, $\Delta\tilde{x}_t^a$:

$$\Delta\tilde{x}_t^a = \tilde{C}_e^a(\tilde{x}_t^e - \tilde{x}_{t-1}^e)$$

$$\Delta\tilde{x}_t^a = C_o^a C_p^o C_s^p \tilde{C}_e^s(\tilde{x}_t^e - \tilde{x}_{t-1}^e)$$

The perturbed position at time t, realized in earth frame $\tilde{x}_t^e$ consist of a true value x_t^e and the perturbation δx_t^e. The perturbed rotation matrix $\tilde{C}_e^a$ transform the position from earth to the SE-NDT frame. The entire rotation error is assumed to be located in the perturbed rotation matrix $\tilde{C}_e^s$, where the angle perturbation is realized in the skew-symmetric matrix Ψ_t^e.

$$\Delta\tilde{x}_t^a = C_o^a C_p^o C_s^p C_e^s(I + \Psi_t^e)((x_t^e - \delta x_t^e) - (x_{t-1}^e - \delta x_{t-1}^e)) \tag{3}$$

The observation equation:

$$\delta Z^o = C_a^o(\Delta x_t^a - \Delta\tilde{x}_t^a) \tag{4}$$

Inserting Equation 2 and 3 into Equation 4:

$$\delta Z^o = C_a^o(x_t^a - x_{t-1}^a + \varepsilon^a) - C_a^o(C_o^a C_p^o C_s^p C_e^s(I + \Psi_t^e)((x_t^e - \delta x_t^e) - (x_{t-1}^e - \delta x_{t-1}^e))$$

$$\delta Z^o = (x_t^o - x_{t-1}^o + \varepsilon^o) - (C_e^o + C_e^o\Psi_t^e)((x_t^e - \delta x_t^e) - (x_{t-1}^e - \delta x_{t-1}^e))$$

Neglecting the product of small terms and using $\Psi_t^e \equiv \psi_t^e \times$ gives:

$$\delta Z^o = (x_t^o - x_{t-1}^o + \varepsilon^o) - x_t^o + x_{t-1}^o + C_e^o(\delta x_t^e - \delta x_{t-1}^e) - C_e^o\Psi_t^e(x_t^e - x_{t-1}^e)$$

$$\delta Z^o = C_e^o(\delta x_t^e - \delta x_{t-1}^e) - C_e^o\Psi_t^e(x_t^e - x_{t-1}^e) + \varepsilon^o$$

$$\delta Z^o = C_e^o(\delta x_t^e - \delta x_{t-1}^e) + C_e^o(x_t^e - x_{t-1}^e) \times \psi_t^e + \varepsilon^o \tag{5}$$

Equation 5 shows that the observation equation is independent of the SE-NDT frame assuming C_a^o can be updated with negligible error at each step, based on incremental orientation from the SE-NDT scan matching. This ensures that the SE-NDT aiding can start and stop without having knowledge of the orientation offset between the object frame and the SE-NDT frame. The uncertainty of the rotational part of the scan matching is implicitly contained in ε^{o}. The covariance matrix for ε^{o} has a full bandwidth. Before the covariance was imported into Terrapos they were scaled with a factor ten. This was done in a best guess approach and adds a certain uncertainties. Equation 2-5 describes the general implementation in Terrapos. In this study, a simplified method was used. This study assumes that the orientation was without errors and the position increment was imported in a specified mapping frame. This simplifies the equation, but also provide significant limitation regarding the orientation.

2.3.3 Circle fit algorithms and Linear adjusted diameter at breast height

There is a large variety of different circle fit algorithms available. In the second stage, three different methods were tested. The first method was coded by Izhak Bucher in 1991 and called "circfit" [61]. The method is based on the general circle equation. It creates one observation equation for each measured point and estimates the best-fit circle parameters. The second method called "CircleFitByPratt" was made by Vaughan Pratt [62] and implemented by Nikolai Chernov. The method is presented as well suited for a situation where just a small arc with points is present. It is a noniterative least-squares fitting method. The third method used is called "fitcircle" and was implemented by Richard Brown in 2007. The method is described in Gander et al. [63]. The method fits a circle to the points by minimizing the sum of the squared distance from the points to the circle. The process uses a nonlinear least squares method. All three methods were used to calculate the tree position and DBH.

A study performed by Forsman et al. [64] made a simulation showing that a positive bias on the diameter estimation can occur. This happens when the laser beam footprint becomes too large compared to the tree stem diameter. The study registered an error higher than 10% on the diameter estimation where the footprint was more than 14% of the diameter. The effect occurred on the edges of the cylinder where the footprint from the laser beam partly hit the cylinder. The simulation in the study [64] was evaluated using a SICK LMS 221 scanner [65]. This scanner has a large beam divergence of 0.8°. They also tested different surfaces. The results were stable when the surface was diffusing the light properly. They used white paper, white shiny cloth, black matter cloth and paint with the result of an error in the same region. When they used aluminum foil, the result was different, and they discovered an increased error. This is important information when measuring potential pipes inside a building. When using a laser scanner with large beam divergence, the diameter of the pipe might be overestimated, and if the surface is a high reflecting target similar to an aluminum foil, special considerations should be made. This might be a problem when new ventilation pipes are surveyed, that might have similar characteristics as aluminum foil. The study suggests excluding the measurements with a lower intensity, which is the measuring points, located on the edge of the cylinder. Other actions would be to select a scanner with sufficient beam divergence or to ensure that the diameter footprint relation is kept below 14%. An option that Forsman et al. [64] suggested was to model and adjust the bias. All three circles fit methods used in this study were analyzed for potential biases and adjusted with a linear function.

2.4 Definitions

The tree measurement in this study was evaluated by calculating the mean difference, RMSE, and RMSE% using Equation 6-8. There are different definitions of these parameters. The definition of each parameter is given here to reduce the possibility of misunderstanding:

$$\text{mean difference} = \frac{1}{n}\sum_{i=1}^{n}(y_i - y_{ri}) \tag{6}$$

$$\text{RMSE} = \sqrt{\frac{\sum_{i=1}^{n}(y_i - y_{ri})^2}{n}} \tag{7}$$

$$\text{RMSE\%} = \frac{\text{RMSE}}{\overline{y_r}}\,100 \tag{8}$$

In the equations y_i is the estimate, $\bar{y}_i$ is the mean estimate, y_{ri} the reference, $\overline{y_r}$ is the mean reference value, and n the number of observations. For the forestry projects, the reference was the result from the calipered DBH and manual tree position registrations using a total station. The tree position accuracy was evaluated using Equation 6 and the RMSE from Equation 7. The standard deviation, σ was found using Equation 9.

$$\sigma = \sqrt{\frac{\sum_{i=1}^{n}(y_i - \bar{y}_i)^2}{n-1}} \tag{9}$$

3. Results

3.1 Product specification development (paper I, IV and V)

This thesis has been involved in different tendering processes to purchase building surveys using terrestrial laser scanning. Two different projects have been used in the thesis. Altogether 15 tenders and 11 different building surveys were used to develop a product specification through different versions. Version 0 was presented by Hjelseth et al. [4] and shown in Table 6. This version was the starting point in the development of the product specification.

Table 6. Product specification at version 0.

Accuracy level	Level 1 (cm)	Level 2 (cm)	Level 3 (cm)
Relative accuracy*	0.3	1	3
Maximum average deviation*	1	4	10

*Calculated on 20 cm x 20 cm control area.

The requirements from step 0 was used in the tendering process for the measurements of the Realtek building. The relative accuracy in step 0 was an expression of the noise level within a control area. The maximum average deviation requirement was interpreted as the average offset to the requested global coordinate frame. To fit the measurements to a global coordinate frame a network of known points was established surrounding the building.

The evaluation found that it was time-consuming and challenging to establish a network of known points with sufficient accuracy in a global coordinate frame. It was also concluded that in most cases it would be sufficient to perform the accuracy evaluation in a local coordinate frame. This required that the network of known points and the laser point cloud are realized in the same local coordinate frame. An additional requirement was that a set of transformation parameters should be established to transform the laser point cloud to a global coordinate frame with sufficient accuracy. The evaluation also concluded that additional requirements were needed to match the selected framework used for the accuracy evaluation. The framework is described in GeodataQuality and uses gross error, standard deviation and average deviation as accuracy indicators. The average deviation was present, but the standard deviation for the average deviation and gross error was missing. We assume that the maximum average deviation defined a

99.7% confidence interval. Based on this assumption the maximum average deviation were divided by a factor of 3. This was used to set the standard deviation requirements. The evaluation also concluded that additional requirements regarding point thickness were recommended. This provides a simplified method to get a rough impression of the scan location pose quality and the laser measurements noise level. The result from the Realtek building project ended up with the result called version 1 and is presented in Table 7.

Table 7. Product specification at version 1.

Accuracy level	Level 1 (cm)	Level 2 (cm)	Level 3 (cm)
Number of gross errors	0	0	0
Max. Point cloud thickness	1.8	6	24
Standard deviation *	0.3	1	4
Maximum average deviation *	1	3	12

* Calculated on 20 cm x 20 cm surfaces separately in three orthogonal directions.

Additional requirements for version 1 were that the number of known points should be at least four. The tolerance for the known points should be at the same level as the maximum average deviation in a local coordinate frame and 6 cm tolerance in a global coordinate frame. The tolerance demand in the global frame ensure that the RTK GNSS measurement method is allowed according to NS3580:2015 [66]. A gross error is present where the maximum point cloud thickness is exceeded. It is also recommended to set a maximum distance between the laser points within the final point cloud. One of the deliveries in the Realtek project was a text file with the size of 4 TB containing laser points. Such a large file is difficult to handle. First of all the file format should be avoided and large files should be split up into a set of smaller files.

The product specification version 1 was used in the framework agreement competition in Ullensaker municipality. Some minor changes were done. The accuracy requirement was set to a global reference frame, and the density requirement was set to a maximum point distance of 0.4 cm.

After the evaluation of the Ullensaker project the product specification was updated accordingly and became the product specification version 2. The major changes were done in the accuracy levels which were synchronized with DIN18710. Due to the lack of documentation from the participants, a new requirement regarding documentation was added.

The product specification was adjusted and summarized in the following:

- Accuracy evaluation follows the principles in GeodataQuality.
- A project report should be delivered following the requirement for geodetic mapping described in GeodataProduction. All requirements should be documented in a project report, and all used coordinates and height systems should be described.
- Density requirement and maximum point distance should be stated as a fixed distance. Typical distance is between 0.2-1.0 cm.
- A network of known points should be established in the surroundings of the building and have a clear view towards the building. The coordinates for the known points should be surveyed with a tolerance equal or better than the maximum average deviation, realized in a local coordinate frame. In the global coordinate frame, the recommended tolerance was set to 6 cm. The laser point cloud should be realized in the local coordinate frame described by the known points. The network of know points should be used in accuracy evaluation purposes and to transform the point cloud into a global coordinate frame.
- The properties of the delivered laser point cloud should be stated accordingly to Table 8.

Table 8. Product specification at version 2.

Accuracy level	Level 1 (cm)	Level 2 (cm)	Level 3 (cm)	Level 4 (cm)	Level 5 (cm)
Number of gross errors	0	0	0	0	0
Max. Point cloud thickness *	6x**	30	9	3	0.6
Standard deviation *	x**	5	1.5	0.5	0.1
Maximum average deviation *	3x**	15	4.5	1.5	0.3

* Calculated based on 20 cm x 20 cm surfaces. ** x: custom standard deviation

The general impression after analyzing the different tenders and delivery process is that the producer often promised more than they achieved. Especially when it came to accuracy and point density. In Oveland et al. [12] it is shown that all ten participants in the Ullensaker project failed to deliver the requested point density and height accuracy.

3.2 Laser-based system

3.2.1 Laser-based system first and second stage

The survey system developed in this study is referred to as BackPack Laser Scanner (BPLS). In the first and second stage, the developed system was used to survey sample plots for forest inventory. The laser system from the first stage was able to survey a 250 m^2 sample plot in 30 seconds. The data collection was done with only one walk through the sample plot. The time estimate did not include the startup time and the walking distance to the sample plot. In total 14 of 18 tree stems were detected and measured. All of the undetected trees had a DBH < 10 cm. An average position was calculated for each center point group. Equations 6 and 7 were used to calculate the mean difference and RMSE. The result is summarized in Table 9.

Table 9. The result from the first stage and the first backpack laser scanner (BPLS).

Method	Omission (Not Found) %	Commission (False Trees) %	Detected Trees %	Diameter at Breast Height (cm)			Position (cm)	
				Mean (Eq. 6)	RMSE (Eq. 7)	RMSE% (Eq. 8)	Mean (Eq. 6)	RMSE (Eq. 7)
BPLS	22	-	78	0.9	1.5	7.5	21	23

In the second stage seven different sample plots were surveyed, each with an area of 500 m^2. All sample plots were surveyed with the BPLS survey system developed for the second stage, a Faro focus 3D x130[25] referred to as Terrestrial Laser Scanner (TLS), and a GeoSlam ZEB1[2] referred to as a Handheld Laser Scanner (HLS). The results from all three methods were compared with traditional caliper measurements and shown in Table 10.

Table 10. The results derived from the terrestrial laser scanner (TLS), handheld laser scanner (HLS) and the second stage referred to as backpack laser scanner (BPLS).

Method	Omission (Not Found) %	Commission (False Trees) %	Detected Trees %	Diameter at Breast Height (cm)			Position (cm)	
				Mean (Eq. 6)	RMSE (Eq. 7)	RMSE % (Eq. 8)	Mean (Eq. 6)	RMSE (Eq. 7)
TLS	37.9	5.4	61.8	-2.0	6.2	28.6	69	82
HLS	26.0	4.8	74.0	0.3	3.1	14.3	17	20
BPLS	12.5	9.9	87.5	0.1	2.2	9.1	54	62

3.2.2 Circle fit algorithms and Linear adjusted diameter at breast height

The survey system developed in the second stage was used to measure the tree stems DBH. In Figure 19 the DBH deviations from the true values are presented and organized after DBH and the red linear trend lines shows that the bias changes accordingly to the tree stem diameter.

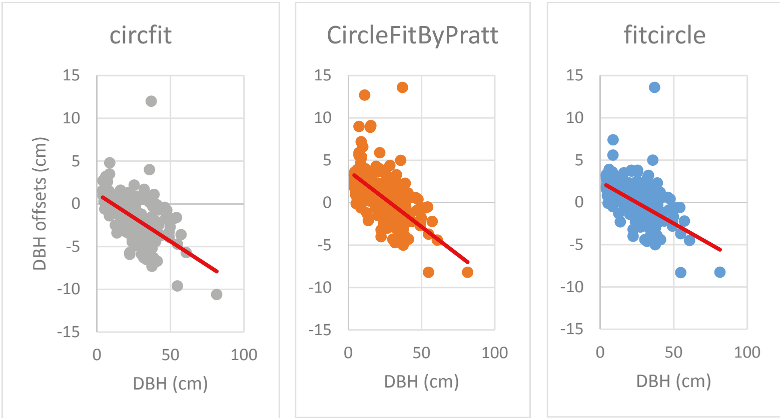

Figure 19. The Diameter at breast height offset shows the difference between the estimated DBH and the caliper measurements. The linear trend lines are shown in red color.

Each scan rotation has 16 different laser channels. In a situation with a clear view from the scanner to the tree stem, it will be possible to create 16 different tree stem profiles. This means that every tree stem was measured multiple times as shown in Figure 20. Smaller trees have fewer observations than the larger trees. This is an expected result since smaller trees are more difficult to spot than larger trees. Oveland et al. [49] showed a relation between the diameter and the distance to the tree. If a large tree has a clear view, it can be observed from all location within the plot while a small tree has a maximum observation distance shorter than the sample plots radius. This means that a small tree only can be observed from a certain region within the sample plot. This effect is shown in Figure 20, where the larger trees have more observations than smaller trees.

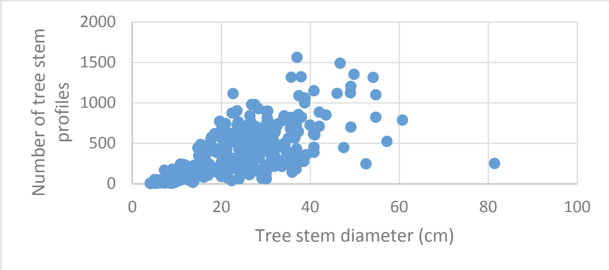

Figure 20. The number of tree stem profiles sorted by diameter.

The final tree stem diameter was estimated by averaging the diameter estimation from each tree stem profile. For each tree, a standard deviation for the diameter estimation is calculated, and a trend line is created for each method. The result is shown in Figure 21. The vertical axis for the CircleFitByPratt is bounded in such a way that 14 trees exceed the plot. The trend line shows that the tree stem diameter estimated for the smaller trees had a lower standard deviation compared to the larger trees.

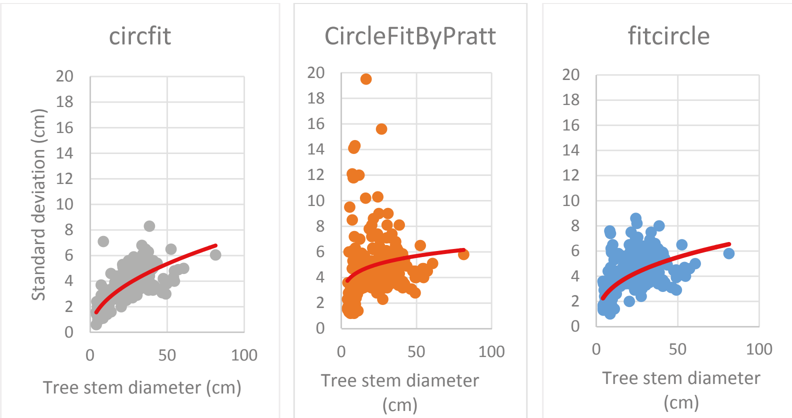

Figure 21. The estimated standard deviation for each method. The red lines are the power trendline and show that the standard deviation is changing with the tree stem diameter.

One method to evaluate the different circle fit methods is to analyze the variation in the tree stem result. The average standard deviation for all trees is present in Table 11. The different circle fit methods are described in section 2.3.3. The method “circfit” has the lowest standard deviation.

Table 11. Result using different circle fit method

Circle fit method	implemented by	st.dev (cm)	Diameter at Breast Height (cm)		
			Mean (Eq. 6)	RMSE (Eq. 7)	RMSE % (Eq. 8)
circfit	Izhak Bucher	3.6	-1.5	2.8	11.7
CircleFitByPratt	Nikolai Chernov	7.3	0.6	3.6	15.4
fitcircle	Richard Brown	4.2	0.1	2.2	9.3

Another method is to evaluate the mean difference, RMSE and RMSE% presented in Table 11. All of the different circle fit methods have different characteristics and use different approaches to fit the circle to the measured points. In the studies from Oveland et al. [49, 51] the tree stem measurements will never cover the entire tree stem, but less than 50% of the tree stem. This is due to the splitting of the laser data into scan rotations or frames. Each of the circle fit methods has different robustness to handle this type of problem. Table 11 shows that the method Fitcircle had the lowest mean difference, RMSE, and RMSE% and was selected in the study by Oveland et al. [51].

In Figure 19 the tree stems are sorted by DBH. This shows that the DBH error varies with the diameter. For the smallest trees, there was a positive mean difference. This corresponds to the simulation made by Forsman et al. [64]. For the larger trees, the mean difference change to a negative bias. This was not an expected result.

The linear trend line shown in Figure 19 indicates a correlation between the DBH offset and the DBH from the caliper result. To further evaluate this the study area was divided into a training dataset and a test dataset. For the training dataset sample plot number 1,3 and 5 were selected, in total 107 trees. For the test dataset the sample plot number 2, 4, 6 and 7 were selected, in total 190 trees. The training dataset was used to fit a trend line to the dataset, shown in Figure 22. The trend line shows a correlation between the tree stem diameter at breast height and the DBH offsets.

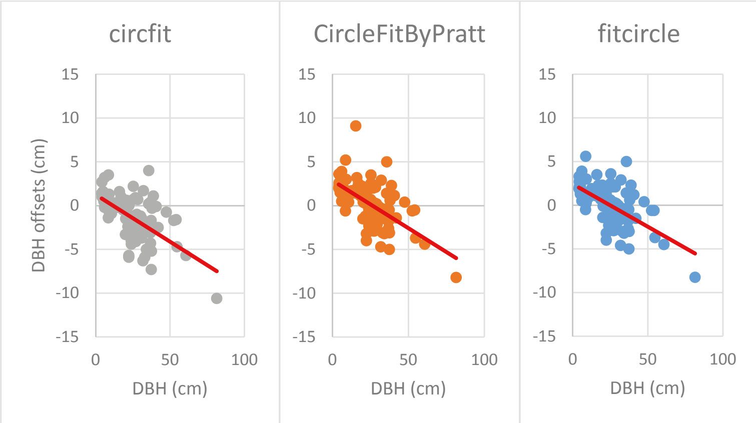

Figure 22. The sample plots number 1, 3 and 5 were used as a training dataset to estimate a trend line for the Diameter at breast height offset.

The R-squared or the confidence of determination were estimated for each trend line and gives the relation between the variation explained by the linear function and the total variation in the dataset. The value ranges from 0 to 1. The highest value indicate a good fit and 0 indicate a poor fit. The confidence of determination was stable in between the different circle fit methods and varied from 0.34 to 0.35, shown in Table 12.

Table 12. The linear trend line function for each circle fit method with the corresponding confidence of determination made from the sample plots 1,3 and 5.

Circle fit method	confidence of determination	Linear function
circfit	0.34	y =-0.1074x +1.2472
CircleFitByPratt	0.35	y =-0.1087x + 2.8575
fitcircle	0.34	y =-0.0976x + 2.4166

The trend line was used to correct the DBH estimation for the test sample plots 2,4,6 and 7. This was done by subtracting the corresponding linear function found in Table 12 from the DBH estimation. Figure 23 shows the result after the adjustment and shows that the correlation between the estimated DBH offset and the DBH was reduced.

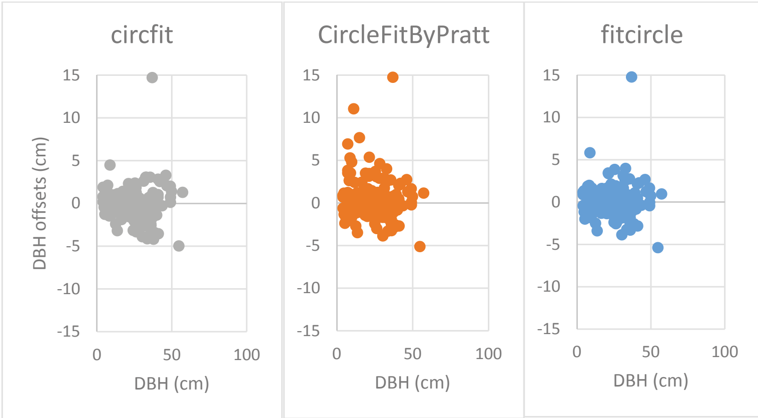

Figure 23. The Diameter at breast height offset after a linear adjustment for the sample plot 2,4,6 and 7.

Based on the linear adjusted result a set of statistics was calculated using Equation 6-8. The result is presented in Table 13. The Mean difference is now closer to zero for all circle fit methods. This was expected since the trend line equation takes the mean difference into account. Additionally, the RMSE and RMSE% changed with the linear correction. Both values were improved for all circle fit methods. The circfit had the largest improvement with 30%, CircleFitByPratt was improved by 10%, and the fitcircle reduced the RMSE and RMSE% by 16%.

Table 13. Result using linear adjustment.

Circle fit method	Diameter at Breast Height (cm) for sample plots 2,4,6 and 7.			Linear adjusted Diameter at Breast Height (cm) for sample plots 2,4,6 and 7.		
	Mean (Eq. 6)	**RMSE (Eq. 7)**	**RMSE % (Eq. 8)**	**Mean (Eq. 6)**	**RMSE (Eq. 7)**	**RMSE % (Eq. 8)**
circfit	1.5	2.7	11.9	0.2	1.9	8.1
CircleFitByPratt	0.9	4.2	18.1	0.5	3.8	16.3
fitcircle	0.2	2.2	9.5	0.0	1.8	8.0

The linear trend line was made from plot 1,3 and 5 and was used to correct the DBH estimations from sample plot 2,4,6 and 7. The result shows a large improvement. This indicates that the linear bias is stable throughout the project.

3.2.3 Laser-based system third stage

The Third stage was used for building surveys and had two different inertial navigation systems. The idea was to evaluate the difference between the two navigation solutions and to evaluate the effect the different solutions had on the final trajectory. The first analysis was performed with the IMU and the GNSS data only. The system was started up outside the building where the GNSS conditions were good. An initialization procedure was performed to ensure good initial values of the orientation parameters and bias and scale corrections. When the system was entering the building, no GNSS signals were received, and the system just relied on the IMU data to estimate the pose. A low-grade IMU will drift significantly over time, while a medium graded IMU can keep the pose for a longer period. There were two trips inside the building and the total time inside the Realtek building was 4 minutes for the first trip. The second trip inside the building was not considered in this thesis. An individual pose estimation was calculated for both IMU systems and used to realize individual laser point clouds. The evaluations were done by comparing the processed laser point clouds with a traditional terrestrial laser scanning of the building. The terrestrial laser scanning is further described in Oveland et al. [11] and act as the true solution. The result is presented in Figure 24 and Figure 25, and shows a large difference between the solutions achieved with the Applanix APX 15 UAV and the Applanix POS AV 510.

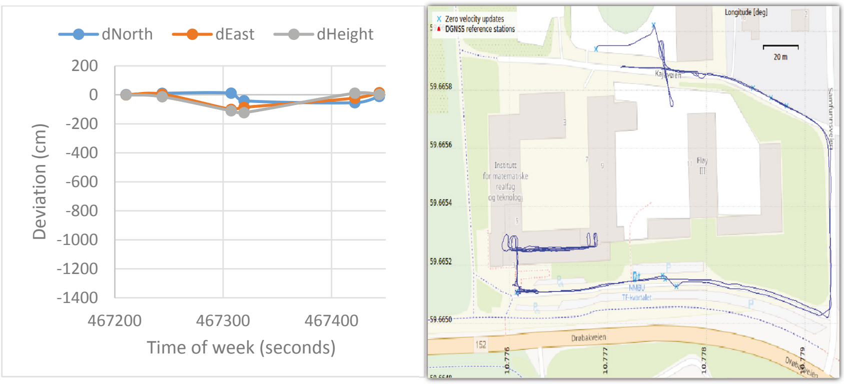

(a) (b)

Figure 24. (a) The deviation from the true solution during the first trip into the building using the Applanix POS AV 510. (b) Shows the entire trajectory with initialization and two separate trips into the building.

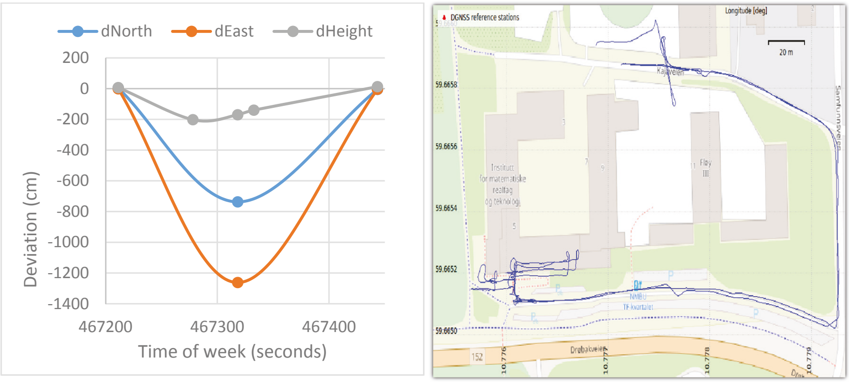

(a) (b)

Figure 25. (a) The deviation from the true solution during the first trip into the building using the Applanix APX 15 UAV. (b) Shows the entire trajectory with initialization and two separate trips into the building.

The maximum error for the Applanix APX 15 UAV solution was 12.6 m and 2.2 m for the Applanix POS AV 510 system. This was an expected result. To maintain an accurate pose estimation the inertial navigation system needed additional information. This was typically received from the GNSS system, but inside the building an additional source would be required. With a 3D laser scanner and scan matching, it was possible to estimate the pose increment from one time frame to another. The frame rate was decided by the scanner speed or scan rotation speed. The Velodyne scanner rotates around the z-axes and continuously performs laser measurements. In this study, the laser measurements were divided by the scan rotation for the horizontal scanner. One scan rotation became one laser point cloud. To improve the result achieved with the Applanix APX 15 UAV, the collected laser data was run through the SE-NDT framework. The result provides a transformation that fits the sequential point cloud to the reference. The result from the SE-NDT framework includes the corresponding covariance, which tells how good the transformation was expected to be. The transformation was used to make the trajectory shown in Figure 26 as red dots. To minimize σ_v in Equation 1, the laser point cloud rate was reduced from 10 Hz to 3.3 Hz. This trajectory was imported into Terrapos v. 2.5.90 [53], where the software used the trajectories to calculate the position increment.

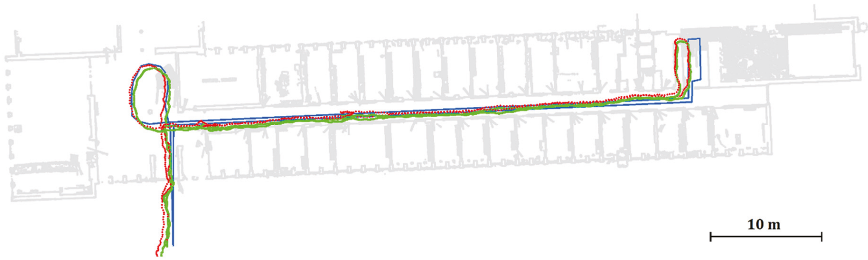

Figure 26. The approximately walking path is shown with blue color. The red dots are the trajectory from the SE-NDT framework, and the green line are the result from Terrapos v. 2.5.90 where the SE-NDT result was used to support the Applanix APX 15 UAV solution.

The result using the Applanix APX 15 UAV with SE-NDT aiding was compared with the terrestrial laser scanning of the building and shown in Figure 27. The maximum deviation was 1.1 m.

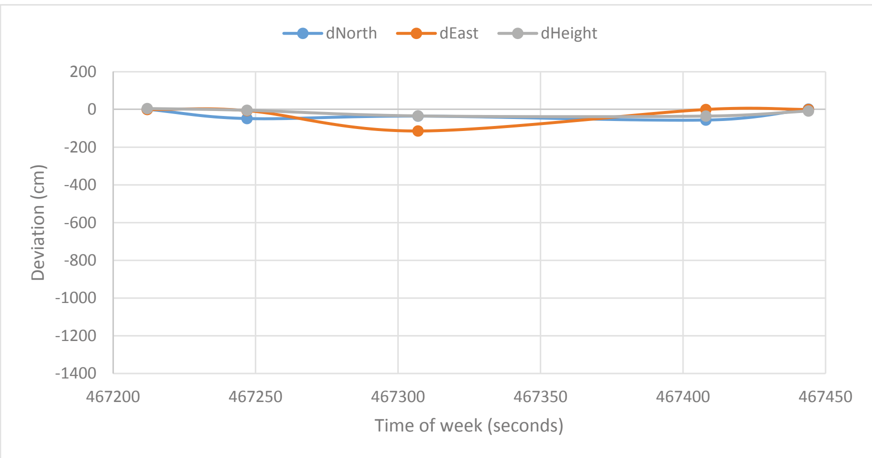

Figure 27. The result from stage 3 using the Applanix APX 15 UAV with aiding from the scan matching.

The covariance from SE-NDT was used to ensure that the SE-NDT result was given the correct weight. In situations where the SE-NDT result is bad and diverge to much from the IMU observation, the filter relied on the IMU observation alone. This was an efficient method to exclude scan matching failure. To test this capability the result from the SE-

NDT was given a 10 m false offset in north direction at a given time. The manipulated result was fed back into Terrapos, and the result showed that the sudden shift was rejected. The result is shown in Figure 28 where the manipulated SE-NDT result and the result from Terrapos are plotted.

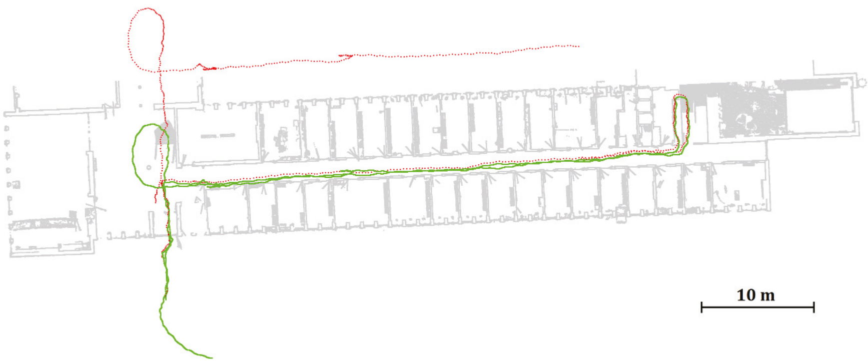

Figure 28. Trajectory from SE-NDT with a manipulated 10 m shift shown in red. The manipulation trajectory was fed back into Terrapos, and the result is shown in green color.

To be able to achieve a similar detection of a potential orientation error it is necessary to include the rotation from the SE-NDT result back into the pose calculation in Terrapos. This was not done in this thesis, but can be done using Equation 5. This will ensure that the imported increments will be independent of the main reference frame.

4. Discussion

This thesis has focused on the research questions called “Product specification development” and “Laser-based systems”. The topics include a number of issues and challenges. In the following, a few of them have been selected and discussed.

4.1 Product specification development

4.1.1 Multiple purpose BIM

In the introduction section, a hypothesis was presented saying that a product specification could increase the potential usage of the BIM. Hjelseth el al. [4] used the theoretical framework Integrated Design and Delivery Solutions (IDDS) [67] to explore and understand the different imperatives in the process of establishing a BIM. The goal was to establish a BIM with multiple purposes within facility management. In Hjelseth et al. [4] the different imperatives were given the following content:

- Involvement of relevant people (Collaborating People): architects, engineers, land surveyors, BIM specialists, landlords, residents,…
- Available scanning technologies (Interoperable Technologies): drawings, tape measure, laser scanner, total station, rangefinder, and camera.
- Processes and methods for enrichment of BIM (Integrated Processes): Software and methods for creating BIM.

The different imperatives and how they interact is illustrated in Figure 29. The size and position of the circles decide the size of the common area or the union of the three circles. When the common area is large, the possibility for a multiple purpose BIM increases. When the accuracy of the product is not stated, the "Collaborating People" do not have the necessary information to understand which possible purposes that lie in the product. An example is the Norwegian Mapping Authority which has a long-term goal to use BIM to update the national map [68]. To achieve this, it is important that information about the model's accuracy and the location is present. Essential information about the product is important to achieve a multiple purpose BIM. The main motivation to have a multiple purpose BIM is to be able to use the product for many different applications and to include as many "Collaborating People" as possible. This has the potential to improve the cost-benefit ratio and could be achieved through the proposed product specification.

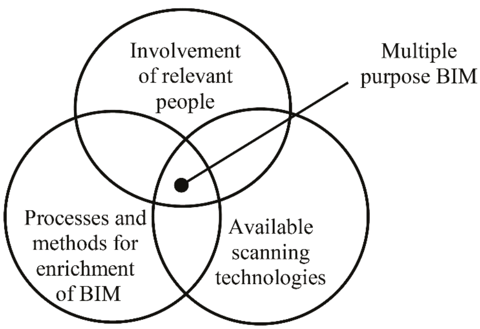

Figure 29. The different imperatives for multiple purpose BIM based on IDDS as proposed by Hjelseth et al. [4].

4.1.2 Fair competition

A comprehensive product specification is an important tool to ensure a fair competition situation in the tendering process. The product specification should clearly state requirements that have an impact on the data capture cost. A typical parameter that highly influences the cost is the accuracy. Different data capture methods have different time consumption during data capture. Typically, a human carried scanner system is faster to use than a tripod and has the potential to capture the data cheaper than a traditional tripod mount. These two methods provide building surveys with different accuracies and characteristics. This makes it important to specify which accuracy level you would request to ensure the best cost-benefit ratio and to ensure fair competition. The accuracy requirement is important, but also which coordinate frame the accuracy should be referred to is important. In Oveland et al. [11] it was found that the requested accuracy was time-consuming to achieve. The requested accuracy was set in a global frame and the time consumption was close to the time consumption of scanning the entire building. To achieve the accuracy in a global frame, it was necessary to perform static GNSS measurements with long observation time and combine this with a closed traverse measurement. A BIM project is located inside a building. Therefore your GNSS measurements often need to be performed close to the building. This might give you poor sky visibility. To ensure acceptable reliability, it might be necessary to repeat the static GNSS measurements. To achieve the same accuracy in a local frame would just take a fraction of the time and is achievable with real-time kinematic GNSS in combination with a closed traverse. Another example of a parameter that strongly influences the data capture cost is point density. In the first years of airborne laser scanning in Norway, the product specifications had an ambiguous description of the point density requirement. The result was that the different suppliers interpreted the density requirement differently. Some estimated the point density by dividing the total number of laser measurements by the total project area while others calculated the point density on smaller subareas down to one m^2. Since the point distribution from an airborne laser system is not uniform, this small difference leads to a significant difference in the data capture time. This had influence on the total price estimate for the tendering process. In the framework agreement competition in Ullensaker municipality, none of the participants achieved the requested point density. The point density for an indoor scanning relies mainly on the scanner settings, the distance between each scan position, range, and the laser beam angle of incidence. The problem with an increasing angle of incidence is that the distance between to laser points increases proportionally. The scanner achieves an optimal distribution of the laser point when it is located in the middle between the floor and ceiling. If the scanner is located too close to the ceiling, the point density in the ceiling will be much smaller at a certain distance from the scan position. This lead to an uneven point density between the ceiling and floor. Each company had proper equipment and used proper scanning settings, but all had a combination of too few scan positions or mounted the laser scanner so close to the ceiling that the angle of incidence became a problem. The number of scan positions is one of the factors that increase the data capture cost. It is therefore important to have a clear description and understanding of the point density requirement to ensure a fair competition situation.

4.1.3 Open up for new technology

The contractor has a responsibility in the tender request to provide a comprehensive product specification. This allows the producer to select the best possible technology for the "result requested" in Figure 2. Typically, if the accuracy level is specified the producer has the possibility to select the technology that gives the requested product. The biggest advantage comes where the contractor only needs a low accuracy product. In such a situation, the producer has the possibility to select a technology that captures the data as fast as possible. This will typically be a kinematic scanner carried by a human. This is a fast data capture method that reduces the data capture cost. The existence of a comprehensive product specification has the potential to ensure the best possible cost-benefit ratio.

4.1.4 Point cloud thickness

Point cloud thickness is a useful contributor to a product specification. The point cloud thickness method evaluates the deviation between the point clouds captured from different scan locations. The most common reason for deviation is a bad estimation of the laser scanner poses. Other reasons are instrument error and calibration issues [16, 21]. The method analysis the deviation between the scans covering the same area. The main use is to increase the probability of a successful data acquisition. In a situation where the point cloud thickness is small, it is likely that the pose, instrument error, and instrument calibration are of adequate quality. It is important to notice that this only counts for the scan involved in the point distance evaluation and just within this local area. The method cannot verify the accuracy in a specific local coordinate system, but is a good tool to evaluate the point cloud homogeneity within limited regions. A large point cloud deviation is a strong indication that something went wrong and in most situation, this error is caused by a weak pose for the laser scanner. The point cloud thickness is easily accessible in the delivered point cloud. This makes the point cloud thickness a usable marker. This counts for the laser-based systems, but also for all other data acquisition methods with overlapping measurements.

4.1.5 Local vs. Global Coordinate frame

In the first version of the product specification, all requirements were given in a global coordinate frame. The evaluation concluded that this was not a necessary requirement. Such a requirement would also require that the network of known points surrounding the building are realized in the global frame. The network of known points should be used to transform the laser point cloud into the global frame, but also to perform control measurements of the laser point clouds. It is therefore important that the network of known points has a certain accuracy, and should have a tolerance equal or better than the maximum average deviation defined in the selected accuracy level Table 8. To achieve a tolerance in the same level as the maximum average deviation in the global coordinate frame is a difficult task, especially since the coordinates standard deviation for the permanent GNSS station in the national grid is stated to be 0.005 m. In most cases, it will be sufficient to have the requirement in a local coordinate frame, but additionally, require a transformation to a global frame with a specified tolerance. In most situations, a tolerance of 6 cm would be sufficient in a global frame. The tolerance level is selected so it should be achievable with real-time RTK GNSS equipment with base station network distances around 35 km [69]. This level open ups for RTK GNSS according to NS3580:2015 [66]. Most of all it should be sufficient for the Norwegian building management solution [70].

4.1.6 LoD framework

The LoD is an efficient method to describe the content of the BIM and provide guidelines on how the BIM could be used. An important aspect regarding the laser-based system is the achievable LoD for an existing building. A major issue is an obvious limitation of the laser-based method. This is the fact that just the visible part of the building object is possible to measure. The consequence is that only the visible part of the building object can be modelled. Typically, parts of a window or door object is hidden by the fittings. This means that a laser-based method is not able to obtain the correct size and shape of building objects like windows and doors without additional information. The level called "300" by AiA [43], BIMforum [45] and MMI [44] requires exact position, orientation, size, and shape. Based on this a laser-based system is not able to achieve the level called "300". The levels called "100" and "200" require an approximate position, orientation, size, and shape and is easily achievable with a laser-based system. To get the most out of a survey of an existing building it would have been useful to add a level called "250" with the requirements of exact position and orientation, but approximate size and shape. The proposed level called LoD 250 is shown in Table 14. The level of accuracy described in this thesis could work as a framework to describe the accuracy of the positon and orientation.

Table 14. Level of Development described by BIMForum with the proposed Lod 250

Level of Development	Representation of building objects			Quantities, size, shape, location and orientation		Fabrication, assembly and installation information	Field verificated
	Symbolic or generic represen-tation	Generic system, object or assembly	Specific system, object or assembly	Roughly	Correct		
LoD 100	x			x			
LoD 200		x		x			
LoD 250			*x*	***size, shape***	***location, orientation***		*x*
LoD 300			x		x		
LoD 350			x		x *		
LoD 400			x		x	x	
LoD 500			x		x		x

* Interfaces with other building systems

4.2 Laser-based system

4.2.1 Nonperpendicular tree stem measurements

The result from the first stage showed that the data capture was efficient. The sample plot was collected with just one walk through the sample plot. The rapid data capture was promising. During the analysis of the data, it was clear that the forest floor was difficult to capture. The scanner was mounted in a horizontal position. This orientation was selected to maximize the number of laser channels that hit the tree stem and to ensure that the measurements were done as perpendicular as possible. When the laser beams hit the tree stem perpendicularly, the circle fit function could be used directly without considering the angle of impact to the tree stem. Figure 30 illustrates the difference between the semi-minor axis and the semi-major axis on a cylinder-shaped tree stem from different laser channels using the VLP16 scanner.

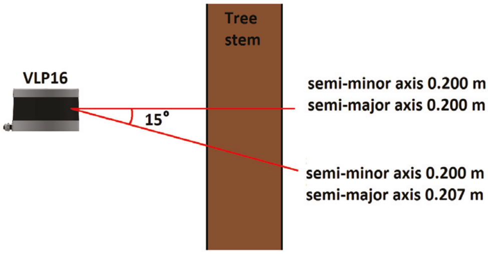

Figure 30. A column shape tree with a 0.200 m radius will appear as an ellipse with a semi-major axis of 0.207 m, when the laser beam deviates with 15° from the tree stems perpendicular line.

The VLP16 scanner has 16 laser channels. All channels have a different vertical angle spanning from -15° to +15°. In a situation where the scanner is mounted horizontally, a vertical tree stem will be measured with an impact angle varying from 75° to 105° to the tree column. The method used in [49, 51] estimated the diameter separately for each scan rotation and laser channel. For one scan rotation, it was possible to estimate 16 different diameters for a single vertical tree stem if all laser channels hit the stem. In Figure 31 it is shown how the estimated diameter will change between the different laser channels due to a different angle of incidence to the tree stem. Figure 31 shows how the measured diameter would vary. For a tree stem with 20 cm diameter, the measured diameter would vary from 20 cm to 20.7 cm with an average diameter of 20.3 cm. The size of the offset will vary linearly with the tree stem diameter. The effect was not compensated for in [49, 51] and would give a theoretical positive bias of 0.3 cm for the diameter at breast height calculation for a clear view tree stem with a diameter of 20 cm.

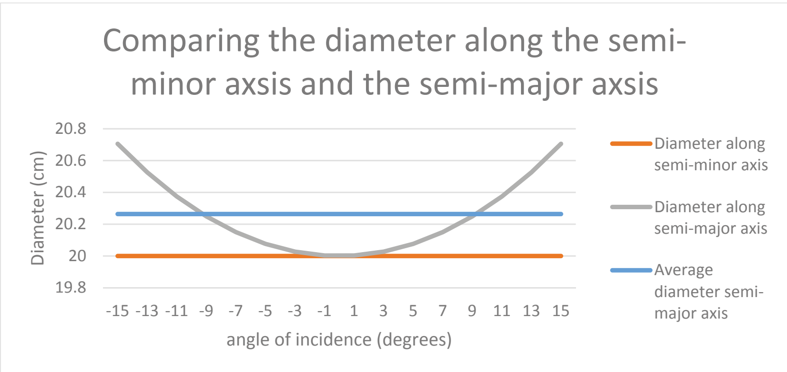

Figure 31. Diameter along the semi-major axis for a tree stem observed with different impact angles.

In practice, the lowest laser channels were often excluded since all observations 0.5 m above the ground level were excluded. This reduced the positive bias slightly. The effect could also be reduced by calculating the impact angle. This could be done by using the laser scanner pose and the tree stem orientation. The orientation of the scanner is known from the pose calculation, and the tree orientation can be found using the laser observations. The tree segmentation was performed with the rule saying that minimum five laser channels should have observed the tree. Based on this observation the tree stem orientation could be calculated. With help from the laser channel information and the laser calibration file, the impact angle could be estimated. Another method is to assume that the tree stem is an ellipse and calculate the semi-minor and semi-major axis. This requires more laser observation on the tree stem and would have influenced the maximum possible distance observation to the tree. The measurements from the VLP scanner have a certain noise level and when the number of parameters increases, it becomes more difficult to get a robust estimation.

4.2.2 Error in cylinder diameter estimation

Forsman et al. [64] showed that cylinder shaped objects might be measured inaccurately due to overestimation of the cylinder diameter, but a flat surface will not have the same inaccuracy. This means that an indoor laser scanning might have different accuracies for different building objects. A cylinder formed shaped pipe might have lower accuracy than a flat wall. Based on the argumentation in Forsman et al. [64] it might be possible that the same effect can occur on wall corners. This might give an inaccurate measurement of the wall edge, and the wall will not end at the correct position. This can be a potential problem when building objects are extracted from the laser point cloud. The USIBD product specification was constructed so that different objects may have different accuracy. This shows the strength of the USIBD framework. The optimal situation would be to have the same accuracy for all objects inside the building. With a uniform accuracy, there is no need to specify different accuracies on different objects. Where different objects have different accuracies, it is easy to get confused and mix the different accuracy specifications. A uniform accuracy should be possible to achieve by selecting a scanner with a small beam divergence and ensure a maximum distance to the object so that the ratio between the footprint and the diameter of the object is sufficient.

In Figure 21 it is shown that the small trees have a lower standard deviation than the larger trees. This is best showed for the circfit method. One reason for the lower standard deviation might be related to the maximum observation distances for the smaller trees. The maximum distance will in some situations limit the area in which it is possible to observe the tree. This could make the observation more homogenous. The larger trees were observed from a larger area and from many different locations. In a situation where the tree column has an elliptical shape, you will observe different diameters when observing the tree from different directions. A non circular shaped tree will also affect the caliper measurement since the measurements were performed only once. Another aspect with a large tree is that the tree diameter might be measured at several different heights above the forest floor. Measurements taken close to the ground will typically have a larger diameter than a measurement higher above the ground. In the study from Oveland et al. [49, 51] there is a simplified growing model built into the procedure saying that the tree stem decreases with 1 cm per meter above the forest floor. This model can be inaccurate in some situations and might cause an increased standard deviation. One method to reduce this problem is to exclude observations with a large elevation distance from the DBH altitude. Oveland et al. [49, 51] exclude all tree stem profiles lower than 0.5 m above the forest floor. This is because the simplified growing model does not fit well in the lower region. When the tree stem diameter becomes large, the effect of the different impact angles illustrated in Figure 31 will provide a larger error compared to the effect on the smaller trees. This can also result in an increased standard deviation.

In the study Oveland et al. [51] three different measurement methods were evaluated. The different methods were backpack scanner, handheld scanner, and terrestrial scanner. Both the handheld scanner and the terrestrial scanner method use a different processing method compared to the backpack laser scanner. One of the main differences was that the laser point cloud was merged into one common point cloud before the DBH extraction begun. The backpack laser scanner divides the laser measurements into smaller point clouds were each scan rotation defines a point cloud. The result from the backpack scanner shows a correlation between the DBH offsets and the DBH, shown in section 3.3.1. A similar correlation was not found when the same relation was investigated for the handheld laser scanner, and the terrestrial laser scanner. This is shown in Figure 32 and Figure 33.

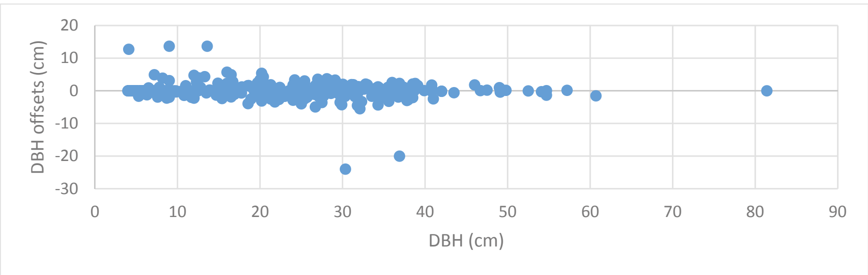

Figure 32. The DBH offsets from the handheld laser scanner.

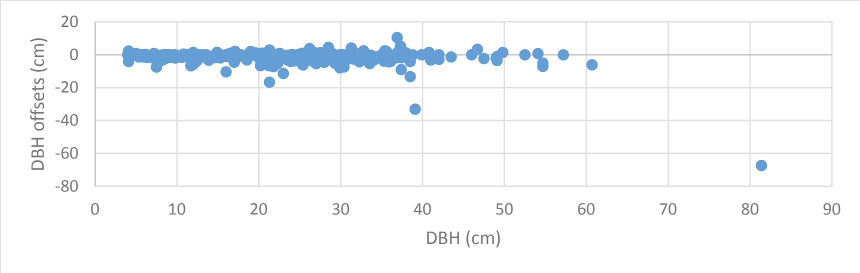

Figure 33. The DBH offsets from the terrestrial scanner

One reason for this lack of bias could be that the backpack scanner calculates the diameter with just a fraction of the complete circle. Under the right circumstances, the potential bias on the diameter estimations described by Forsman et al. [64] will be present. The same situation could also be the case for the terrestrial scanner, but this scanner has 15 times smaller beam divergence compared to the backpack scanner. This makes the system less vulnerable to bias effects on the diameter estimation. The handheld ZEB1 system is a system with a large beam divergence, and a bias effect could be expected. From Figure 32 it is shown that no clear correlation between DHB and DBH offset is present. The handheld data is merged into a common point cloud before the DBH extraction is performed. The effect described by Forsman et al. [64] will only affect the tree stem edge points. The tree stem points between the edges are not affected. Since most of the trees are observed all around the tree stem, there will be observations that are not affected by a false bias surrounding the stem. The points which are affected by the bias will occur as noisy points located further away from the real stem circle.

4.2.3 Scan matching and aided inertial navigation

The third stage was used for indoor survey. The result showed that the tactical graded IMU provided a better pose result than the automotive IMU. This is an expected result. When the automotive pose result was run through the SE-NDT result and fed back into the Inertial processing, the automotive result was at a higher level than the tactical graded result. This shows that a tactical graded IMU can be replaced by an automotive graded IMU if an additional aiding source is added. This is expected and according to Table 2. The goal was that the backpack system should be able to perform within an accuracy level 2-3 according to Table 8. This was not achieved. Commercial backpack versions might be able to achieve an accuracy level 2-3, but this was not tested. The 60 m long corridor is a difficult task for most scan matching methods. With the SE-

NDT method, we experienced a shortening in the trajectory. This shortening might have something to do with the filtering caused by the voxelization. This effect will be more pronounced at higher sample rates. Based on this assumption it would follow that a 3.3 Hz rate, as used in the thesis, was more suitable than the 10 Hz point cloud rate. The 3.3 Hz point cloud had a 1.1 m shortage in the trajectory, and the 10 Hz point cloud had a 2.4 m shortage. This is shown in Figure 34.

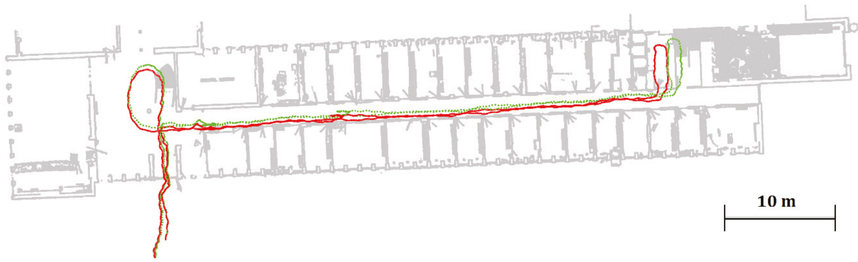

Figure 34. Trajectories from different sample rates. The green dots show the result with 3.3 Hz point cloud, rate and the red dots show the result with 10 Hz point cloud rate. An approximate walking path is shown in Figure 26.

Different voxel sizes ranging from 0.2 m to 0.6 m were tested for the 3.3 Hz solution without discovering any large differences. Other reasons for the shortage in the SE-NDT result might be boresight calibration, lever arm calibration and potential timing issues for the backpack scanner system. The effect described by Forsman et al. [64] could also be a potential reason.

All stages used minimum one IMU and minimum one laser scanner mounted on a backpack baby carrier. The backpack moves and rotate during data collection due to the walking motion. This motion is registered by the IMU. During small time interval the IMU observations can be considered stable, with negligible change in bias or scale. Based on this assumption it was possible to use the IMU observation to ensure that the laser measurements during one scan rotation was realized in the same local frame. Without this possibility, the split point clouds would appear with deformation. The effect of the deformation would depend on the backpack movement like the speed and rotation. Especially in the forest, it is difficult to walk stable without rotations. Deformations in the point cloud is critical for the scan matching and would have a negative effect on the scan matching results.

5. Conclusions

This study has explored the research question on how to rapidly establish a building information model (BIM) for an existing building. Two different aspects have been investigated. The first is related to product specification development and provide a framework for ordering and controlling a laser-based scanning of a building. The second aspect is related to how a laser-based system could rapidly survey a building.

5.1 Product specification development

The research question regarding product specification development was divided into two different aspects. Both aspect is related to the transaction pattern between the customer and producer that is present when a BIM of an existing building is purchased from an external producer. The first aspect focused on the customer request and the second aspect focused on the acceptance actions presented in Figure 2. The customer request is adjusted to the framework used in the “acceptance” actions. The main difference between this study and the standards DIN18710 [13, 14] and USIBD [15] is that this study has a detailed description of the acceptance actions.

The “acceptance” actions are based on well-known and open access standards in the Norwegian geomatics community. The main goal is to document and control the achieved accuracy of the building survey. The first standard is the “GeodataQuality” [18]. This Norwegian standard was used as a framework to evaluate the statistical relevance of the control measurements. The evaluation is based on the following parameters: gross error, standard deviation, and systematic deviation. The product specification has been developed through different stages in this study. Each stage was the result of various commercial BIM projects initiated by different building owners. The final version matched the accuracy indicators in “GeodataQuality,” and the accuracy values were synchronized with DIN 18710 [13, 14]. Additional requirements were added to ensure a fair competition situation. The maximum laser point distance in the laser point cloud is a parameter that directly affects the data capture cost. Another parameter added is the point thickness. This parameter is easily accessible in the point cloud and is a good identifier of gross errors due to errors in the scan location pose estimation. The point thickness method is a simplified version of the control method described by Tang et al. [20] , Anil et al. [16, 21] and the airborne laser industry [22].

The study has proposed a control method for indoor laser scanning projects based on unmarked targets. The method is based on the Norwegian standard

"GeodataProduction" [17]. The standard describes a procedure to control an airborne laser scanning project and controls the accuracy in one dimension, typically in height. The proposed method scales the procedure up to three dimensions. Since the targets are unmarked, it is not necessary to mark the targets before the laser data collection. This makes the control method flexible, and measurements can be performed at any time and anywhere, as long as the building is stable. The proposed procedure requires a network of known points inside or in the building surroundings. The network of known points defines a local coordinate frame, and the captured laser data should be realized in this local coordinate frame. The local network makes it possible to perform control measurements with a reflectorless total station directly through openings in the building, such as windows and doors. The benefit is that closed traverses can be minimized. This improves the reliability and simplifies the control measurements.

The acceptance actions shown in Figure 2 document and control the result. This has the potential to increase the product trust. In the long term, the product trust can increase the possible purposes of the BIM product. A reliable description of the accuracy ensures that the buyer gets the most out of the scanning and the most out of the potential BIM. This is a fundamental step to achieve a multi-purpose BIM [4].

A comprehensive product specification is an important tool to improve the tendering process. With a comprehensive description, the producers have the best possible situation to provide a correct offer to fulfill the customer's desired result. This ensures a fair and reliable competition situation where all producers have the same understanding of the "result requested". The main goal is to ensure that the "desired result" and the "result accepted" is as equal as possible. Another effect of a comprehensive product specification is that the producer has the freedom to select best-suited technology. Typically, if the customer only requires a low accuracy product, the producer can select a technology that is more efficient than a traditional static terrestrial laser scanning. In such a situation, the product specification has the potential to open up for new technology.

The product specification developed is a contribution to the industry. The main goal is that the version 2 of the product specification developed will be accessible for the municipalities in Norway so that the "result requested" and result acceptance methodology can be used by others who would like to establish a BIM for their existing buildings.

5.2 Laser-based system

The second part of the thesis explores how a laser-based system could be used to rapidly survey an existing building. In a low-level accuracy project, the fastest method to survey a building is a human carried system. This method has the potential to survey a building with the same time consumption as it takes to walk through the building. The thesis has explored different aspects of the human carried laser-based system. The focus has been on objects like wall, floor, ceiling, and cylinder shaped objects. In a building environment, cylinder-shaped objects are typical columns and infrastructure like pipes and ventilation.

The new technology proposed in this thesis is a novel laser-based processing method, where the data is collected from instrumentation mounted on a human carried backpack. The development was divided into different stages. The first and second stages were specialized to find cylinder-shaped objects. The practical application was used in a forest environment for the acquisition of ground references data. The data collection provided the tree position and the diameter at breast height. The survey was done within circle shaped sample plots of size 250-500 m^2. The method can be used in combination with airborne laser data for forestry inventory. The novel aspects are related to how the trees are segmented and how the diameters at breast height are estimated without losing precision due to potential reduced position and orientation accuracy. The GNSS signal is typically degraded under the forest canopies due to the reception conditions. Even with relatively coarse positioning and orientation solutions the diameter estimation should not be affected. This was possible because the laser data were divided into limited time frames determined by the lasers scan rotations. An additional novelty is related to the trees position. The position was estimated directly without any additional land surveying. This was done using a GNSS aided inertial navigation system in combination with an iterative closest point algorithm and loop closure. The proposed laser scanning methods were compared with two other laser-based measurement systems in a full-scale test with seven different sample plots. The other laser-based systems were ZEB1 from Geoslam [2] and Faro Focus 3D x130 [25]. The results from all three laser-based system were compared to manual measurements performed with a traditional caliper. The fastest and most accurate method was the proposed laser scanning method. After a linear adjustment of selected sample plots, the mean difference was 0.0 cm, and a root mean square of 1.8 cm. In addition, the method had the largest amount of detected trees with 87.5%. However, the proposed method had also the highest amount of false trees. The tree positions were slightly degraded, but the position accuracy should be acceptable for many forestry inventory purposes.

The third stage was constructed for an indoor environment. An automatic classification routine was developed to classify walls, ceilings, floors and cylinder-shaped objects. The building objects with flat surfaces were given surfaces with corresponding normal vectors. The third stage used two differently graded inertial measurement units (IMU) to get an impression of the needed quality. The result shows that the tactical graded IMU performed significantly better than the automotive graded IMU. At the same time, the automotive graded system was able to perform at a higher level than the tactical graded IMU when it received support from scan matching. The scan matching method is called semantic assisted normal distribution transform and uses each point's floorness, ceilingness and wallness to support the process. The scan matching result provided sequential position increment with corresponding covariance. This was fed back into the aided inertial processing. This novel approach is able to detect scan matching failures and prevent the solution to shift.

5.3 Recommendations for further studies and implementations

The recommendations for further studies are divided into product specification and laser-based system. A product specification for an indoor terrestrial laser scanning projects is an essential tool for the buyer to achieve the best possible cost-benefit ratio, a multiple purpose BIM, a fair competition situation in the tender process, and to opens up for new technologies. It is important to continue evaluating the transaction pattern between the two parties to ensure the potential of the product specification and to ensure that the requested product match the accepted product.

This thesis has the potential to contribute to the industry with a foundation for further standardizations and product specifications for building survey. As a first step, six municipalities in Norway have adopted the proposed product specification. In the long term, it has the potential to take the step into a national or international level.

For a laser-based system, it would be natural to further investigate different laser scanners. New developments have been made on the sensor side that could make a huge contribution to the stability of the scan matchings algorithm. Especially small laser sensors from Velodyne where the number of laser channels have increased from 16 to 128. This has the potential to survey the full environment at a high frequency, with a high level of details. This is a perfect situation for scan matching. Another possible improvement would be to add new instruments, according to Table 2. A visual odometer would be very useful. Due to the high image frame rate, they seem to capture the movement with high reliability. To get the full benefits of the system, the result should be merged into the inertial processing. This requires the covariance from the visual odometer calculation. If the system is tuned and calibrated properly, and the time synchronization is controlled, it has the potential to improve the final pose calculation. In the end, both the visual odometer and the scan matching result could be fed into the aided inertial processing. The benefit is that each measurement method has positive and negative qualities. In a situation where the positive and negative effects between the different methods do not overlap, the aided inertial processing is in a position to highlight the best source for each specific situation. The final goal is to feed in observations with sufficient accuracy to perform a good state estimation in the tightly coupled Kalman filter used in the aided inertial processing. This has the potential to give the best possible pose estimations.

In the third stage, the automatic point classification created surfaces for walls, floors, and ceilings. This is an excellent foundation to create real building objects and could be further developed to create a full BIM at the proposed LoD 250.

In this study every 3rd point cloud was used in the SE-NDT process. In further developments, it will be natural to investigate how every point cloud could be used without losing precision. This might be done by matching not only the sequential point cloud, but also point clouds with different time intervals. Such systems could possibly be extended to handle loop closure situations. The result could be realized and solved in an equation system and fed back into the final inertial processing.

References

1. Azhar, S., *Building information modeling (BIM): Trends, benefits, risks, and challenges for the AEC industry.* Leadership and management in engineering, 2011. **11**(3).
2. Geoslam. *GeoSlam Zeb-1*. [cited 2017 16th november]; Available from: https://geoslam.com/hardware/zeb-1/.
3. Bell, M., D. Gausebeck, and M. Beebe, *Capturing and aligning three-dimensional scenes*, U.S. Patent, Editor. 2016, Matterport, Inc., Mountain View, CA.
4. Hjelseth, E., I. Oveland, and I. Maalen-Johansen, *Framework for enabling scan to BIM services for multiple purposes - Purpose BIM*, in *20th World Building Congress*. 2016, Tampere University of Technology: Tampere (Finland).
5. Fischler, M.A. and R.C. Bolles, *Random sample consensus: a paradigm for model fitting with applications to image analysis and automated cartography.* Communications of the ACM, 1981. **24**(6).
6. Biber, P. and W. Straßer. *The normal distributions transform: A new approach to laser scan matching*. in *IROS*. 2003.
7. Labbe, M. and F. Michaud. *Online global loop closure detection for large-scale multi-session graph-based SLAM*. in *Intelligent Robots and Systems (IROS 2014), 2014 IEEE/RSJ International Conference on*. 2014. IEEE.
8. Dietz, J.L., *What is Enterprise Ontology?* 2006: Springer.
9. ISO, *ISO 29481-1:2016, Building information models, Information delivery manual, Part 1: Methodology and format*. 2016.
10. ISO, *ISO 29481-2:2012, Building information models, Information delivery manual, Part 2: Interaction framework*. 2012.
11. Oveland, I., I. Revhaug, and I. Maalen- Johansen, *Laser scanning, product specification and Level of Accuracy evaluation.* Kart og Plan, in revision, 2018.
12. Oveland, I., *Evaluation of product specification for terrestrial laser scanning to extract a building information model, to be submitted*. 2019.
13. DIN18710-1:2010-09, *Engineering survey*, in *Part 1: General requirements,*. 2010, Deutsches Institut für Normung: Beuth Verlag GmbH, 10772 Berlin, Germany.
14. DIN18710-2:2010-09, *Engineering survey*, in *Part 2: Site surveying, .* 2010, Deutsches Institut für Normung: Beuth Verlag GmbH, 10772 Berlin, Germany.
15. USIBD, *USIBD Level of Accuracy (LOA) Specification Guide*, in *Document C120 - C320, Version 2.0*. 2016, U.S. Institute of Building Documentation.
16. Anil, E.B., et al., *Deviation analysis method for the assessment of the quality of the as-is Building Information Models generated from point cloud data.* Automation in Construction, 2013. **35**.
17. Kartverket. *Produksjon av basis geodata, version 1.0.* Standarder Geografisk Informasjon 2015 01.03.2015; Available from: https://kartverket.no/geodataarbeid/Standarder/Standarder-for-geografisk-informasjon/.

18. Kartverket. *Geodatakvalitet, version 1.0*. Standarder Geografisk Informasjon, 2015 01.01.2015; Available from: https://kartverket.no/geodataarbeid/Standarder/Standarder-for-geografisk-informasjon/.
19. EN-ISO19157, *geographic information-Data quality*. 2013, International Standards Organisation.
20. Tang, P., et al., *Efficient and effective quality assessment of as-is building information models and 3D laser-scanned data*, in *Computing in Civil Engineering (2011)*. 2011.
21. Anil, E.B., et al. *Assessment of the quality of as-is building information models generated from point clouds using deviation analysis*. in *Three-Dimensional Imaging, Interaction, and Measurement*. 2011.
22. Klang, D. and H. Burman. *Airborne Laser Scanning, an Efficient Revision Procedure for the Swedish Digital Elevation Model*. in *Proceedings of the 7th Conference on Optical, 10*. 2005.
23. Brown, R.G. and P.Y. Hwang, *Introduction to random signals and applied Kalman filtering*. Vol. 4. 2012: john Wiley & Sons, Inc.
24. Liang, X., et al., *International benchmarking of terrestrial laser scanning approaches for forest inventories.* ISPRS Journal of Photogrammetry and Remote Sensing, 2018. **144**.
25. Focus, F.L.S., *3D X-130.* FARO Technologies Incorporation, USA.
26. Leica. *Leica Cyclone REGISTER*. [cited 2019 14. January]; Available from: https://leica-geosystems.com/products/laser-scanners/software/leica-cyclone/leica-cyclone-register.
27. *Velodyne Lidar, PUCK, VLP16*. [cited 2017 01.08]; Available from: http://velodynelidar.com/vlp-16.html.
28. Ouster. *Ouster*. [cited 2018 23. August]; Available from: https://www.ouster.io/.
29. 3DLaserMapping. *Mobile indoor mapping using world leading 3D Geospatial SLAM technology*. [cited 23. July 2018]; Available from: https://www.3dlasermapping.com/indoor-mapping/.
30. CSIRO. [cited 23. July 2018]; Available from: https://www.csiro.au/.
31. Bosse, M. and R. Zlot. *Continuous 3D scan-matching with a spinning 2D laser*. in *Robotics and Automation, 2009. ICRA'09. IEEE International Conference on*. 2009. IEEE.
32. Bosse, M., R. Zlot, and P. Flick, *Zebedee: Design of a spring-mounted 3-d range sensor with application to mobile mapping*. IEEE Transactions on Robotics, 2012. **28**(5).
33. Nocerino, E., et al. *Investigation of indoor and outdoor performance of two portable mobile mapping systems*. in *Videometrics, Range Imaging, and Applications XIV*. 2017. International Society for Optics and Photonics.
34. Kaarta. [cited 2018 23. July]; Available from: http://www.kaarta.com/.
35. Holland, D., et al., *The Topographic Data Deluge–Collecting and Maintaining Data in a 21st Century Mapping Agency.* The International Archives of Photogrammetry, Remote Sensing and Spatial Information Sciences, 2016. **41**.

36. Vexcel. *UltraCam Panther*. [cited 2018 23. July]; Available from: http://www.vexcel-imaging.com/ultracam-panther/.
37. Nistér, D., O. Naroditsky, and J. Bergen. *Visual odometry*. in *Computer Vision and Pattern Recognition, 2004. CVPR 2004. Proceedings of the 2004 IEEE Computer Society Conference on*. 2004. Ieee.
38. Vassena, G. and A. Clerici, *Open pit mine 3d mapping by TLS and digital photogrammetry: 3D model update thanks to a slam based approach.* International Archives of the Photogrammetry, Remote Sensing & Spatial Information Sciences, 2018. **42**(2).
39. Gexcel. *Heron, Wearable mobile mapping*. [cited 23. July 2018]; Available from: https://gexcel.it/it/soluzioni/heron-mobile-mapping.
40. 3DLaserMapping. *ROBIN – The World's Most Flexible Mobile Mapping System*. [cited 2018 23. July]; Available from: https://www.3dlasermapping.com/robin-mobile-mapping-system/.
41. Riegl. *Riegl, Laser measurments systems*. [cited 2018 24. July]; Available from: http://www.riegl.com/.
42. Riegl. *Riegl VUX-1HA*. [cited 2018 23. July]; Datasheet VUX-1HA]. Available from: http://www.riegl.com/uploads/tx_pxpriegldownloads/DataSheet_VUX-1HA__2015-10-06.pdf.
43. AiA, *Document G202 TM Project BIM Protocol*. 2013, the American Institute of Architects
44. *EBA - Entrepenørforeningen Bygg og Anlegg, RIF - Rådgivende Ingeniørers Forening, Arkiktektbedriftene. MMI – Modell Modenhets Indeks*. Available from: https://www.eba.no/globalassets/dokumenter/mmi-utvalget/mmi-modell-modenhets-indeks.pdf.
45. Reinhardt, J.B., J, *Level of Development (LOD) Specification Part I commentary*, in *For building infromation moedels and data*. 2018, BIMForum.
46. Soininen, A., *TerraScan User's Guide*, in *For the 32-bit version of TerraScan*. 2016, Terrasolid Ltd.
47. Business_Wire. *Velodyne LiDAR Opens Megafactory in San Jose for Large-Scale Production of 3D LiDAR Sensors*. 2017 [cited 2018 15. August]; Available from: https://www.businesswire.com/news/home/20170117005644/en/Velodyne-LiDAR-Opens-Megafactory-San-Jose-Large-Scale.
48. Masiero, A., et al., *Comparison of low cost photogrammetric survey with TLS and Leica Pegasus Backpack 3D models.* International Archives of the Photogrammetry, Remote Sensing & Spatial Information Sciences, 2017. **42**.
49. Oveland, I., et al., *Automatic Estimation of Tree Position and Stem Diameter Using a Moving Terrestrial Laser Scanner.* Remote Sensing, 2017. **9**(4).
50. Applanix. *APX-15 UAV*. [cited 2018 18. July]; Available from: https://www.applanix.com/downloads/products/specs/APX15_DS_NEW_0408_YW.pdf.
51. Oveland, I., et al., *Comparing Three Different Ground Based Laser Scanning Methods for Tree Stem Detection.* Remote Sensing, 2018. **10**(4).

52. SBG_Systems. *Ellipse 2 Series, Miniature high performance Inertial Sensors*. [cited 2018 18. july]; Available from: https://www.sbg-systems.com/docs/Ellipse_Series_Leaflet.pdf.
53. Terratec. *GNSS/INS post processing software*. Terrapos; Available from: https://www.terratec.no/terrapos.
54. Northrop_Grumman. *LN-200 FOG Family*. [cited 2018 12. june]; Available from: http://www.northropgrumman.com/Capabilities/LN200FOG/Documents/ln200.pdf.
55. Applanix. *POS AV*. [cited 2018 18. July]; Available from: https://www.applanix.com/downloads/products/specs/2017_POSAV_One_Trimble_web.pdf.
56. Fischler, M.A. and R.C. Bolles, *Random sample consensus: a paradigm for model fitting with applications to image analysis and automated cartography*, in *Readings in computer vision*. 1987, Elsevier.
57. Mathworks. *pcfitplane, Fit plane to 3-D point cloud*. [cited 2019 14. January]; Available from: https://se.mathworks.com/help/vision/ref/pcfitplane.html.
58. Torr, P.H. and A. Zisserman, *MLESAC: A new robust estimator with application to estimating image geometry*. Computer vision and image understanding, 2000. **78**(1).
59. Bergström, P. *Iterative Closest Point Method*. 2016 [cited 2016 3. Nowember]; Available from: https://se.mathworks.com/matlabcentral/fileexchange/12627-iterative-closest-point-method.
60. Zaganidis, A., et al. *Semantic-assisted 3D Normal Distributions Transform for scan registration in environments with limited structure*. 2017. IEEE/RSJ.
61. Bucher, I. *Circle fit*. 2004 [cited 2016 15.12]; Available from: https://se.mathworks.com/matlabcentral/fileexchange/5557-circle-fit/content/circfit.m.
62. Pratt, V. *Direct least-squares fitting of algebraic surfaces*. in *ACM SIGGRAPH computer graphics*. 1987. ACM.
63. Gander, W., G.H. Golub, and R. Strebel, *Least-squares fitting of circles and ellipses*. BIT Numerical Mathematics, 1994. **34**(4).
64. Forsman, M., et al., *Bias of cylinder diameter estimation from ground-based laser scanners with different beam widths: A simulation study*. ISPRS Journal of Photogrammetry and Remote Sensing, 2018. **135**.
65. SICK. *LMS200/211/221/291 Laser Measurement Systems*. [cited 2018 14th December]; Available from: https://cdn.sick.com/media/docs/3/33/933/Technical_information_LMS200_211_221_291_Laser_Measurement_Systems_en_IM0027933.PDF.
66. Standard_Norge, *NS 3580:2015 Site grids for constrution, Distribution of responsibility, quality acceptance requirements and methods*. 2015.
67. Owen, R., et al., *Research Roadmap Report CIB Integrated Design and Delivery Solutions (IDDS)(CIB Publication 370). International Council for Building*. 2013, ISBN 978-90-6363-072-0. http://site.cibworld.nl/dl/publications/pub_370.pdf.
68. Kartverket. *Hva skal FKB-data være i fremtiden?* Geovekst-forum 2018 29.-30. may; Available from:

https://www.kartverket.no/globalassets/arkiv/kart/geovekst/geovekst-forum/mars-2018/sak-5_18-hva-skal-fkb-vare-i-framtiden---kvalitetsplan.pdf.
69. kartverket. *CPOS - Kvalitet*. 2018 [cited 2018 23. August]; Available from: https://www.kartverket.no/posisjonstjenester/cpos/.
70. Kartverket, *Produktspesifikasjon FKB-Bygning 4.6*. 2016, The Norwegian Mapping Authority.

Appended Papers (individual page numbering)

PAPER I

Framework for enabling scan to BIM services for multiple purposes – Purpose BIM

Eilif Hjelseth,
Department of Civil Engineering and Energy Technology,
Oslo and Akershus University College of Applied Sciences
email: Eilif.Hjelseth@hioa.no

Ivar Oveland,
Department of Mathematical Sciences and Technology,
Norwegian University of Life Sciences
email: ivar.oveland@nmbu.no

Ivar Maalen-Johansen
Department of Mathematical Sciences and Technology,
Norwegian University of Life Sciences
email: ivar.maalen@nmbu.no

Abstract

Technology for scanning is in rapid development. More advanced solutions are available for lower cost of scanning, and simple methods are available for everyone. Use of a building information model (BIM) for facility management is gaining interest, there is still a large number of existing buildings without BIM representation. As-built drawings are not updated or unreliable. However, establish a BIM for an existing property is often costly, and hard to utilize for new purposes. Time and cost effective methods for flexible use is therefore wanted. Integrated Design and Delivery Solutions is used as theoretical frame for this study. The analysis explores the steps in the process of scanning and modelling, collaboration between people in establishing the BIM, and further use for multiple purposes within facility management. An overview of technology presents in relation to process and people to give support for ordering commercial scanning and BIM services. A scan to BIM project of an old apartment building is used as case for demonstrating a framework for "Purpose BIM". This framework combines relevant technology, processes and personal resources for flexible and stepwise processes of ordering scan to BIM services. An outcome of this approach can be add-on services that can enable reuse previous work. This can result in extended use of BIM to multiple purposes in facility management.

Keywords: Purpose-BIM, process specification, product specification, scanning technology

1. Introduction

There is an increasing interest for integrating laser scanning as basis for establishing building information model (BIM). Laser scanning technology is in rapid development, likewise development of BIM software. Detailed scanning of heritage buildings is often presented as an example of the potential of scan to BIM, but most buildings are ordinary and need a more simple approach to maximize the cost/benefit relation. Even if there is a lot of available theology for scanning and modelling a BIM, the projects are often motivated by solving one single task, by use of one technological approach, often by one single provider. Development of technology contributes to reduced cost, but the traditional processes have limited flexibility and the cost must be covered by only one use-case, or benefit. Often will small changes in requirements to the BIM – result in repeating almost the entire scan to BIM process. The impact is limited establishment of BIM for existing facilities, despite the benefits for using BIM for multiple purposes within facility management.

There is an increased number of papers regarding integration of BIM, based on various methods for laser scanning in BIM related conferences. This can be illustrated by activity at following BIM related conferences; the BIM 2015 conference had one entire sessions about BIM and GIS integration (Breibba et al., 2015), and the CIB-W78 IT in construction conferences have included papers which cover solutions where BIM can be established based on laser scanning (Issa et al, 2014 and Beetz et al. 2015). This integrated focus has also reaches standardization, where ISO/ TC 211 about GIS and ISO/TC58/SC13 about BIM have joint workshop (Kim, 2012). The general focus of research is on issues related to technical interoperability, demonstration of laser scanning hardware and use of software for transforming point clouds into 3-D geometrical models and BIM.

The outcome of this concept paper is useful for building owner / facility manager (client) for design of specification or requirement for ordering scan and BIM services – especially when the purpose is not limited to only one purpose. Expected impact is increase return of investment. The outcome for service providers of scan and BIM services is in improved accuracy of deliverables in relation to client current and future needs. The proposed framework is called "Purpose BIM" and includes all elements from preparing of the project, capturing information by laser scanning, processing of information into BIM, and various ways of presenting results for different users and use cases.

2. Technology overview

2.1 Overview of methods and processes for scan to BIM solutions

The process from the decision to capture geometrical data describing the building to establish a BIM for solving one or more purposes consists of several steps. To be aware of these steps and the options within each steps can make it possible to order according to the principles of "purpose BIM", see figure 1. This is possible even if purpose is unknown or multiple.

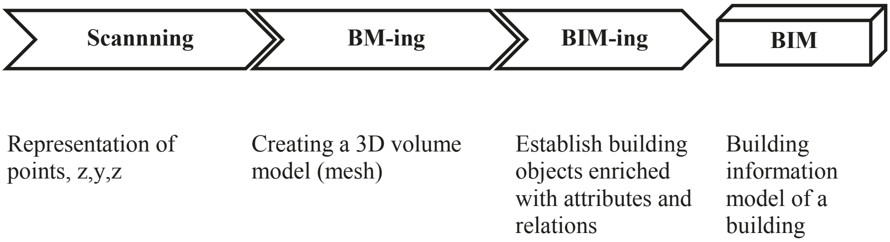

Figure 1: Overview, main stages in the scan to BIM process

Awareness of these steps, and potential between the steps and within each step, is one of the main motivation for this study, and will be explored later on in this paper. Use of the "Purpose BIM" is presented as a framework for an improved ordering of services to enable flexible use and options for future use with positive cost/benefit of the BIM model.

2.2 Overview of capturing geometrical data

Today there is a large variety of instruments used to create a BIM for an existing building. In this paper, we will refer to this as Interoperable Technologies, with reference to IDDS (2013) presented later in this paper. The different technics are mainly:

- Use the original building drawings (both digital and paper based)
- Tape measure (ruler or handheld laser)
- Static point based laser measurement (e.g. "Flexijet" or total station)
- Static laser scanner (terrestrial laser scanner mounted on a tripod)
- Laser scanner and other instruments mounted on a moving platform

We focus on the laser-based methods. These approaches have developed dramatic in recent years and have changed the way we capture indoor data. The "static point based laser measurement" approach use the concept "less is more". This technique has a direct link into the modelling software, e.g. by use of Flexijet. The modelling and enrichment of the model is done on site. Which in many cases has a big advantage. On the other end of the scale, you find "laser scanner and other instruments mounted on a moving platform" which use a "more is less" approach. The goal is to measure as much as possible and also the same objects as often as possible. This method has taken technics from the robotics into use. The technique is called Simultaneous localization and mapping (SLAM). This is the key concept in autonomous robotics. The robot use SLAM to create a map of the surrounding and at the same time place itself in the map. This concept is now used by many manufactures of indoor measurement systems. These systems are special made to rapid create a building model. These techniques give new opportunities and new challenges. One problem with the more is less approach is that you also collect information that might be sensitive for the people living or working there. In such a situation, the data need to be handled with care. Different techniques have different accuracy capability and the performance improve rapidly with time. We have manly talked about laser scanners, but new software can put the traditional photogrammetry into new life. Examples of software are Autodesk Memento (https://memento.autodesk.com/about) and Agisoft photoscan (http://www.agisoft.com/).

2.3 Software for processing and enriching of scanned data

There are many different software, that can be used to perform the modelling work, adding attributes and relations to the building objects. Typically software is EdgeWise Building™ from ClearEdge3D (www.clearedge3d.com/), Pointsence for Revit from Faro (http://faro-3d-software.com/) and RECAP from Autodesk (http://www.autodesk.com/). It is also relevant to mention the DURAAK project (http://duraark.eu/).

To fulfil a real BIM the collected measurement of a building has to be enriched. This process is called Integrated Processes (see figure 2) in this paper (BIM-ing). To enrich the measurements different software solutions can be used. Some software are standalone solution, but most are plugins into typical architectural software like Revit from Autodesk, Archicad from Graphisoft and Microstation from Bentley. One important difference between the software solutions is the level of operator interactions, which is needed to create the BIM. This is often a time and cost consuming operations. Another difference is how the building objects are placed related to the point cloud. In most cases, the operator can select different settings, which will place the object based on Gaussian distribution, best fit or with different kind of assumption. Typical assumption is that two walls should meet perpendicular and that a wall should always be vertical.

3. Framework for scan to BIM

The dominating focus when exploring scan to BIM has been technology, which is presented in a systematic way. Other organisational issues are often very randomly explored and presented. It is therefore a need for a framework that include technology in a systematic way. In this respect is the Integrated Design and Delivery Solutions (IDDS, 2013) as theoretical framework. IDDS can be regarded as simplification of the socio-technical theory (Bostrom & Heinen, 1977) which is adapted to the AECOO construction industry. The IDDS framework is developed by the International Council for research and Innovation in Building and Construction (CIB) in order to optimize construction projects. IDDS is a powerful framework to explore and understand interactions between different imperatives. The three imperatives of the IDDS are illustrated in figure 2.

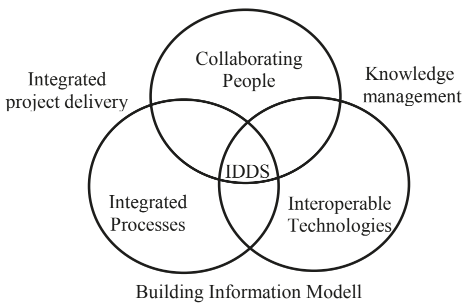

Figure 2: The three imperatives of IDDS (2013), figure simplified by the authors

In our study of the process of establishing a BIM for multiple purposes within facility management, we have used the model in figure 3 to describe the collaboration. Figure 4 illustrat the current situation in the case used in this study.

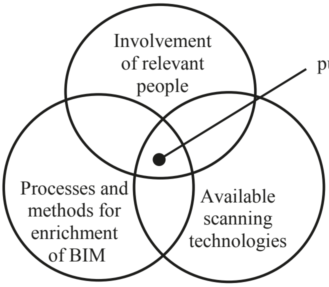

Figure 3: Identifying imperatives for multiple purpose BIM based on IDDS

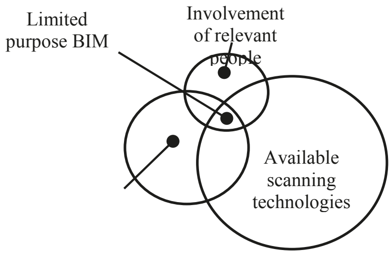

Figure 4: Example of unbalanced IDDS and limited purposes of scan to BIM

The different imperatives are in our case exemplified by the following content:

- Involvement of relevant people (Collaborating People): architects, engineers, land surveyors, BIM specialists, landlords, residents,…
- Available scanning technologies (Interoperable Technologies): drawings, tape measure, laser scanner, total station, Flexijet, rangefinder, camera,…
- Processes and methods for enrichment of BIM (Integrated Processes): Software and methods for creating BIM.

The size of each circle can be changed due to current resources, e.g. the amount of relevant and available technology or the number of collaborating people. The relative position of the circles may also change according to the interaction in between the imperatives. Examples of this are the degree of harmonization of software and hardware or the maturation of new processes in the user communities. The resulting size of the centre region can then be regarded as an indicator for the possibilities for success. Small circles with large internal distance make it difficult to succeed. An example with very good harmonization of hardware and software, but with a limited number of skilled and collaborating people is shown in figure 4. The two lower circles are highly overlapping in figure 4. The problem is that the circle representing the relevant people purpose is small. The consequence is that command area for all three circles is very limited compare to figure 2 and 3. This means that the resulting BIM has very limited purposes.

4. Framework for Purpose BIM

Our evaluation of the case study is that an ordering guide would be useful for the collaborating people. The goal of an ordering guide is to maximize the common area between collaborating people, technologies and processes. The purpose is to help the buyer to order the product, that has the potential to give the best cost benefit ratio. A spin off to this is that the provider of BIM easy can understand the customers demand and expectation. In the early days of airborne laser, the industry had a problem. The buyers of airborne laser data had a poor description of their expectations. They had very different knowledge about airborne laser data and different approaches to control the result. The consequence was that some suppliers took the benefit of this and delivered data with bad quality, knowing that the probability to be discovered was minimal. After some years, the buyers became more professional and establish detailed specification and methods to control the result. The result of the new specification was that the quality of the products became more even. Another important effect was that the different providers could compete based on the same understanding of the customers expectations.

The first step in our framework is to establish a development plan with focus on collaborating people. This will decide which persons who have interest in the project and who should have access to the result. Another aspect is who should continue to work with the BIM to ensure that it is up to date. When the BIM is up to date, it is a "Living BIM". The second task is to get an overview of the different challenges the collaborating people have and how BIM can be used as a tool to solve their problem. Based on this the accuracy level of the data capture can be established.

Table 1: Accuracy Levels of Data Input to further proceeding BIM model

Accuracy level	**Level 1**	**Level 2**	**Level 3**
Description	Rehabilitation	Area information	Management/develop
Relative accuracy *	0.003 m	0.01 m	0.03 m
Maximum average deviation *	0.01 m	0.04 m	0.10 m
Maximum deviation between measurement and model (at 1 meter above the floor)	0.01 m	0.03 m	0.10 m
Modelling assumption	Exact modelling. The object should be placed on the average location of the point cloud	Exact modelling, but walls can be straighten up to be perpendicular to the floor or celling	Walls can be straighten up to be perpendicular to the floor, ceiling and walls

* Calculated on a 0.2 x 0.2 meters surface

The accuracy level give the BIM provider an accuracy expectation to the final product. Both data capture and the modelling work is covered. Based on the accuracy level the provider can select the most cost efficient method to capture the data. One of the important messages in Table 1 is that you do not need a level 1 scanning if you during modelling will straighten up walls, floors and ceiling to ensure that they are perpendicular. This count if your intention is to use your model in further work and not the point cloud.

Table 2: Information contend in BIM model, gives an overview of 3 different level of detail

Level of Detail (LOD)	**Class A**	**Class B**	**Class C**
Description	*Full BIM*	*Slim BIM*	*BM (overview)*
Relative content of information in BIM	Volume model, standard objects with attributes and relations	Volume model, standard objects *Defined (limited) information*	Volume model

The next step is the integrated processes. In this step, the measurements become a real BIM. Again, it is important for the buyer to have a conscious relation to the content of the BIM. A simple volume model is cheap, and this is classified as BIM class C. If you add standard objects, it is more expensive and more useful. Finally, if you add attributes and relations you get a full BIM and BIM class A.

Table 3: Framework for Purpose BIM

Accuracy level / **BIM class**	**Level 1**	**Level 2**	**Level 3**
Class A	Multiple purpose (Expensive)		Limited purpose (Moderate price)
Class B			
Class C	Limited purpose (Moderate price)		Single purpose (inexpensive)

Table 3 illustrate the relation between the cost and applicability based on the criteria accuracy level and BIM classes. The highest accuracy product is level 1. If you combine this with the BIM class A, you get the most expensive product. BIM class A gives you a BIM with standard objects with attributes and relations. On the other end of the scale, you find accuracy level 3 and BIM class C. This is the cheapest product with less accuracy and no building objects. The accuracy level 1 has the highest flexibility. With high flexibility, you have the opportunity to change your BIM from an accuracy level 1 to accuracy level 3. You also have the opportunity to change from BIM class A to C and vice versa. If you create your BIM with the accuracy level 3, you are not able to change you BIM to the accuracy level 1 without new measurement, but the BIM class can be change. This means that accuracy level 3 has a lower flexibility than accuracy level 1.

Table 4: Framework for Purpose BIM examples

Accuracy level / BIM class	Level 1	Level 2	Level 3
Class A	Rehabilitation		Facility management
Class B			
Class C	Absolute documentation of geometry		Volume sketch and planning

Table 4 illustrate which purposes, which accuracy level and BIM class are suitable for some example purposes.

5. Examples from the case study

The case study used in this paper is based on a project in Oslo, Norway. The building was built in 1890 and has a co-ownership organization with 16 different sections. A board selected by the co-owners controls the building. An important aspect was distribution of cost related to the total area of each section. The area of each section was unknown. It was disused to use the existing drawings to create the BIM. The problem was that the drawings where old and did not give a correct picture of the areal situation. Another problem was that the basement was not present in the drawings. The boarder also had maintenance tasks waiting ahead where they would like to using a BIM. The dream was to link the maintenances history, the today's status and scheduled maintenance directly to building objects in the model. Additionally they needed a fire and evacuation plan. They also had a project where they needed to control the chimneys. Based on these needs the scan to BIM project was started. The Norwegian Building Authorities was interested in the project and decided to finance the project. The company Rendra won the project after public announcement. Rendra has developed an application for interoperability in construction projects based on BIM. Sweco BIMlab consulting engineers performed the measurement and modelling of the building. The data capture and modelling was scheduled to take 5 weeks. The static point based laser measurement called Flexijet 3D 4ARCHITECTS was used for data capture. The system is directly linked to Archicad, which means that the BIM is created directly on site. The total budget for the project was 200 000 NOK (approximately 22.000 €).

The result from the project was good. The boarder got a BIM they could use for area calculation of each section, storage room in the basement and storage room in the attic. This solved an ongoing conflict in the basement. From the BIM they can extract drawings like fire and escape plans, extract volume of the walls, framework to store information about the past, present and further for each building object. The new established BIM is a good starting point to establish a maintenance plan (DIBK, 2015).

In the evaluation of the BIM one of the section owners discovered that his apartment was 10 m2 larger than the report form the latest valuer report (DIBK, 2015; chapter 4.6). It is likely that the areal in this report has been calculated with a tape measurement device, manual or digital. It is therefore likely to claim that the BIM provide the correct area calculation. The price pr. square meter in this area is higher than 50 000NOK (5400 €). This has a big influence on the value of the property.

The experience from the project shows that it is very time consuming to arrange access to all the different sections. Sweco BIMLab performed the measurement and informed that 25% of the time was used just to get access to the different sections DIBK (2015, chapter 4.7). In the evaluation of the result, the board claim that the model has a higher quality and richness than they actually needed (DIBK, 2015; chapter 4.3). There are for instance more objects present than they expected. This model is therefore a good opportunity to use the BIM for more purposes than initially intended.

We have concluded that it would have been beneficial to use a data capture method, which use less time on site and more time in the office. The main reason is that approx. 25% of the time was spent on getting access to the different sections. Flexijet scanning contain only what has been presented in the model. There is no extra data for further processing. This makes the method sensitive for missing registrations and it is difficult to document the quality of the model.

Table 5: Identification of possible purposes for the example case

Accuracy level / BIM class	Level 1	Level 2	Level 3
Class A	No Possible expansion	No Possible expansion	No Possible expansion
Class B	No Possible expansion	Case study	Possible expansion
Class C	No Possible expansion	Possible expansion	Possible expansion

The case study have an accuracy level 2 and a BIM Class B. Table 5 illustrate which direction it is possible to expand the BIM. The main reason for this limitation is the Flexijet method where you collect limited amount of data. It is not possible to enrich the model without revisit the building. If a “more is less approached” had been use it might have been possible to enriched the BIM without revisit the building. Then all BIM classes with accuracy level 2 and 3 would have been an option for expansion. If we assume the same starting point. This is illustrated in Table 6.

Table 6: Possible purposes for the example case collected with a "more is less approach"

Accuracy level / BIM class	Level 1	Level 2	Level 3
Class A	No Possible expansion	Possible expansion	Possible expansion
Class B	No Possible expansion	Case study	Possible expansion
Class C	No Possible expansion	Possible expansion	Possible expansion

6. Discussion

This concept paper is based on a literature overview of available technologies within hardware for scanning and software for processing captured data, in addition to use a real project as case. The practice of today is driven by use of technology offered by the selection of services from the scan to BIM provider. The proposed "purpose BIM" framework intent to enable an overview of applicable technology for capturing data, and by processing the data into BIMs applicable for multiple purposes. Overview of technology, process and competency (with reference to the trinity in the IDDS framework) enables the building project owner to manage the scan to BIM process by ordering or purchasing process. This study is therefore not a study of selecting the best technology, but how different technologies can be combined to enable a potential for multiple purposes in the future based on reuse of previous work (normally done at low additional cost as supplement to the primary job, e.g. a cloud scanning, when doing point scanning).

A real case was used as example for the scan to BIM process to explore how the "purpose BIM" can be applied. However, further empirical studies are needed to assess the reliability of the framework, in addition to further detailing and guidance. We have focused on accuracy level in the data collection, accuracy in modelling and the level of detail in the building objects. Especially the level of detail is general and need further detailing. In a comprehensive product specification, it will be necessary to have a full list of objects, which should be included in the model. It is also necessary to define which attributes and relation each object should have. In a complex building, this list may be long and complicated. If possible, it will be an advantage to create general rules instead of a complexed list. The comprehensive product specification is important to make sure that the model is created and enriched according to the contractor's expectation. Additionally the providers have the possibility to calculate the cost more precise. This will contribute to a more fair competition situation where the provider know precisely what to deliver.

7. Conclusions

This study has introduced the “Purpose BIM" as a framework to support flexible ordering of services to solve multiple purposes at positive cost/benefit. This framework structure the ordering processes to combinations off accuracy level from scanning related to BIM classes for processing of scanned data for defined purposes and potential purposes.

An overview of technology and services is presented and illustrates possibilities for a more flexible process. Detailing the overview by current commercial solutions is recommended before practical use. On the other side, we see that the Purpose BIM as a framework will become more relevant to enable increased numbers of solutions by combining technology and processes and personal resources. An important aspect is to break-down into small work-packages or services that can act as options for further processing and enabling of new purposes.

Development of technology will increase the possibilities to combine various technologies at low cost and enable possible multiple use. This will be a key factor to make it common to use BIM in the facility management. With lower prices and flexible processes, the purposes can be extended to purposes we have not thought about or minor tasks, which normally are taken care off in a manual way. One key aspect in this framework is to set up development and feasibility plan to ensure a multiple purpose BIM. Another key aspect is to use the purpose BIM framework to select technology and process to maximize the cost /benefit ratio.

References

Beetz, J., Berlo, L., Hartmann, T., Amor, R. & Vries, B. (2015). CIB W78 IT in Construction conference, Eindhoven, The Netherlands, October 27th -29th 2015, Eindhoven, The Netherlands. http://cib-w78-2015.bwk.tue.nl/

Bostrom, R. P., & Heinen, J. S., (1977). MIS problems and failures: A socio-technical perspective, MIS Quarterly, Vol. 1, No. 3, pp. 17-32. http://misq.org/cat-articles/mis-problems-and-failiures-a-socio-technical-perspective-part-i-the-causes.html

Breibba, C.A., Mahdjoubi, L. & Laing, R. (2015). BIM 2015 - Building Information Modelling (BIM) in Design, Construction and Operations, 626pp WIT Press, Print ISBN: 978-1-84564-914-2; eISBN: 978-1-84564-915-9. Conference in Bristol, UK, September 9th – 11th 2015. http://www.wessex.ac.uk/conferences/2015/bim-2015

DIBK (2015). “Bruk av BIM i borettslag og sameier”, (Norwegian), The Norwegian Building Authorities (DIBK). http://dibk.no/no/Tema/Eksisterende-bygg/Eksisterende-bygg-publikasjoner/bruk-av-bim-i-borettslag-og-sameier/

IDDS (2013). Research Roadmap Report CIB Integrated Design and Delivery Solutions (IDDS), Editors: Owen, R., Amor, A., Dickinson, J., Matthjis, P., & Kiviniemi, A. CIB Publication 370, ISBN 978-90-6363-072-0. http://site.cibworld.nl/dl/publications/pub_370.pdf

Issa, R. and Flood, I. (2014). ICCCBE and CIB W078IT in Construction conferences, Orland, Florida, June 23th – 25th 2014. http://128.227.160.197/icccbe2014/

Kim, I. (2012) ISO/ TC 211 about GIS and ISO/TC 58/SC13 about BIM have joint workshop, builingSAMRT International conference, Tokyo, Japan, 18th October 2012. http://iug.buildingsmart.org/resources/itm-and-iug-meetings-2012-tokyo/itm-meeting-2012-tokyo/GIS-BIM_Workshop_20121014_summary_v2.pdf/at_download/file

PAPER II

remote sensing

MDPI

Article

Automatic Estimation of Tree Position and Stem Diameter Using a Moving Terrestrial Laser Scanner

Ivar Oveland [1,*], Marius Hauglin [2], Terje Gobakken [2], Erik Næsset [2] and Ivar Maalen-Johansen [1]

1 Faculty of Science and Technology, Norwegian University of Life Sciences, 1432 Ås, Norway; ivar.maalen@nmbu.no
2 Faculty of Environmental Sciences and Natural Resource Management, Norwegian University of Life Sciences, 1432 Ås, Norway; marius.hauglin@nmbu.no (M.H.); terje.gobakken@nmbu.no (T.G.); erik.naesset@nmbu.no (E.N.)
* Correspondence: ivar.oveland@nmbu.no; Tel.: +47-672-31-649

Academic Editors: Parth Sarathi Roy, Clement Atzberger and Prasad S. Thenkabail
Received: 15 February 2017; Accepted: 1 April 2017; Published: 6 April 2017

Abstract: Airborne laser scanning is now widely used for forest inventories. An essential part of inventory is a collection of field reference data including measurements of tree stem diameter at breast height (DBH). Traditionally this is acquired through manual measurements. The recent development of terrestrial laser scanning (TLS) systems in terms of capacity and weight have made these systems attractive tools for extracting DBH. Multiple TLS scans are often merged into a single point cloud before the information extraction. This technique requires good position and orientation accuracy for each scan location. In this study, we propose a novel method that can operate under a relatively coarse positioning and orientation solution. The method divides the laser measurements into limited time intervals determined by the laser scan rotation. Tree positions and DBH are then automatically extracted from each laser scan rotation. To improve tree identification, the estimated center points are subsequently processed by an iterative closest point algorithm. In a small reference data set from a single field plot consisting of 18 trees, it was found that 14 were automatically identified by this method. The estimated DBH had a mean differences of 0.9 cm and a root mean squared error of 1.5 cm. The proposed method enables fast and efficient data acquisition and a 250 m^2 field plot was measured within 30 s.

Keywords: automated tree positioning; diameter at breast height; forest inventory; iterative closest point

1. Introduction

Forest inventories are of paramount importance for sustainable and effective management of forest resources. Airborne laser scanning (ALS) is now widely used in forest inventories [1]. An essential part of forest inventories based on ALS is field reference data collection. Field data are typically acquired by manual measurements on circular sample plots of 200–400 m^2 in size distributed over the landscape in question according to statistically rigorous sampling principles [2]. The use of terrestrial laser scanning (TLS) to acquire field reference data in these ALS-based forest inventories has been proposed. In a recent review study by Liang et al. [3] it is acknowledged that there is a potential for utilization of TLS in forest inventories. A TLS system uses a laser to measure distances in a regular pattern around the scanner. This information is used to create a dense point cloud covering the surroundings of the scanner position. A setup where the scanner position is fixed is often referred to as a static TLS. If the scanner moves during data capture, the system can be referred to as a kinematic TLS.

There are several studies providing methods for highly detailed description of single trees from single or multiple scanning positions in the field, often including all branches and leaves [4,5]. Tree architecture modeling has been used for biomass estimation [6–8] and forest structure description [9] at the plot or single tree level.

The use of TLS for the acquisition of specific biophysical tree parameters has been investigated in several studies, including estimation on diameter at breast height (stem diameter at 1.3 m above ground level; DBH) and tree stem volume [10–15]. A full or partial reconstruction of individual trees has also been investigated [5,16–19]. Direct estimation of single tree biomass from TLS data has been described in [6,8]. Others have estimated biomass from TLS data through tree stem reconstruction [20] or by using related TLS-estimates with existing allometric models [15,21].

Yang et al. [9] used multiple scans in individual field plots and found good agreement between field reference DBH, tree heights, and number of trees and corresponding properties derived from the TLS data. Positioning field plots using global navigation satellite system (GNSS) in forests can be affected by unfavorable conditions for reception of satellite signals, and reliably obtaining an accurate geo-referenced position typically requires a survey-grade GNSS receiver [22]. As an alternative to GNSS positioning of field plots and trees in the field, Hauglin et al. [23] demonstrated that the ALS data that exist in many forest inventory projects can be used together with TLS data for positioning purposes by matching ALS and TLS data and exploiting the inherent absolute positions of the ALS data. Both the use of multiple TLS scans and the use of a single scan—the latter typically acquired from the plot center—have been proposed. By using only a single scan, the data acquisition and post-processing procedures are greatly simplified and the acquisition time is reduced [24–26]. The main challenge in using a single scan setup is to handle the tree shadows that will occur in the TLS data. This is acknowledged in previous studies [12,27]. Depending on the tree density and factors such as the presence of undergrowth and low branches, a number of trees will be occluded from the view of the scanner and hence cannot be detected. Automated detection algorithms are in practice associated with omission and commission errors, which means that some trees visible from the scanner will go undetected and that some patterns in the data occasionally will cause the algorithm to detect trees that are actually not present. For these reasons, some of the trees within a field plot will often not be detected from a single TLS scan. Liang et al. [28] reviewed several previous studies and reported that 10–32% of the trees were reported to be occluded from the plot center, depending on tree density and plot size. In the same studies, an additional 4–33% of the visible trees were not detected, depending on the algorithm that was applied and other factors. Tree occlusion and handling of omission errors when using multiple scanning positions were the main objectives of the studies [29,30]. Astrup et al. [31] tested several approaches to estimating a corrected stand volume, taking into account the omitted trees. They found that without a correction the volume was substantially underestimated using single-scan TLS data. When applying a statistically founded correction, they obtained results which were closer to the volume computed from field measurements, but differences could still be observed. This suggests that it could be beneficial to investigate other methods to handle or avoid tree occlusion.

Time consumption is an important factor when considering the use of TLS on forest field plots. Bauwens et al. [32] noted that a plot typically can be measured within 10 min with a single static scan setup. The use of multiple scan locations in order to reduce occlusion will substantially increase the time needed for each plot.

As an alternative to the use of multiple static scanner positions, the problem of occlusion can be eliminated by moving the scanner while scanning, typically referred to as mobile laser scanning. A few studies have described the application of this technique in forests. Forsman et al. [33] used a laser scanner and cameras mounted on a car to measure trees along a forest road. Bauwens et al. [32] used a wearable rig consisting of a TLS scanner and additional sensors such as a GNSS receiver and an inertial measurement unit (IMU), which can be referred to as a kinematic TLS system. Walking with this rig through the forest produced a point cloud from which positions and other single tree properties could be derived. Bauwens et al. [32] and Ryding et al. [34] used a hand-held laser scanner with an integrated IMU to produce similar point clouds by walking through a forest area with the scanner.

In these and other studies, point cloud data are typically captured from multiple positions and merged prior to a feature extraction such as detection of tree stems. Accurate position and orientation are needed in order to merge multiple scans, and lack of accuracy will produce noisy point clouds due to errors when aligning data captured from different positions. In the present study, we propose a novel approach by which point data from as little as a single scanner rotation of a moving laser scanner is used for tree stem detection. In the current set-up of the method, a scanner rotation typically would take 0.05 s. This approach ensures that a spatially consistent point cloud is used for tree stem detection, and could form the basis for simultaneous localization and mapping (SLAM) using the detected trees. Thus, the aim of the current study was to develop and implement the proposed method and test it in a real forest environment by assessing the obtained accuracy of tree detection, tree position, and estimated DBH.

2. Instrumentation and Data Collection

2.1. Study Area and Field Reference Data Collection

The study area is located in Gran municipality in southeastern Norway (60°27′ N 10°33′ E, 500 m above sea level). The forest in Gran is boreal and dominated by Norway spruce (*Picea abies* (L.) Karst.) and Scots pine (*Pinus sylvestris* L.). An existing circular sample plot of 250 m^2 in a pine-dominated forest stand was subjectively selected from a dataset collected as part of another research project in the area. The plot was measured in field in August 2015. At the plot, all trees with a DBH >4 cm were accurately positioned, using an SOKKIA SET5 total station with additional measurements to at least two known points. The position of the two known points was obtained by post-processed GNSS baselines with base station data obtained from the Norwegian Mapping Authority. The receiver logged satellite data for more than 30 min. For all positioned trees, the DBH and species were also registered. The individual tree stems were calipered for diameter only once (a single measurement). In Table 1 a summary of the trees in the sample plot is given.

Table 1. Summary of tree diameter at breast height (DBH).

Species	Number of Trees	DBH Min (cm)	DBH Max (cm)	DBH Mean (cm)
Pine	12	19	39	25
Spruce	6	4	23	9
All	18	4	39	19

2.2. ALS Data Acquisition

The present study took advantage of ALS data acquired as part of an operational stand-based forest inventory. The ALS data were acquired on June 2015 with a Leica ALS70 sensor mounted on a fixed-wing aircraft, and the mean point density of the acquired ALS data was five points per m^2. The ALS echoes were classified into "ground" and "non-ground" points by the data provider using the TerraScan software (Version 015, Terrasolid: Kanavaranta, Finland) [35]. From the ALS points classified as ground points, a triangular irregular network (TIN) was created to represent the terrain surface height. The vertical accuracy of the surface model was expected to be approximately 20–30 cm [36]. Only the ALS echoes classified as ground points were used in the present study.

2.3. TLS Data Acquisition

TLS data were collected on the sample plot in April 2016 using an instrumentation integrating three primary components. The three hardware components used are illustrated in Figure 1. The VLP16 from Velodyne [37] was used as the terrestrial laser scanner. This instrument can be referred to as a low-cost laser scanner compared to traditional TLS systems. All laser measurements were timestamped with GPS time during data capture. The Velodyne VLP16 laser scanner has 16 individual laser beams rotating around the z-axis. The rotation speed is 5–20 rotations per second, referred to as scan rate. The vertical angle distance between each beam is 2 degrees. This gives a total field of view of 30 $\times$ 360 degrees. In this project, the pulse repetition rate was 300 kHz and the scan rate was 20 Hz. The data were stored and exported with VeloView v3.1.1.

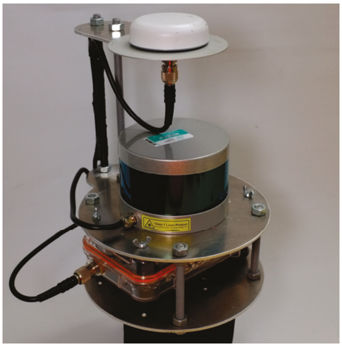

Figure 1. The complete measurement unit with global navigation satellite system (GNSS) antenna, Velodyne VLP16 laser scanner, and the Applanix APX-15 UAV sensor with an inertial measurement unit (IMU) at the bottom. The instrumentation was mounted and carried on a backpack during data capture in the field.

The Applanix APX-15 UAV [38] system was used to capture GNSS and IMU data. Position and orientation were post processed with Applanix POSPAC UAV v7.2. The algorithm used an inertial aided differential GNSS technique [39] with a baseline length up to 30.5 km. The GNSS reference station was obtained from the Norwegian Mapping Authority. Figure 2a shows how the position dilution of precision (Pdop) varied during data capture. The average estimated root mean squared error (RMSE) for the position in the horizontal direction was 0.22 m and 0.32 m in the vertical direction. The estimated RMSE for the orientation in roll and pitch was 0.06 degrees, and 1.30 degrees in heading. Some studies have shown that the GNSS solution can be improved by using the digital elevation model obtained from high-resolution ALS data. The techniques are often referred to as terrain aided GNSS [40], but was not tested in this study.

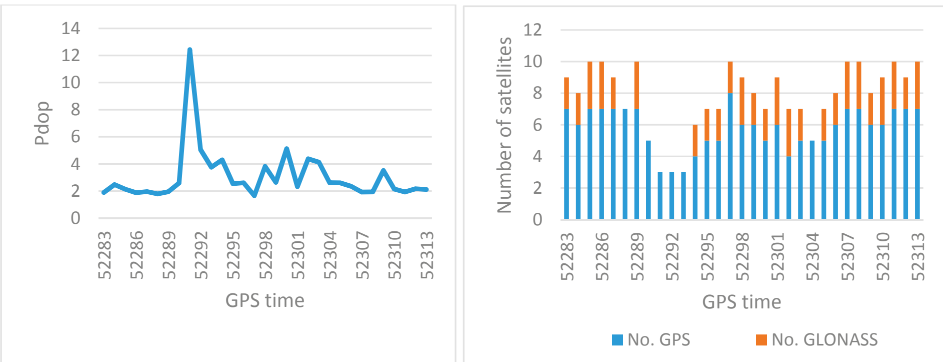

(**a**) (**b**)

Figure 2. The position dilution of precision (Pdop) during data capture is shown in (**a**) and (**b**) shows the number of satellites in the same time period.

The estimated positions were transformed to the coordinate system called EUREF89 Norwegian Transversal Mercator projection, which has a mapping scale value close to 1. The same coordinate system was applied for the ALS data. All other processing was performed using Matlab [41].

3. Data Processing and Analysis

3.1. Processing Method

The data processing was divided into nine different processing steps, which can be seen in Scheme 1.

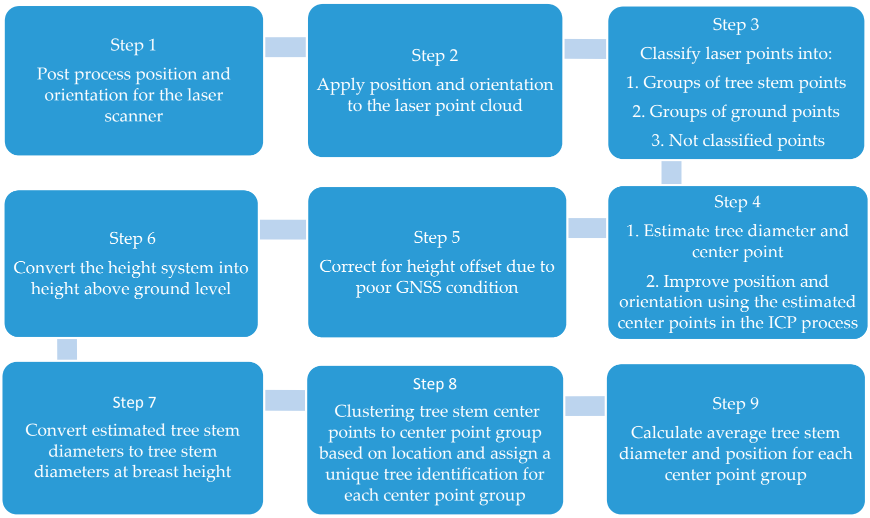

Scheme 1. Each step in the proposed method is illustrated in the scheme. IPC in step 4 means iterative closest point algorithm, see text in Section 3.3 for details.

The first step in this processing method was to calculate position and orientation of the laser scanner, described in Section 2.3. The second step was to apply the post processed position and orientation to the laser measurement. The laser points were realized in a local coordinate system. The position and orientation together with the installation calibration parameters provided the information to transform the laser points from this local coordinate system into the global coordinate system described in Section 2.3.

3.2. Point Group Classification

Step number 3 in Scheme 1 starts a classification process. Figure 3 shows the laser points from one scan rotation before the classification were performed. All laser measurements were classified into "groups of tree stem points," "groups of ground points," and "not classified points" based on a distance increment analysis for each of the 16 laser beams, also called laser channels. This is a sort of spike landmark extraction, where we searched for points that stands out from the rest [42]. The technique is often used in leg detecting algorithms in robotics [43], but it was also used for tree classification by Forsman et al. [33]. In this method, all laser points were separated into different point groups where each laser channel was treated separately. Two neighboring points were placed into the same point group if the difference between the measured distances was below a given threshold. Based on the evaluation of the field data, the following classification parameters were used:

- Distance measurement increment threshold was set to 0.1 m;
- Maximum tree diameter was set to 0.5 m;
- Trees were assumed to be vertical.

Based on these three classification parameters, all measurements were automatically classified into the three mentioned classes. No manual editing of the point classification was performed.

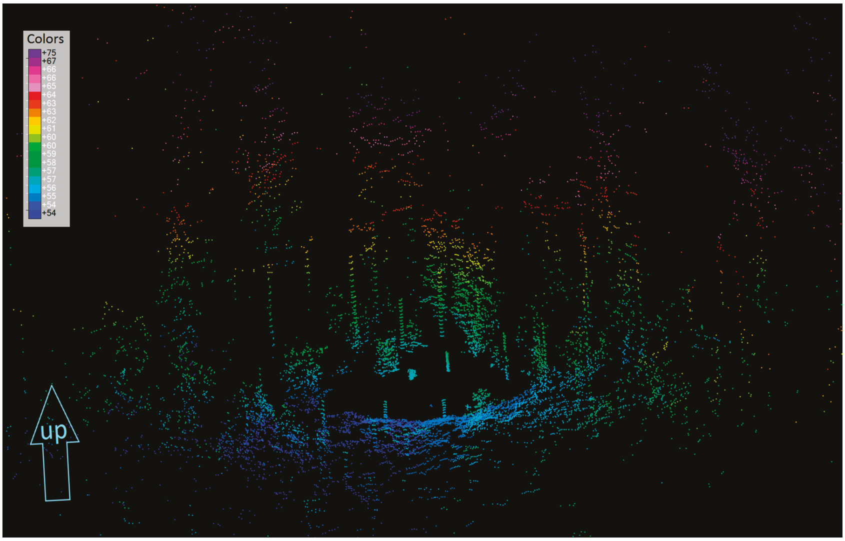

Figure 3. Approximately 10,000 laser points are collected during one scan rotation. Figure 3 shows an example of one scan rotation from an oblique perspective where the points are colored by elevation. The symmetric vertical structures are tree stems.

A point group was classified as a potential group of tree stem points if the distance increment was less than 0.1 m within one laser channel (see Figure 4a). In addition, the horizontal distance between the first and last point in the group had to be smaller than the maximum tree diameter. The analysis was done individually for each of the 16 laser channels. For each point group, a center point and tree radius were estimated using a circle fit algorithm [44]. It is necessary to have three measurements to be able to estimate a center point of the tree stem and a tree diameter. Based on the construction of the laser scanner we can estimate the theoretical maximum distance for a tree detection. Due to the precision and beam divergence, the minimum detectable tree diameter is set to 4 cm. The minimum detectable tree diameter ($\mathrm{Min_{stem}}$) depends on the distance to the scanner, and can be estimated with

$$\mathrm{Min_{stem}} = 2 \times \mathrm{distance} \times \sin\left[\frac{360 \times \mathrm{scan\ rate}}{\mathrm{puls\ repetition}/16}\right] \tag{1}$$

The tree stems were assumed to be vertical and well defined, i.e., clearly visible from the scanner and not hidden behind obstacles such as branches and other trees. The tree stem center points established from the different laser channels were subsequently merged together. The vertical distance between each laser channel is two degrees and this was used to decide if two center points belonged to the same tree. To be classified as a tree, there must be five consecutive center points with a vertical distance of two degrees (see Figure 4b). The minimum free visible tree stem ($\mathrm{S_{stem}}$) of a tree stem can be estimated as

$$\mathrm{S_{stem}} = \tan(2^\circ \times 4) \times \mathrm{distance} \tag{2}$$

A group of points was classified as ground if the distance increment was smaller than 0.1 m and the horizontal distance was larger than the maximum tree diameter. Finally, a point group was classified as “not classified” if the distance increment was greater than 0.1 m or if the distance increment was below 0.1 m for less than three consecutive measurements.

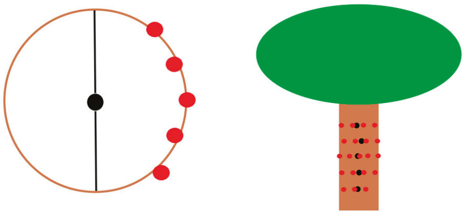

(**a**) (**b**)

Figure 4. Each of the 16 laser channels was treated separately. (**a**) Illustrates points from the same laser channel reflecting on a tree stem. The red points have all shorter observation distance increment than the given threshold and forming a group of tree stem points. These points are used to estimate a tree stem center point and diameter marked with black color. (**b**) Illustrates five different groups of tree stem points with the center point marked as a black point and the red points are the laser points. If the number of consecutive tree stem center points were five or more the center points were accepted as a tree and used in step 9 illustrated in Scheme 1.

3.3. Processing Method, Position, and Orientation Improvement

The post processed position and orientation solution described in Section 2.3 had a degraded result due to unfavorable conditions for reception of satellite signals. The proposed method is not very sensitive to position and orientation accuracy, but if the distances between the trees become small, tree identification might become unsuccessful. To avoid unsuccessful identification, it was decided to test scan matching. A version of the iterative closest point algorithm (ICP) called iteratively re-weighed least squares [45] was implemented by adding a Matlab function created by Bergström [46]. In the processing, the robust Welsch criterion function was used. The function estimates a three-dimension translation and rotation between two different point clouds. The first point cloud was locked and called model points. The other point cloud was fitted to the model points and called data points. For each scan rotation, a point cloud was created and a translation and rotation was estimated between the model points and the new data points. It was found that the ICP became more robust if just the estimated tree center points calculated for each scan rotation were entered. Since the amount of estimated tree center points was limited, we allowed the model points to be built up sequentially. After the new data points were transformed to fit the model points, the new transformed data points were added to the model points. In the end, the model points contained all estimated center points. The process is referred to as step 4 in Scheme 1.

3.4. Processing Method, Height Adjustment

To estimate DBH, the heights obtained from the scanner were adjusted. Due to the properties of the scanner and the acquisition, ground points were not present in the entire area for each scan rotation. The ground points from the ALS data were therefore utilized when calculating each center points height above ground and the conversion of the estimated diameter to DBH. The method involves three different height adjustments and was performed separately for each scan rotation. The estimated position accuracy was assumed to be sufficient in the horizontal direction to correspond to the ALS data. The method is further described below.

3.4.1. Height Adjustment Due to Poor 268 GNSS Conditions

Due to the poor GNSS conditions under tree canopies, the TLS data were not accurately aligned in height with the ALS data. The points classified as "ground" from the ALS acquisition were therefore used to estimate a height offset between the ALS and TLS data. This operation is referred to as step 5 in Scheme 1. Since the Velodyne laser scanner has a vertical field of view of 30 degrees, some laser channels were pointing down and others were pointing more upwards. In Figure 5, it is shown that the laser channels pointing down had a higher reliability when estimating the height difference between the ALS ground and the terrestrial ground points. Based on the findings in Figure 5, the laser channels 0, 2, and 4 having vertical observation angles corresponding to −15, −13, and −11 degrees, respectively, in the laser scanner frame system were used in the height difference estimation.

All estimated tree stem center points were adjusted for the estimated height difference between the TLS and ALS data.

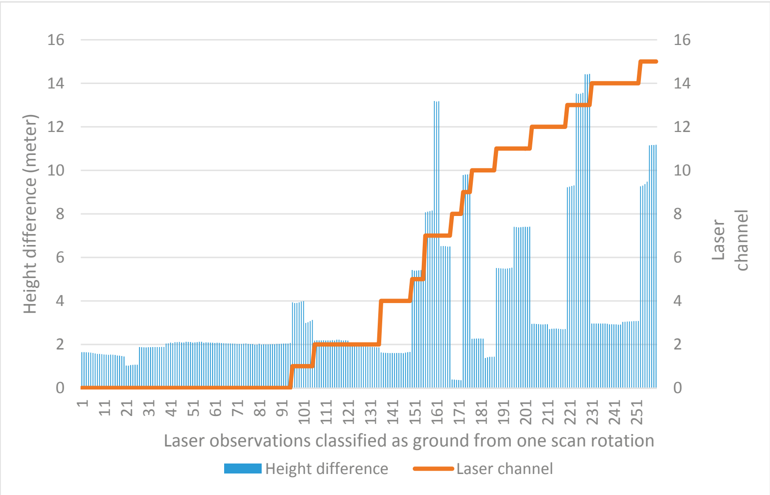

Figure 5. The height difference between the airborne laser scanning (ALS) ground points and terrestrial laser scanning (TLS) ground points was compared and evaluated based on the 16 different laser channels of the Velodyne laser scanner. The blue bars give the height difference between the ground classified points from TLS data and ground classified points from the ALS data. The orange line tells which laser channels are associated with the corresponding blue bar. The figure shows that laser channels pointing down are more likely to hit the true ground level.

3.4.2. Conversion into Height above Ground

After the height adjustment due to poor GNSS observations, the TLS data refer to the same coordinate and height system as the ALS point cloud. Normalized heights (height above ground) for the TLS data were then computed for all TLS points by subtracted their respective ALS TIN heights at the corresponding x and y coordinates, referred to as step 6 in Scheme 1.

3.4.3. Conversion of Estimated Tree Stem Diameters to Tree Stem Diameters at Breast Height

Most of the TLS points were obtained in the region from ground to 3 m above ground. To extract the diameter at breast height, a simple model that assumed that the stem diameter was reduced by 1 cm per m along the stem was used. This is referred to as step 7 in Scheme 1. Points obtained between 0 to 0.5 m were excluded from the processing due to the irregular taper of the lower stem section.

3.5. Clustering of Center Points

In step 8 in Scheme 1, the tree stem center points were clustered based on location and distance analysis. All points closer than 0.3 m to each other were clustered together into one center point group. Each center point group represents a tree with a unique identification. In step 9, the average tree stem diameter and position for each center point group was calculated.

3.6. Evaluation

Finally, the estimated tree coordinates and DBH were compared to the corresponding field reference measurements. Based on these results, mean differences, RMSE, and RMSE% were calculated as

$$\text{mean difference} = \frac{1}{n}\sum_{i=1}^{n}(y_i - y_{ri}), \tag{3}$$

$$\text{RMSE} = \sqrt{\frac{\sum_{i=1}^{n}(y_i - y_{ri})^2}{n}}, \tag{4}$$

and

$$\text{RMSE\%} = \frac{\text{RMSE}}{\overline{y_r}}100 \tag{5}$$

where y_i is the estimate, y_{ir} the reference, $\overline{y_r}$ is the mean reference value, and n the number of observations. The tree positon accuracy was evaluated using Equations (3) and (4).

4. Results

The proposed method was able to detect 14 of the 18 trees on the 250 m^2 plot. The actual data capture time consumption was 30 s, which did not include the startup time, shutdown time, and the walk in and out of the forest to reach the sample plot. Startup and shutdown can be done while walking to the area of interest. The actual walking path during data capture is shown in Figure 6a. A total of 9.5 million points were measured and 0.2 million of these were automatically classified as tree stems. Based on these points, 3249 center points with a corresponding diameter were estimated. The result is shown in Figure 6b. The center points were clustered to center point group based on location and given a unique tree identification.

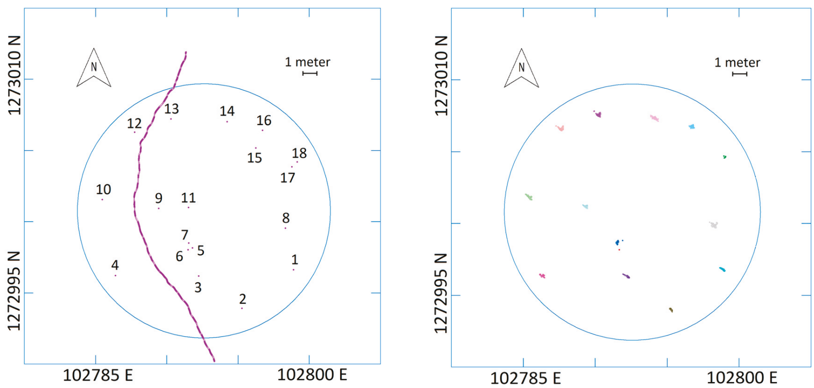

(**a**) (**b**)

Figure 6. The walking path (purple line) during data capture and field measured position of the trees are shown in (**a**). In (**b**), all estimated center points are shown. Each tree stem center point is colored by a unique color for each tree.

Table 2 summarizes the result of the tree stem diameter estimation. The difference between the field measured DBH and the estimated DBH varied between −1 cm and 3 cm for the detected trees. The undetected trees were all small, with a field measured DBH <10 cm, which was smaller than the minimum detectable tree diameter except for one of the four undetected trees. The minimum detectable tree diameter depends on the distance from the scanner to the tree, and is given for each tree in the rightmost column in Table 2. Figure 7 summarizes this minimum detectable tree stem diameter versus distance from the scanner to the tree. For example, if the scan rate is 20, the maximum distance to allow tree detection of a tree with 10 cm in diameter is 7 m.

Table 2. Summary at the individual tree level: Estimated DBH, the number of laser points used for detection. The minimum (Min. dist.) and maximum (Max dist.) observed distance to the tree, and field measured DBH. Minimum detectable tree diameter calculated for each tree. All distances are given in cm.

Tree ID	Estimated DBH	No. of Laser Points	Min. Dist.	Max Dist.	Field Reference DBH	Difference between Field Reference and Estimated DBH	Detect-Able Tree Diameter [a]
1	20.3	2800	728	820	20.4	0.1	10
2	25.3	18,628	385	1630	27.2	1.9	5
3	21.4	22,707	248	630	22.6	1.2	4
4	22.2	1850	699	1190	22.5	0.3	9
5	8.3	26	240	180	7.9	−0.4	4
6	NIL		250	1140	5.6		4
7	26.0	7994	574	950	27.0	1.0	8
8	23.6	5689	944	1310	23.6	0.0	13
9	19.8	29,719	398	940	20.7	0.9	5
10	19.3	20,203	651	1210	21.4	2.1	9
11	NIL		370	9300	4.2		5
12	24.7	33,816	450	1310	27.3	2.6	6
13	17.9	33,122	364	1000	19.0	1.1	5
14	23.8	11,624	741	1050	23.5	−0.3	10
15	NIL		720	1380	5.8		10
16	26.1	9496	826	1080	25.1	−1.0	11
17	NIL		1010	1350	7.0		14
18	36.0	160	1050	1160	39.0	3.0	14

[a] Calculated based on the field measured tree positions and the scanner location. See Figure 7 for further details.

In Scheme 1, step 9, an average DBH was calculated for each center point group. This was used as the estimated DBH for each detected tree and was compared to the field reference DBH. The result is presented in Table 2 and was used to estimate the mean difference, RMSE, and RMSE%. The estimation was based on Equations (3) to (5). Table 3 summarize these findings. The mean difference between the field reference DBH and the estimated DBH was 0.9 cm, with an RMSE of 1.5 cm.

Table 3. Comparison of estimated DBH and field reference DBH. Mean difference and root mean squared error (RMSE).

Number of Trees	Mean Difference (cm)	RMSE (cm)	RMSE%
14 of 18	0.9	1.5	7.5

An average position was calculated for each center point group. Equations (3) and (4) were then used to calculate the mean difference and RMSE. The result is summarized in Table 4.

Table 4. Comparison of estimated tree positions and field reference positions.

Number of Trees	Mean Difference (m)	RMSE (m)
14 of 18	0.21	0.23

5. Discussion

The results showed that small trees were difficult to extract with the proposed method. The main reason was that three measurements were required to be able to calculate the tree stem center point and diameter. Based on Equation (1), it is possible to estimate the minimum tree stem diameter observed from different distances. Figure 7 summarizes this minimum detectable tree stem diameter versus distance from the laser scanner to the tree.

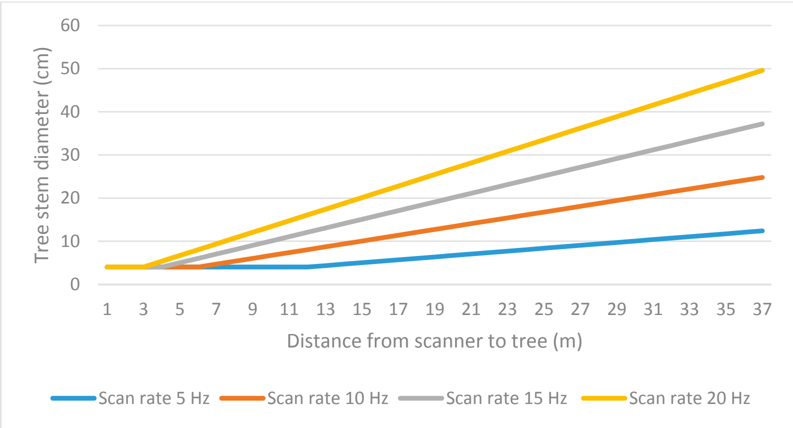

Figure 7. Minimum diameter at breast height as a function of observation distance and scan rate calculated from Equation (1). Each diameter estimation requires minimum three laser points hitting the tree stem. Then minimum detectable diameter is set to 4 cm.

In the practical test, there were four trees that were not detected (Table 2). For each of the non-detected trees, the maximum detectable distance was calculated and for three of the four trees, the observed distance was too large for the tree to be detected. The smaller trees would be detected if observed distance or the scan rate had been reduced (Figure 7). If the scan rate is reduced from 20 Hz to 10 Hz, the possible detectable tree diameter is reduced with the same ratio, which means that 17 of 18 trees should theoretically be detectable by reducing the scan rate to 10 Hz. For the tree with ID number 6, the possible detectable tree diameter was smaller than the actual diameter of the tree. This means that one should have expected a positive detection. The actual reason for this was not found, but branches or other vegetation blocking the visibility of the stem might be one explanation.

The classification algorithm requires five continuous center points along the stem to be classified as a potential tree. The main reason for this is to filter out points that were falsely classified as a tree stem. Figure 8 shows the relationship between observed distance and the required minimum free visible tree stem. The calculation is based on Equation (2). This requirement was not a big problem in the test area, but different forest conditions with respect to tree species and ages might give other results.

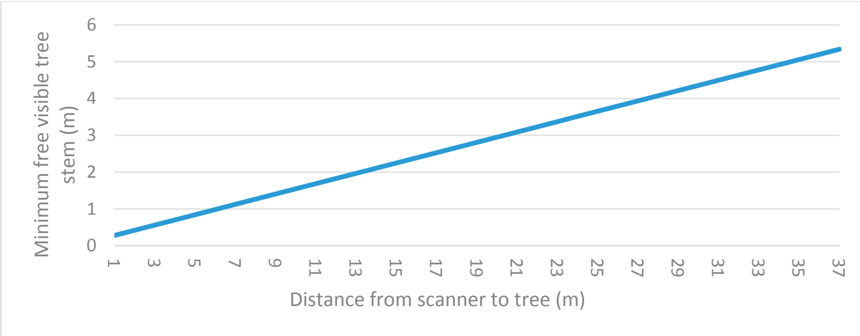

Figure 8. Calculated minimum unobstructed view to the tree stem based on observed distance. The calculation is based on Equation (2).

The position and orientation solution in this study were relative good, but not good enough to merge the different scan rotations into one common point cloud. The main reason for this was the poor conditions for GNSS signal reception under the tree canopy.

For many forest inventory applications, the tree position accuracy achieved in this study is sufficient. It is, however, possible to improve the accuracy of the positions. The positions can be improved by different methods:

- Take actions to improve the GNSS accuracy, such as reduce the distance to the GNSS reference station;
- Use the ALS point cloud to extract the tree positions and perform matching per scan rotation to estimate a 2-dimensional translation and rotation for each scan rotation (c.f. Hauglin et al. [47]);
- Develop the proposed method into a three-dimensional SLAM system;
- The trees are assumed to grow vertically. In cases with low orientation accuracy, the trees can be used to estimate an average initial roll and pitch angle.

In the study presented by Bauwens et al. [32], three different tests were performed. The study area was located in Belgium and consisted of 10 different locations. The locations were chosen to maximize the variation in forest types, tree density, and terrain slope. One test was called FARO1 where the reference field was measured from one location with a Faro focus 3D 120. Another test called FARO5 was performed by measuring with the same instrument from five different locations. Finally, a test called ZEB1 was performed by collecting data with a handheld scanner (ZEB1). In terms of accuracy, the result achieved in the current study was between the FARO1 and the FARO5 tests (Table 5).

Table 5. Result for estimated DBH in the current study compared to Bauwens et al. [32].

Study	Mean Difference (cm)	RMSE (cm)	RMSE%
Current study	0.9	1.5	7.5
FARO1 [32]	−1.2	3.7	13.4
FARO5 [32]	−0.2	1.3	4.7
ZEB1 [32]	−0.1	1.1	4.1

An important factor when collecting data in the field is time consumption. The method with the smallest time consumption achieved by Bauwens et al. [32] was the FARO1 method, which required 10 min of field work. The required time only included the acquisition of data to get the measurements into a local coordinate system. In the current study, the TLS acquisition took 30 s. The latter also included the acquisition of GNSS and IMU data, which enabled us to produce tree positions in a global reference system. To be able to use the data in operational forest inventory, it is necessary to have the measurements in the same global coordinate system as the ALS data. It is, however, difficult to compare the methods directly because the forest conditions were different with respect to forest type, tree density, terrain conditions, and field plot size. In the current study, we used a plot with a radius of 8.9 m while Bauwens et al. [32] used a radius of 15 m.

6. Conclusions

GNSS signal reception conditions are typically degraded under forest canopies, and the proposed method worked with a relatively coarse positioning and orientation solution. This was possible because the laser measurements were divided into limited time frames determined by the scan rotation. For each scan rotation, tree center points and diameters were calculated. This provided a means to circumvent the need for a high accuracy position and orientation of the moving scanner platform. To avoid the different trees from being mixed, the estimated center points were treated by an ICP algorithm to improve the homogeneity in the merged dataset. This process improved the tree identification process and made the entire process more robust. Future work should be devoted to improving the position and orientation solution with different GNSS techniques, different scan matching technics, or SLAM. Although the method proposed in the current study is in an initial phase of development, it has the potential to become a robust method, rapid and cost-effective acquisition of forest field plot data.

Author Contributions: Ivar Oveland wrote the paper, performed the Velodyne fieldwork, conducted the hardware installation, method development, and processed the data. Marius Hauglin co-authored the paper, prepared the field, and prepared the ALS data. Terje Gobakken planned the ALS acquisition and revised the paper. Erik Næsset and Ivar Maalen-Johansen supervised the study and revised the paper.

Conflicts of Interest: The authors declare no conflict of interest.

References

1. Vauhkonen, J.; Maltamo, M.; McRoberts, R.E.; Næsset, E. Introduction to forestry applications of airborne laser scanning. In *Forestry Applications of Airborne Laser Scanning*; Springer: Berlin/Heidelberg, Germany, 2014; pp. 1–16.
2. Næsset, E. Predicting forest stand characteristics with airborne scanning laser using a practical two-stage procedure and field data. *Remote Sens. Environ.* **2002**, *80*, 88–99. [CrossRef]
3. Liang, X.; Kankare, V.; Hyyppä, J.; Wang, Y.; Kukko, A.; Haggrén, H.; Yu, X.; Kaartinen, H.; Jaakkola, A.; Guan, F.; et al. Terrestrial laser scanning in forest inventories. *ISPRS J. Photogramm. Remote Sens.* **2016**, *115*, 63–77. [CrossRef]
4. Bayer, D.; Seifert, S.; Pretzsch, H. Structural crown properties of Norway spruce (*Picea abies* [L.] Karst.) and European beech (*Fagus sylvatica* [L.]) in mixed versus pure stands revealed by terrestrial laser scanning. *Trees* **2013**, *27*, 1035–1047. [CrossRef]
5. Côté, J.-F.; Fournier, R.A.; Egli, R. An architectural model of trees to estimate forest structural attributes using terrestrial LiDAR. *Environ. Model. Softw.* **2011**, *26*, 761–777. [CrossRef]
6. Hauglin, M.; Astrup, R.; Gobakken, T.; Næsset, E. Estimating single-tree branch biomass of Norway spruce with terrestrial laser scanning using voxel-based and crown dimension features. *Scand. J. For. Res.* **2013**, *28*, 456–469. [CrossRef]
7. Hosoi, F.; Nakai, Y.; Omasa, K. 3-D voxel-based solid modeling of a broad-leaved tree for accurate volume estimation using portable scanning lidar. *ISPRS J. Photogramm. Remote Sens.* **2013**, *82*, 41–48. [CrossRef]
8. Kankare, V.; Holopainen, M.; Vastaranta, M.; Puttonen, E.; Yu, X.; Hyyppä, J.; Vaaja, M.; Hyyppä, H.; Alho, P. Individual tree biomass estimation using terrestrial laser scanning. *ISPRS J. Photogramm. Remote Sens.* **2013**, *75*, 64–75. [CrossRef]
9. Yang, X.; Strahler, A.H.; Schaaf, C.B.; Jupp, D.L.B.; Yao, T.; Zhao, F.; Wang, Z.; Culvenor, D.S.; Newnham, G.J.; Lovell, J.L.; et al. Three-dimensional forest reconstruction and structural parameter retrievals using a terrestrial full-waveform lidar instrument (Echidna®). *Remote Sens. Environ.* **2013**, *135*, 36–51. [CrossRef]

10. Bienert, A.; Scheller, S.; Keane, E.; Mohan, F.; Nugent, C. Tree Detection and Diameter Estimations by Analysis of Forest Terrestrial Laser Scanner Point Clouds. In Proceedings of the ISPRS Workshop on Laser Scanning 2007 and Silvilaser 2007, Espoo, Finland, 12–14 September 2007; pp. 50–55.
11. Hopkinson, C.; Chasmer, L.; Young-Pow, C.; Treitz, P. Assessing forest metrics with a ground-based scanning lidar. *Can. J. For. Res.* **2004**, *34*, 573–583. [CrossRef]
12. Lovell, J.L.; Jupp, D.L.B.; Newnham, G.J.; Culvenor, D.S. Measuring tree stem diameters using intensity profiles from ground-based scanning lidar from a fixed viewpoint. *ISPRS J. Photogramm. Remote Sens.* **2011**, *66*, 46–55. [CrossRef]
13. Moskal, L.M.; Zheng, G. Retrieving Forest Inventory Variables with Terrestrial Laser Scanning (TLS) in Urban Heterogeneous Forest. *Remote Sens.* **2012**, *4*, 1–20. [CrossRef]
14. Simonse, M.; Aschoff, T.; Spiecker, H.; Thies, M. Automatic Determination of Forest Inventory Parameters Using Terrestrial Laserscanning. In Proceedings of the ScandLaser Scientific Workshop on Airborne Laser Scanning of Forests, Umeå, Sweden, 3–4 September 2003.
15. Yao, T.; Yang, X.; Zhao, F.; Wang, Z.; Zhang, Q.; Jupp, D.; Lovell, J.; Culvenor, D.; Newnham, G.; Ni-Meister, W.; et al. Measuring forest structure and biomass in New England forest stands using Echidna ground-based lidar. *Remote Sens. Environ.* **2011**, *115*, 2965–2974. [CrossRef]
16. Gorte, B.; Pfeifer, N. Structuring laser-scanned trees using 3d mathematical morphology. *Int. Arch. Photogramm. Remote Sens.* **2004**, *35*, 929–933.
17. Lefsky, M.; McHale, M.R. Volume estimates of trees with complex architecture from terrestrial laser scanning. *J. Appl. Remote Sens.* **2008**, *2*, 023521.
18. Pfeifer, N.; Gorte, B.; Winterhalder, D. Automatic Reconstruction of Single Trees from Terrestrial Laser Scanner Data. *ISPRS Int. Arch. Photogramm. Remote Sens. Spat. Inf. Sci.* **2004**, *XXXV*, 114–119.
19. Raumonen, P.; Kaasalainen, M.; Åkerblom, M.; Kaasalainen, S.; Kaartinen, H.; Vastaranta, M.; Holopainen, M.; Disney, M.; Lewis, P. Fast Automatic Precision Tree Models from Terrestrial Laser Scanner Data. *Remote Sens.* **2013**, *5*, 491–520. [CrossRef]
20. Yu, X.; Liang, X.; Hyyppa, J.; Kankare, V.; Vastaranta, M.; Holopainen, M. Stem biomass estimation based on stem reconstruction from terrestrial laser scanning point clouds. *Remote Sens. Lett.* **2013**, *4*, 344–353. [CrossRef]
21. Vonderach, C.; Voegtle, T.; Adler, P.; Norra, S. Terrestrial laser scanning for estimating urban tree volume and carbon content. *Int. J. Remote Sens.* **2012**, *33*, 6652–6667. [CrossRef]
22. Andersen, H.-E.; Clarkin, T.; Winterberger, K.; Strunk, J. An Accuracy Assessment of Positions Obtained Using Survey- and Recreational-Grade Global Positioning System Receivers across a Range of Forest Conditions within the Tanana Valley of Interior Alaska. *West. J. Appl. For.* **2009**, *24*, 128–136.
23. Hauglin, M.; Lien, V.; Næsset, E.; Gobakken, T. Geo-referencing forest field plots by co-registration of terrestrial and airborne laser scanning data. *Int. J. Remote Sens.* **2014**, *35*, 3135–3149. [CrossRef]
24. Bienert, A.; Scheller, S.; Keane, E.; Mullooly, G.; Mohan, F. Application of terrestrial laser scanners for the determination of forest inventory parameters. *Int. Arch. Photogramm. Remote Sens. Spat. Inf. Sci.* **2006**, *36*, 5.
25. Brolly, G.; Király, G. Algorithms for stem mapping by means of terrestrial laser scanning. *Acta Silv. Lignaria Hung.* **2009**, *5*, 119–130.
26. Liang, X.; Litkey, P.; Hyyppa, J.; Kaartinen, H.; Vastaranta, M.; Holopainen, M. Automatic Stem Mapping Using Single-Scan Terrestrial Laser Scanning. *IEEE Trans. Geosci. Remote Sens.* **2012**, *50*, 661–670. [CrossRef]
27. Hopkinson, C.; Lovell, J.; Chasmer, L.; Jupp, D.; Kljun, N.; van Gorsel, E. Integrating terrestrial and airborne lidar to calibrate a 3D canopy model of effective leaf area index. *Remote Sens. Environ.* **2013**, *136*, 301–314. [CrossRef]
28. Liang, X.; Litkey, P.; Hyyppä, J.; Kaartinen, H.; Kukko, A.; Holopainen, M. Automatic plot-wise tree location mapping using single-scan terrestrial laser scanning. *Photogramm. J. Finl.* **2011**, *22*, 38–48.
29. Puttonen, E.; Lehtomäki, M.; Kaartinen, H.; Zhu, L.; Kukko, A.; Jaakkola, A. Improved Sampling for Terrestrial and Mobile Laser Scanner Point Cloud Data. *Remote Sens.* **2013**, *5*, 1754–1773. [CrossRef]
30. Trochta, J.; Král, K.; Janík, D.; Adam, D. Arrangement of terrestrial laser scanner positions for area-wide stem mapping of natural forests. *Can. J. For. Res.* **2013**, *43*, 355–363. [CrossRef]
31. Astrup, R.; Ducey, M.J.; Granhus, A.; Ritter, T.; von Lüpke, N. Approaches for estimating stand-level volume using terrestrial laser scanning in a single-scan mode. *Can. J. For. Res.* **2014**, *44*, 666–676. [CrossRef]

32. Bauwens, S.; Bartholomeus, H.; Calders, K.; Lejeune, P. Forest Inventory with Terrestrial LiDAR: A Comparison of Static and Hand-Held Mobile Laser Scanning. *Forests* **2016**, *7*, 127. [CrossRef]
33. Forsman, M.; Holmgren, J.; Olofsson, K. Tree Stem Diameter Estimation from Mobile Laser Scanning Using Line-Wise Intensity-Based Clustering. *Forests* **2016**, *7*, 206. [CrossRef]
34. Ryding, J.; Williams, E.; Smith, M.; Eichhorn, M. Assessing Handheld Mobile Laser Scanners for Forest Surveys. *Remote Sens.* **2015**, *7*, 1095–1111. [CrossRef]
35. Terrasolid. *TerraScan User's Guide*; Terrasolid Ltd.: Helsinki, Finland, 2011.
36. Kraus, K.; Pfeifer, N. Determination of terrain models in wooded areas with airborne laser scanner data. *ISPRS J. Photogramm. Remote Sens.* **1998**, *53*, 193–203. [CrossRef]
37. Velodyne Lidar, PUCK, VLP16. Available online: http://velodynelidar.com/vlp-16.html (accessed on 8 January 2017).
38. Direct Mapping Solutions for UAVs. Available online: http://www.applanix.com/products/dms-uavs.htm (accessed on 8 January 2017).
39. Hutton, J.; Bourke, T.; Scherzinger, B.; Hill, R. *New Developments of Inertial Navigation Systems at Applanix*; Wichmann: Heidelberg, Germany, 2007; pp. 201–213.
40. Danezis, C.; Gikas, V. An iterative LiDAR DEM-aided algorithm for GNSS positioning in obstructed/rapidly undulating environments. *Adv. Space Res.* **2013**, *52*, 865–878. [CrossRef]
41. MathWorks. Matlab. 2017. Available online: https://se.mathworks.com/ (accessed on 7 February 2017).
42. Riisgaard, S.; Blas, M.R. *SLAM for Dummies. A Tutorial Approach to Simultaneous Localization and Mapping*; BibSonomy: Würzburg, Germany, 2003; p. 126.
43. Arras, K.O.; Mozos, O.M.; Burgard, W. Using boosted features for the detection of people in 2d range data. In Proceedings of the 2007 IEEE International Conference on Robotics and Automation, Roma, Italy, 10–14 April 2007.
44. Bucher, I. Circle Fit. 2004. Available online: https://se.mathworks.com/matlabcentral/fileexchange/5557-circle-fit/content/circfit.m (accessed on 15 December 2016).
45. Bergström, P.; Edlund, O. Robust registration of point sets using iteratively reweighted least squares. *Comput. Optim. Appl.* **2014**, *58*, 543–561. [CrossRef]
46. Bergström, P. Iterative Closest Point Method. 2016. Available online: https://se.mathworks.com/matlabcentral/fileexchange/12627-iterative-closest-point-method (accessed on 11 March 2016).
47. Hauglin, M.; Næsset, E.; Gobakken, T. Assessing the accuracy of co-registered terrestrial and airborne laser scanning data in forests. In Proceeding of the ForestSat 2014, Garda, Italy, 4–7 November 2014.

PAPER III

remote sensing

Article

Comparing Three Different Ground Based Laser Scanning Methods for Tree Stem Detection

Ivar Oveland [1,*], Marius Hauglin [2], Francesca Giannetti [3], Narve Schipper Kjørsvik [4] and Terje Gobakken [2]

1 Faculty of Science and Technology, Norwegian University of Life Sciences, 1432 Ås, Norway
2 Faculty of Environmental Sciences and Natural Resource Management, Norwegian University of Life Sciences, 1432 Ås, Norway; marius.hauglin@nmbu.no (M.H.); terje.gobakken@nmbu.no (T.G.)
3 Department of Agricultural, University of Florence, 50145 Firenze, Italy; francesca.giannetti@unifi.it
4 TerraTec AS, 0281 Oslo, Norway; narve.kjorsvik@terratec.no
* Correspondence: ivar.oveland@nmbu.no; Tel.: +47-4022-0711

Received: 4 February 2018; Accepted: 30 March 2018; Published: 31 March 2018

Abstract: A forest inventory is often carried out using airborne laser data combined with ground measured reference data. Traditionally, the ground reference data have been collected manually with a caliper combined with land surveying equipment. During recent years, studies have shown that the caliper can be replaced by equipment and methods that capture the ground reference data more efficiently. In this study, we compare three different ground based laser measurement methods: terrestrial laser scanner, handheld laser scanner and a backpack laser scanner. All methods are compared with traditional measurements. The study area is located in southeastern Norway and divided into seven different locations with different terrain morphological characteristics and tree density. The main tree species are boreal, dominated by Norway spruce and Scots pine. To compare the different methods, we analyze the estimated tree stem diameter, tree position and data capture efficiency. The backpack laser scanning method captures the data in one operation. For this method, the estimated diameter at breast height has the smallest mean differences of 0.1 cm, the smallest root mean square error of 2.2 cm and the highest number of detected trees with 87.5%, compared to the handheld laser scanner method and the terrestrial laser scanning method. We conclude that the backpack laser scanner method has the most efficient data capture and can detect the largest number of trees.

Keywords: backpack laser scanner; forest inventory; handheld laser scanner; lidar; terrestrial laser scanner; tree stem detection

1. Introduction

Updated information about forest resources is important on different scales ranging from the individual tree up to regional, national and global levels. Remote sensing has played a key role in the past decades' development of modern forest inventory methods. Optical sensors on airborne and spaceborne platforms are being used for mapping of forest resources, and, in the boreal forest in the Nordic countries, a majority of operational forest inventories are today carried out using a combination of aerial imagery and data from airborne laser scanning [1]. In this inventory method, the relationship between remotely sensed data and field measured properties is modeled for area units [2]. Complete coverage forest inventory data are produced by utilizing the remotely sensed data and the established relationship with biophysical forest characteristics from the field measurements. A requirement in this approach is that field reference data are available. At a regional and national scale, similar methods have been used with satellite imagery [3]. Field reference data are also required and used in this case.

Manual field registrations including tree positioning, as required in many forest inventory methods, can be time consuming (cf. [4]), and several studies have investigated how remote sensing technologies can aid or replace manual work in the field. Liang et al. [5] reviewed research aiming at using terrestrial laser scanner (TLS) in forest inventories. TLS produces three-dimensional data in the form of dense point clouds, and by processing and analyzing these point clouds several biophysical characteristics related to the forest and the trees can be extracted. Methods have been developed for automatic identification of tree stems and extraction of stem diameters [6–11]. Others have developed methods for more detailed reconstruction of the tree stem and branch structure [12]. It has been suggested that the field reference data that are used in remote sensing based forest inventories can be collected using TLS. Field reference data for forest inventories typically consist of measurements on field plots of size 200–400 m^2. Several challenges must be overcome to effectively use TLS for registrations on field plots, and many of them are discussed in the review studies by Liang et al. [5] and Dassot et al. [13]. Scanning from a fixed position on a field plot will for example lead to occluded areas, or areas where the point cloud data are sparse or missing due to obstructions between the trees and the scanner position. The presence of such occluded areas in the dataset can be reduced by scanning from multiple positions. This is however time consuming, and some studies investigate methods to correct for the missing trees that will be obstructed from the view of the scanner [14]. Reducing the chance of having occluded areas in the data from a field plot can also be achieved by using mobile laser scanning (MLS). Rather than scanning from fixed positions, such systems will continuously record data while the instrument is carried through the forest field plot. The instrument can be carried by a human [8,15,16], or mounted on a vehicle [17,18].

Oveland et al. [8] have developed and described a MLS-based system for acquisition of single tree positions and diameters at forest field plots. This system used data from an airborne laser scanning to determine the ground level. The dependence on additional external data limited the use of the system. It was therefore desirable to develop a system that could be used without the need for additional data. The system described in the current study solves this by including an additional scanning device, and therefore does not depend on additional data. In the following, this system will be referred to as the backpack laser scanner (BPLS). The BPLS system has similar laser instrumentation as the Leica Pegasus backpack tested by Masiero et al. [19].

Previous studies on laser scanner based systems for mapping of trees are briefly described in the following. Pierzchala et al. [20] used an unmanned vehicle-based MLS system and simultaneous localization and mapping (SLAM) to map trees and estimate diameter at breast height (DBH). A root mean square error (RMSE) of 2.4 cm was obtained when estimating the DBH. Based on a novel method for tree stem identification, Heinzel and Huber [21] used TLS to estimate DBH, and obtained an RMSE of 2.9 cm. In a study by Bauwens et al. [15], three systems based on TLS and MLS were compared on trees with DBH > 10 cm. For DBH estimation, an RMSE of 1.1 cm was obtained using the MLS-based system. When using TLS for DBH estimation an RMSE of 3.7 cm was obtained for a single scan and 1.3 cm was reported for multiple scans. For a single TLS scan, 78% of the trees were detected. Forsman et al. [17] used a vehicle-mounted MLS system to estimate DBH. Three-dimensional data were obtained by the combination of a two-dimensional laser scanner and the movement of the vehicle. For the trees within 10 m from the vehicle, an RMSE of 3.7 cm was obtained for the estimation of DBH and with a stem detection accuracy variation from 63% to 78%. Liang et al. [22] demonstrated a BPLS system based on a TLS laser scanner in combination with an inertial measurement unit (IMU) and a global navigation satellite system (GNSS) receiver. A tree stem detection accuracy of 82.6% and an RMSE of 5.1 cm on estimation of DBH were reported in that study. Liang et al. [23] proposed a method using separate processing of multiple TLS scans on a forest field plot. They obtained a stem detection accuracy of 95.3% and an RMSE for the DBH estimation in the range from 0.9 cm to 1.9 cm. Corresponding results for a single scan setup were a detection rate of 73.4% and an RMSE for the DHB in the range from 0.7 cm to 2.4 cm. In a study comparing different TLS scanner setups and detection algorithms, Pueschel et al. [24] estimated the DBH with an RMSE of 0.7–1.2 cm when using multiple TLS scans. For single TLS scans, the RMSE varied from 1.4 cm to 2.4 cm.

Field plots used in remote sensing based forest inventories are required to be accurately positioned. This is typically achieved in manual field work by using survey-grade GNSS receivers. TLS and MLS instruments which record laser data in a local coordinate system must be related to a global coordinate reference system to be used in the inventory process. The three-dimensional point cloud obtained from the laser instruments are usually rotated and translated from the local coordinate system to a global coordinate reference system using targets. Accurate positioning of targets within forests using GNSS can be challenging, and post-processing is often used [25]. The difficulties are poor sky visibility due to the tree canopy. The trees interrupt the GNSS signals, resulting in poor conditions for GNSS measurements. The movement of a MLS system through the forest means however that favorable conditions for GNSS signals are likely to occur at some locations, where the canopy is less dense or absent. This can be utilized, and in combination with information about the orientations and movements, it can be used to retain the current position in areas with poorer GNSS conditions. Use of IMU in combination with GNSS in forests was applied, e.g., by Kaartinen et al. [26], Forsman et al. [17] and Oveland et al. [8], to handle information about the orientations and movements. In the current study, tightly coupled GNSS-IMU post processing software called TerraPos [27] was used to obtain the position throughout the data collections. Additionally, iterative closest point (ICP) algorithm were used to improve the position accuracy within the plots. TerraPos is a multi-purpose software for aided inertial navigation. In addition to standard ambiguity fixed differential GNSS aiding, a wide range of aiding sources and sensors may be used. Typical aiding examples are wheel-based and visual odometry, magnetometers, slave GNSS antenna, velocity constraints and digital elevation model. TerraPos is usually applied to positioning of planes, ships and cars and not commonly used in an MLS system in the forest.

The aim of the current study was to describe a BPLS system for collection of single tree data on field plots in boreal forest. The target was to obtain DBH and tree position in a global reference frame as efficient as possible. The BPLS system used a novel method to extract the DBH without losing precision due to poor GNSS conditions and to extract the tree position in a global reference frame using a GNSS aided inertial navigation system (INS) in combination with a two-step iterative closest point approach. Data obtained with the BPLS system were compared to similar data from two existing scanning systems, namely the handheld laser scanner (HLS) GeoSlam ZEB1 (GeoSlam, Ruddington Fields Business Park, Ruddington, Nottinghamshire, NG11 6JS, United Kingdom) and the TLS Faro Focus 3D x130 (Faro, 250 Technology Park Lake Mary, FL 32746, USA). Data from all three systems were validated against manual field measurements.

2. Materials and Methods

2.1. Study Area

This study was conducted in a boreal forest in Ås municipality in the southeastern part of Norway (59°40′N 10°46′E, 100 m above sea level). The main tree species in this forest are Norway spruce (*Picea abies* (L.) Karst.) and Scots pine (*Pinus sylvestris* L.). Birch (*Betula pubescens* Ehrh.), larch (*Larix deciduae*) and silver fir (*Abies alba* Mill.) are also present. In total, seven circular plots of 500 m^2 were located in the forest. Two of the plots were located in hilly terrains and five plots were located in flat terrains. The plots were measured with four different measurement methods. The different methods were caliper, TLS, HLS and BPLS. The caliper dataset act as the reference in this study. All other observations were compared to the reference.

2.2. Reference Data Collection

The reference data were collected in May 2017 and October 2017. In total, 335 trees were measured, where 92 trees had a DBH < 10 cm. Table 1 summarizes the number of trees and species. The stem density varied from 380 to 1380 stems/ha with an average of 967 stems/ha.

Table 1. Summary of trees with species and diameter at breast height (DBH).

		DBH (cm)		
Species	**Number of Trees**	**Min**	**Max**	**Mean**
Spruce [1]	144	4.0	60.7	22.3
Pine	137	9.3	43.5	28.2
Silver fir	32	4.1	81.4	9.4
Birch	22	4.1	9.8	6.1

[1] Norway spruce with larch.

For each tree, the DBH was measured with a caliper, and the position of the tree was recorded. There were different stages involved when the data were established. The first step was to register the center of the plot. GNSS registrations are not well suited for dense forest conditions. To establish a high accuracy position for the center point, two additional points were established. The additional points were located in locations where the sky visibility was more suitable for GNSS measurements. The positions of the two known points were obtained with a survey-grade GNSS receiver and the logging of satellite data for more than 30 min. Accurate positions were derived through post processing using GNSS base station data obtained from the Norwegian mapping authorities. An accurate position for the plot center was then found using a SOKKIA SET5 (Sokkia Topcon, 75-1 Hasunuma-cho, Itabashi-ku, Tokyo 174-8580, Japan) total station and the two GNSS measured points. The time consumption for measuring the center point coordinate was approximately 15 min. Finally, tree positions were obtained using the total station and a prism placed in front of the tree center. The prism constant and tree radius were added to the distance measurements. All trees inside the plot with a DBH larger than 4 cm were registered with position, DBH and species. The DBHs were measured once with the caliper in a random heading direction.

The expected standard deviation of the measured tree position was estimated by adding the different error contributors. This was summed up in an error budget shown in Table 2.

Table 2. Error budget for the tree positions. Standard deviations are approximated based on output from the GNSS post processing software, and inspection of the data.

Description	Standard Deviation (cm)
GNSS points coordinates	1
Plot center point coordinate	3
Tree center alignment	3
Distance from tree surface to tree center	1

We assumed that the errors were independent and summarized the variance to estimate the standard deviation for the tree positions:

$$\sqrt{1^2 + 3^2 + 3^2 + 1^2} = 4.5 \tag{1}$$

The reference tree positions were estimated to have a standard deviation of 4.5 cm.

2.3. TLS Data Collection

TLS data were collected with a Faro Focus 3D x130 scanner in May 2017. The laser scanner settings were set to give a point density of 70,000 points per m^2 at 5 m distance from the scanner. Bauwens et al. [15] measured the time consumption for a similar TLS and plot and for one single scan the time consumption was 10 min and 75 min for five scans, without positioning the scan in a global coordinate system. To have a comparable time consumption with the other methods in this study, we decided to only use one single scan per plot. A tripod with the laser scanner was placed at the center of each plot. During the reference data collection, the plot center was physically marked and the global coordinates measured. The center point coordinates were used for positioning the scanner in a global coordinate system. The laser scanner had a build-in magnetometer that was used to orient the scanner. The declination at the project location was 1.9° and the meridian convergence was 1.5°. The magnetometer reading was therefore adjusted with +0.4°. The laser point clouds were extracted using Faro Scene version 7.0. The DBH and tree positions were estimated in Computree, version 3.0 [28] using the "onfensamv2" plugin. The following gives a brief outline of the processing step using the "onfesamv2" plugin for each plot: First, the point cloud was classified into ground and vegetation points. The vegetation points were then filtered using two Euclidean filters to remove noise points. A digital terrain model was created using the points classified as ground, and a slice of points between 1.0 m and 1.5 m above the terrain was extracted. From this slice, large clusters of points were identified. The large clusters were then used to segment the point cloud into single tree clouds. From the single tree clouds, the DBH and the center coordinate of each identified tree stem were automatically extracted. The procedure was developed using the SimpleTree plugin in the Computree Software [29]. The main result was a set of positions and DBH for all automatically identified trees and referred to as the TLS tree data.

2.4. HLS Data Collection

The HLS system GeoSlam ZEB1, was used to collect data in May 2017. The system weight was 665 g and had a 15 m outdoor range [30]. It consisted of a laser ranging device mounted on a spring, and the motion created when the operator walked through the forest was an important part of the measurement technique. A comprehensive description of the instrument can be found in Bosse et al. [31], Bauwens et al. [15], Ryding et al. [16] and Giannetti et al. [32].

A star-shaped walking path used by Bauwens et al. [15] was followed to minimize occluded areas. Bauwens et al. [15] reported the HLS data capture time to be 24 min per plot without positioning the scan in a global coordinate system. This time consumption corresponds to our experience. The data capture started and ended in the plot center. The fixed walking path also ensured several loop closures which improved the navigation solution. To ensure an accurate position and orientation in the local frame SLAM was used. The processing was carried out using the Geoslam cloud processing services [15]. The result was one point cloud for each plot.

Three spherical targets were placed within each plot. The positions of these targets were derived using a total station mounted on a tripod at the plot center, with a time consumption of approximately 5 min. The total station was positioned in the same procedure as described in Section 2.2. The accurate position of each of the spherical targets was therefore known. The point cloud obtained from the GeoSLAM processing was rotated and translated from the local coordinate system to a global coordinate system (EUREF89 UTM32N) using the position of the three spherical targets. The targets were automatically detected and the coordinate system assigned using the Align tool in the CloudCompare software [33]. The RMSE values of the registration reported by CloudCompare, were <6 cm for all plots. Tree positions and DBH were derived from the point cloud using the same approach as for the TLS data, described above. The resulting dataset of tree positions and DBH is referred to as the HLS tree data.

2.5. BPLS Data Collection

A BPLS was developed as an extension of the scanner presented in Oveland et al. [8]. The BPLS was an in-house-build. Standard components were assembled in a metal frame and mounted on a backpack. The complete unit is shown in Figure 1. The main hardware improvement from the scanner presented in Oveland et al. [8] was that an additional laser scanner was added and the navigation system was changed. In this version, the navigation system was a combined IMU and dual GNSS board. The unit was called SBG Ellipse 2D (SBG systems, 1 avenue Eiffel, 78,420 Carrières-sur-Seine, France) and received GNSS signals from the Global navigation system (GPS), Globalnaja navigatsionnaja sputnikovaja Sistema (GLONASS) and the Satellite-based Augmentation System (SBAS). A GNSS antenna called PolaNt-X MF (Septentrio, Greenhill Campus, Interleuvenlaan 15i, 3001 Leuven, Belgium) worked as a master antenna. This antenna collected the main GNSS signals. A GNSS reference station operated by the Norwegian University of Life Sciences was used to calculate the initial position of the system. The maximum distance between the reference station and the plots was 800 m. An additional slave GNSS antenna manufactured by Antcom (Antcom Corporation, 367 Van Ness Way, Suite 602, Torrance, California 90501, USA) was a part of the real time heading calculation.

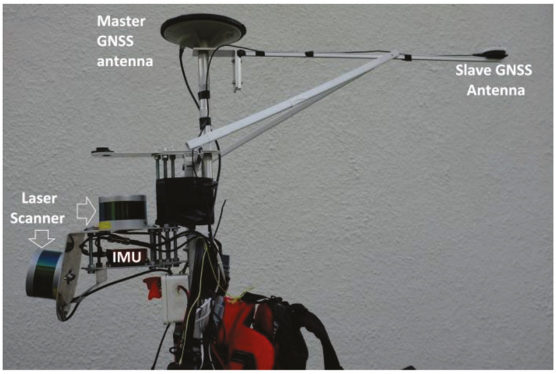

Figure 1. In-house-built backpack laser scanner.

Two laser scanners were mounted on the backpack. Both scanners received time information from the GNSS system. The main scanner collected data horizontally and the secondary scanner collected vertically. The main function of the horizontal scanner was to detect the tree stems, while the vertical scanner's main purpose was to detect the ground. Both scanners had the product name VLP16 (Velodyne LiDAR, 5521 Hellyer Avenue, San Jose, CA 95138, USA) [34]. Each scanner had 16 individual laser beams with an angle separation of two degrees. This gave a Field of view (FOV) of 30°. All 16 beams rotated continuously around the z-axis, as shown in Figure 2. This provided in total a FOV of $30° \times 360°$. The rotation speed used was 10 scan rotations per second and the pulse repetition rate was 300 KHz. All data were stored and exported to ASCII by Veloview version 3.1.1.

The data collection was performed in July 2017 and the data were collected in a star-shaped pattern similar to the HLS. The data capture was carried out by walking across the plot in a straight line through the plot center. This line was defined as a scan line. For the BPLS system, three scan lines were used per plot while the HLS system used four scan lines. With the BPLS scan pattern, the longest possible distance from a random point inside the plot to the scanner was 6.3 m. To be able to detect a tree, it was necessary to create a circle that represented the tree stem. It is necessary to have three measurements on a tree stem to be able to fit a circle to the measurements. From Oveland et al. [8], we have a formula telling that the smallest detectable tree from 6.3 m has a DBH of 4.2 cm. The resulting dataset of tree positions and DBH is referred to as the BPLS tree data. The startup and initialization of the BPLS system took approximately 10 min and the average data capture time was 6 min per plot.

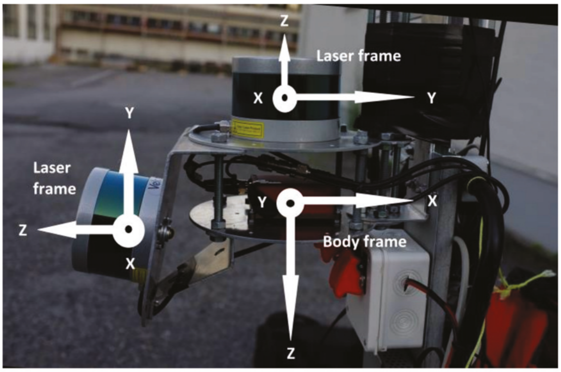

Figure 2. Location and orientation of the vertical and horizontal laser frames and body frame.

BPLS Data Processing

The novel BPLS data processing was divided into nine main steps, as shown in Scheme 1. Steps 2 and 3 are described in more detail by Oveland et al. [8]. In Step 1, position and orientation of the measurement system are calculated. The position and orientation of the measurement system will further be referred to as the pose. In the next steps, the laser data are processed to improve the pose accuracy, and finally calculate the DBH and tree position.

Step 1, illustrated in Scheme 1, was the pose calculation performed in TerraPos version 2.4.90 [27] made by Terratec AS. The input data were raw GNSS data from the main GNSS antenna, 200 Hz IMU data and the heading observation from the combined master and slave GNSS antenna solution. Additional precise ephemeris, clock correction files and earth rotation parameter files were provided from the Center for Orbit Determination in Europe (CODE). The final processing was performed in a tightly coupled GNSS/IMU/heading observation solution. The estimated poses were applied to the laser observations. This was carried out by transforming the measured laser point cloud. There were different reference frames in the BPLS system. The following frames were used:

- laser frame (l), defined by each laser scanner
- body frame (b), defined by the IMU: x-axis: in speed direction; z-axis: down
- local geodetic frame (g), same origo as the body frame: x-axis: north; y-axis: east; z-axis: down
- mapping frame (m), defined by the mapping grid: x-axis: east; y-axis: north; z-axis: up

All laser observations were realized in the laser frame x^{li}, where “i” denoted the vertical or horizontal laser scanner. The laser points in the laser frame were first transformed to body frame x^b. The transformation was performed with the following equation:

$$x^b = C^b_{\tilde{b}i} C^{\tilde{b}i}_{li} x^{li} - dx^{li}_b \quad (2)$$

where dx^{li}_b defined the vector from the body frame origo to the specified laser frame origo, measured with a total station. The rotation matrix $C^b_{\tilde{b}i}$ was used to correct for smaller rotations, also called boresight corrections. $C^{\tilde{b}i}_{li}$ performed the rough transformation from the laser to the body frame. Figure 2 shows the orientation of the axes for the horizontal laser frame, vertical laser frame and body frame. The rotation matrix was different for the vertical and horizontal laser scanner and can be written as follows:

$$C_{li}^{\tilde{b}i}\begin{pmatrix} i = vertical \\ scanner \end{pmatrix} = \begin{bmatrix} 0 & 0 & -1 \\ 1 & 0 & 0 \\ 0 & -1 & 0 \end{bmatrix}, \tag{3}$$

$$C_{li}^{\tilde{b}i}\begin{pmatrix} i = horizontal \\ scanner \end{pmatrix} = \begin{bmatrix} 0 & 1 & 0 \\ 1 & 0 & 0 \\ 0 & 0 & -1 \end{bmatrix} \tag{4}$$

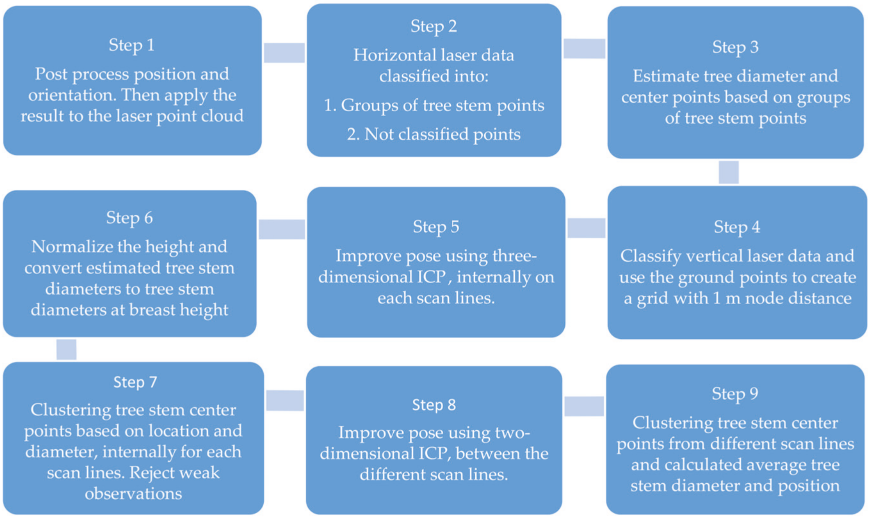

Scheme 1. Flowchart describing each step in the proposed method.

A calibration field was established with two perpendicular lines that were measured in both directions. The field was a parking lot and a road with surrounding buildings, poles and trees. The buildings were additionally measured with a traditional TLS to verify the calibration. The main purpose of the calibration was to estimate the boresight corrections $C_{\tilde{b}i}^{b}$, and verify the dx_b^{li} vector for each of the scanners. The next transformation was from the body frame to the local geodetic frame x^g. This task was performed using the rotation matrix, C_b^g, created from the orientation estimated in the navigation solution:

$$x^g = C_b^g x^b \tag{5}$$

The last transformation step was from the local geodetic frame to the mapping frame x^m:

$$x^m = C_g^m x^g + dx_g^m \tag{6}$$

The vector dx_g^m was created from the position in the navigation solution. For the BPLS data, the mapping frame was the EUREF89 Norwegian Transversal Mercator projection that has a mapping scale value close to 1 and a small grid conversion. We assumed that the grid conversion was negligible for this project. The projection gave the rotation matrix C_g^m, transforming from local geodetic to mapping frame:

$$C_g^m = \begin{bmatrix} 0 & 1 & 0 \\ 1 & 0 & 0 \\ 0 & 0 & -1 \end{bmatrix} \tag{7}$$

The pose result had a sampling rate of 200 Hz. It was assumed that the movement during one pose epoch was negligible. Laser points collected in the same time frame as the pose epoch were therefore transformed with the same parameters.

In Step 2, the horizontal laser data were segmented and classified into groups of tree stem points. The method followed the description in Oveland et al. [8].

In Step 3, all groups of tree stem points were used and tree stem diameter and position for each individual group were estimated. It was assumed that the trees were vertical. When four individual point groups were located above each other, they were assumed to be part of the same tree [8].

In Step 4, data from the vertical laser scanner were classified into ground points and non-ground points. After the classification, it was verified that the ground points covered the entire plot and the points were used to establish a grid with node distance of 1 m. These tasks were carried out in TerraScan version 16.004 from Terrasolid [35]. It is assumed that the pose error was relatively stable during one scan line. Between two scan lines, the difference can be significant, especially in height. Thus, for every scan line, a new grid was established. Points classified as ground from different scan lines were not mixed. This reduced the potential influence of deviation in the pose to a minimum.

Due to the poor GNSS condition in the forest, the pose accuracy was reduced compared to a clear sky situation. This made it difficult to merge tree observations based on positions observed at different scan rotations. In Step 5, this problem was reduced by performing scan matching using ICP. Scan matching was divided into two main parts. The first part performed scan matching between sequential scan rotations within a scan line, and the second part performed scan matching between entire scan lines described in Step 8. In both parts, the tree center points were used as input for the scan matching. The estimated tree center points from the first scan rotation at a scan line were used as fixed points. The center point estimation from the next scan rotation was then fitted to the first scan rotation with the ICP algorithm. When the data were fitted, the data were added to the fixed points and so on. One side-effect of this approach was that the entire line inherited the pose accuracy from the first fixed points. This effect was reduced by calculating the average estimated translation from the ICP and applied this to the estimated tree center points.

In Step 6, the established grid from the given scan line was used and the elevation values at the estimated center points were subtracted from the height values. This resulted in tree center positions above ground level. All observations less than 0.5 m above ground were rejected. The goal was to extract the DBH, i.e., 1.3 m above ground level. The estimated diameters were adjusted to diameter at 1.3 m above ground by applying a simple model assuming that the tree diameter was reduced by 1 cm for each meter along the tree stem.

In Step 7, the tree center points were clustered based on position and diameter. We assumed that the diameter was estimated with a standard deviation below 5 cm. If there were two groups within the search radius and the groups had a diameter difference above 15 cm, they were given a different tree identification. The circle points within a scan rotation were analyzed using random sample consensus. This technique was used to reject observations. Tree stem circle points which did not fit in a straight line were rejected. Additional identified trees with five or fewer circle observations per scan line were also rejected.

Step 8 ensured that the result from the different scan lines fitted each other. This was performed with a two-dimensional ICP method between the clustered tree stem center points from the different scan lines.

In Step 9, the results from the different scan lines were merged based on location. Finally, the average position and DBH were derived and compared to the reference.

2.6. Evaluation

The resulting tree positions and DBHs from the TLS, HLS and BPLS tree datasets were compared to the reference data. The estimated DBH were evaluated by calculating the mean difference, RMSE and RMSE% with the following equations:

$$\text{mean difference} = \frac{1}{n}\sum_{i=1}^{n}(y_i - y_{ri}) \tag{8}$$

$$\text{RMSE} = \sqrt{\frac{\sum_{i=1}^{n}(y_i - y_{ri})^2}{n}} \tag{9}$$

and

$$\text{RMSE\%} = \frac{\text{RMSE}}{\overline{y_r}}100 \tag{10}$$

In the equations, y_i is the estimate, y_{ri} the reference, $\overline{y_r}$ is the mean reference value, and n the number of observations. The reference was the result from the calipered DBH and manual tree position registrations using total station as described above. The tree position accuracy was evaluated using Equations (8) and (9).

3. Results

The TLS had a built-in magnetometer that was used to orient the scanner. The magnetometer readings were evaluated by rotating the laser scanner result until a best possible fit to the reference tree positions was achieved. Table 3 summarizes the result.

The average heading error was −0.8° with a 6.1° standard deviation. Additionally, the tree positions were calculated based on the magnetometer readings and with the corrections found in Table 3. The result is presented in Table 4.

The evaluation of the magnetometer accuracy showed that the tree position can be significantly better by improving the orientation method. The final result based on the magnetometer readings are presented in Table 5. The DBH estimation for the TLS method had two major outliers. By removing these two outliers, the mean difference was 1.5 cm, the RMSE 3.4 cm and the RMSE% 15.5.

Table 3. The heading error in the magnetometer readings, found by comparing the estimated tree positions from the terrestrial laser scanner method and the tree position from the reference.

Plot ID	Angle Difference in Heading (Degrees)
1	2.0°
2	−9.0°
3	4.9°
4	7.4°
5	1.1°
6	−6.5°
7	−5.2°

Table 4. The result from comparing the archived tree position accuracy with two different orientation methods.

Orientation Method	Mean Difference (cm)	RMSE (cm)
Magnetometer	69.1	81.8
Reference tree position	8.5	9.9

The results obtained from the HLS revealed that small trees were difficult to detect. To illustrate this, one of the plot with a high number of small trees was used as an example. In Figure 3a, the HLS tree data are plotted in green together with the reference trees in red. Figure 3b shows the laser point in the region 1.0 m to 1.5 m above ground level. By comparing Figure 3a,b, it seems that the missing trees occurred where there were no half or full donut shaped pattern in the laser data.

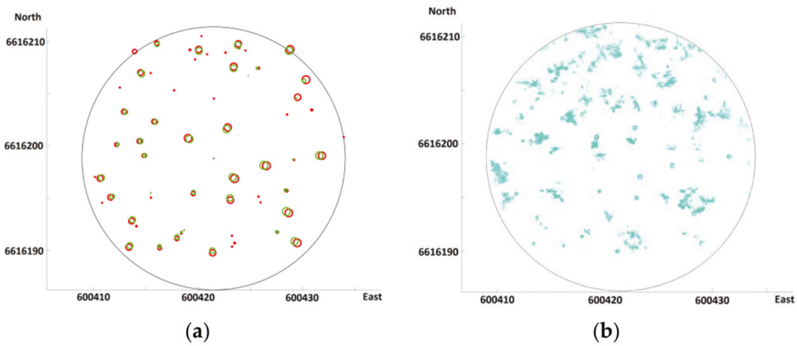

Figure 3. (**a**) Detected trees by HLS (green circle) and ground reference tree data (red circles). The size of the circle represents the DBH and the coordinate system is EUREF89 UTM zone 32. (**b**) HLS data used to extract trees.

An important factor for the BPLS method was the calculated pose accuracy. The estimated standard deviation for the position was better than 0.5 m. For roll and pitch it was better than 0.13° and for heading it was better than 0.9°. The combined master and slave GNSS antenna heading system had only 134 epochs with valid observations. The heading system was very useful during system orientation initialization. Inside the forest the position dilution of precision (PDOP) varied from 1.1 to 17. Typically, TerraPos was able to create fixed solutions when the PDOP dropped down and float solutions when it rose. Approximately 60% of the epochs had a fixed solution, but in the densest forest there were up to 18 min in-between two fixed solutions. Due to the tightly coupled solution, there were continually pose observations for the entire mission. The main result from the different methods is presented in Table 5.

The results presented in Table 5 show that up to 37.9% of the trees were not found. Table 6 presents the average DBH for the omission trees and the number of trees with DBH larger and smaller than 10 cm.

Table 5. Comparison of the results derived from the terrestrial laser scanner (TLS), handheld laser scanner (HLS) and the backpack laser scanner (BPLS). The total number of trees were 335.

Method	Omission (Not Found) %	Commission (False Trees) %	Detected Trees %	Diameter at Breast Height (cm)			Positions (cm)	
				Mean Difference	RMSE	RMSE %	Mean Difference	RMSE
TLS	37.9	5.4	61.8	-2.0	6.2	28.6	69	82
HLS	26.0	4.8	74.0	0.3	3.1	14.3	17	20
BPLS	12.5	9.9	87.5	0.1	2.2	9.1	54	62

Table 6. The average diameter at breast height (DBH) for omission trees.

Method	Average DBH for Omission Trees (cm)	Number of Omission Trees with DBH < 10 cm	Number of Omission Trees with DBH > 10 cm
Terrestrial laser scanner	16.9	67	60
Handheld laser scanner	8.7	68	19
Backpack laser scanner	7.5	36	6

4. Discussion

The coordinate for the plot center point was determined using GNSS measurements in relatively clear sky locations and measured using a total station. These established center points were also used to position the HLS and TLS data. This gave a correlation between these measurement methods and the reference data while the BPLS data were independent. Thus, the resulting uncertainties in the center point coordinates would not affect the HLS or TLS data positions statistics but would give a false position offset for the BPLS result. We assume that there were no major errors in the center point position estimation and that the errors were independent of each other. The errors presented in Table 2 are summarized:

$$\sqrt{st.dev\ GNSS\ measurment^2 + st.dev\ plot\ center\ point\ measurment^2} = \sqrt{1^2 + 3^2} = 3.2\ \text{cm} \qquad (11)$$

The center point coordinates were estimated to have a standard deviation of 3.2 cm. This was substantially less than the achieved standard deviation for all the laser scanning methods.

The caliper measurements of the DBH were conducted with one measurement in a random heading direction. Since tree stems can be ellipse-shaped, DBH measured from a different direction might deviate from this reference measurement. This can be viewed as a small uncertainty in the reference measurements, and might have an influence on the achieved DBH accuracy. The uncertainties could have been reduced by using an additional perpendicular caliper measurement or using diameter tape to measure the girth.

As shown in Figure 3a, the HLS had difficulties to detect smaller trees and this confirmed the results underlined by Bauwens et al. [15] and Ryding et al. [16]. In the situation where the HLS data formed a half or full donut shape pattern, the tree detection technique worked well (Figure 3b). Other shapes such as filled circle and odd shapes did not succeed at the same level. One reason for the blurry shapes describing the smaller trees might be the point cloud precision. Another reason might be a change in the stem inclination due to wind conditions [21]. All laser scanners had problems to detect the smaller trees. Additionally, the TLS had problems with occluded areas, since the scanning was performed only from the center. The average tree density in our study area was 969 stems/ha, but also the high number of small trees that created a complex understory vegetation contributed to the occluded areas. Both the HLS and BPLS were carried around in the plot. This reduced the occluded areas to a minimum, but there will always be some occluded areas left due to branches, leaves and bushes. The BPLS method found the largest number of trees, also when it comes to the smallest trees.

For the BPLS method, it was important to capture all the potential GNSS satellites in the forest. This was important to ensure the best possible position in the global coordinate frame. The GNSS equipment used in the BPLS could not receive signals from the GNSS created by the European Union called Galileo. The base station was able to pick up some signals from the Chinese BeiDou navigation satellite system, but these signals were not present in the BPLS GNSS data. BeiDou and Galileo together consist of 15–20 satellites. Under good GNSS observation conditions, it might have been possible to track 7–10 more satellites. Inside the forest, this could give a huge difference because just one more observed satellite could create a fix solution rather than a float solution. Signals from both Galileo and BeiDou could have improved the position accuracy. The DBH calculation for the BPLS was not vulnerable to poor GNSS condition, but the processing was smoother if the position standard deviation was below 0.5 m. The main reason for the low sensitivity to poor GNSS was the INS and the splitting of the laser data. The proposed method splits the laser data into small time frames, decided by the scan rotation of the horizontal VLP 16 laser scanner. For each 0.1 s, a new point cloud was established. This point cloud was then used to estimate the tree center point and stem diameter. ICP operations were applied to the result and ensured a homogenous localization of each tree with the corresponding attributes. This method ensured that errors from GNSS and IMU are negligible to the stem diameter and DBH calculation. This assumption was acceptable since the pose error can be considered as stable within such time interval. A side effect was the high number of point clouds, where each of them gave diameter calculation for the observed trees. The result was many diameter calculations that were used to estimate the final DBH for each tree. This had a positive impact on the DBH accuracy.

Each method used different workflows with different working tasks involved. The data capture time would mainly vary according to the number of tasks. The most time consuming method was the HLS method. This technique required static GNSS, position of the plot center, spheres position measurements and laser scanning. The total time consumption was estimated as 74 min. Some of the working tasks can be done in parallel to reduce the time consumption. However, this was not considered in this study. Table 7 summarizes the time consumption from this and previous studies. The overview shows that the BPLS was the method with the fewest working tasks, and therefore, the fastest method with an estimated time consumption of 16 min.

Table 7. The different working tasks and time consumption per plot for each laser based method.

Method	Static GNSS for Reference Points	Position Measurement of Plot Center	Position Measurement of Spheres	Laser Scanning	Total
Terrestrial laser scanner	30 min	15 min		10 min	55 min
Handheld laser scanner	30 min	15 min	5 min	24 min	74 min
Backpack laser scanner				16 min	16 min

The TLS was aligned with a built-in magnetometer. The precision of the final tree coordinates was heavily influenced by the quality of the built-in magnetometer. If the registration of the center point positions was carried out using a total station, it would not be very time consuming to put up spheres to align the scanner and thus obtain a much better precision. On the other hand, the TLS data were very homogenous in the sense that the relative positions within each plot were consistent. Thus, the highly accurate tree positions of the detected trees are a really good starting point as input for matching the data with airborne laser data [36], to improve position accuracy.

The main data capture was performed in May 2017, before the leaves had emerged. The BPLS data collection was delayed due to technical problems and was performed in early July 2017. The leaves had emerged, which might have had an effect on the tree stem visibility and the number of false trees. An example from plot number three is shown in Figure 4a,b. The tree growth between the two points in time were assumed to have a minor effect on the DBH.

The data capture with the BPLS was carried out by walking across each plot in straight lines forming a star-shaped pattern. The number of lines decided the maximum possible distance to the potential trees inside the plot. In this study, we used three scan lines and this gave a theoretical minimum detectable DBH of 4.2 cm for the BPLS. In the reference data, the minimum DBH was set to 4.0 cm. This means that there are small areas at the outer edge where we were unable to detect the smallest trees. In this study, the total area was 0.4% of a plot and was assumed to be at an acceptable level.

For a long time, studies have reported large commission errors [37] when laser based methods have been used. More recent studies confirm these observations [15,22]. Reported commission errors vary from 0% to 31% [15]. The result in our study showed that the number of false trees—i.e., commission errors—were up to 9.9% of the total number of field reference trees. Most of the false trees had a DBH less than 10 cm. In the reference data, all trees with a DBH larger than 4 cm were measured. No trees with a smaller DBH than 4 cm were measured. Since the measurement methods have uncertainties, it is possible that some of the trees which were estimated to have a larger DBH than 4 cm actually were trees with DBH smaller than 4 cm. In such situations, the trees would be registered as false trees. In the BPLS method, the laser point clouds were segmented into tree points, ground points and none classified points. The segmentation was based on a rule based approach. This could in further studies be changed to a machine learning approach. This has the potential to improve the tree segmentation and reduce the commission errors.

(**a**) (**b**)

Figure 4. (**a**) Understory vegetation in May 2017. (**b**) Understory vegetation in July 2017 at the same location as (**a**).

The obtained results for the DBH estimation are compared to results in other recent studies in Table 8. All TLS methods in Table 8 were performed with one single scan in the center of the plot. Our TLS result had a lower accuracy compared to similar studies [15,23,24]. Potential explanations for this might be the tree density and the understory vegetation and how this affect the DBH calculation. Other elements that might affect the DBH extraction are the ranging method in the laser scanner, the scanner characteristics, scan settings and data processing [24]. The TLS method in our study had two large outliers. An outlier search might have detected these outliers and thus reduced the RMSE and RMSE% to 3.4 cm and 15.5, respectively.

Table 8. Comparison of current results with previous studies derived from the terrestrial laser scanner (TLS), handheld laser scanner (HLS) and the backpack laser scanner (BPLS). * mean value calculated from Liang and Hyyppä [23]. ** single scan, Lemen algorithm, beech plot [24].

Reference	Method	Equipment	Mean Difference (cm)	RMSE (cm)	RMSE%
This study	TLS	Faro Focus 3D x130	−2.0	6.2	28.6
[15]	TLS	Faro Focus 3D x120	−1.2	3.7	13.4
[23]	TLS	Leica HDS6100	0.5*	1.5*	7.3*
[24]	TLS	Faro photon 120	−0.1**	1.6**	-
This study	HLS	GeoSlam ZEB1	0.3	3.1	14.3
[15]	HLS	GeoSlam ZEB1	−0.1	1.1	4.1
[16]	HLS	GeoSlam ZEB1	0.5	2.9	23
This study	BPLS	Velodyne VLP 16	0.1	2.2	9.1
[8]	BPLS	Velodyne VLP 16	0.9	1.5	7.5

In general, the TLS, HLS and BPLS result in this study have larger RMSE and RMSE% values compared to other studies. One advantage of our study was that the different methods have the same preconditions regarding stem density, tree species, stem sizes, understory vegetation, reference data and plot size. This makes it easier to compare the different methods used in the study. On the other hand, the DBH extraction algorithm for the TLS and HLS method might vary from the state-of-the-art DBH. In this study, the BPLS method achieved the best accuracy with the smallest level of omissions, however the largest level of commissions was also obtained.

BPLS seems to be a very promising method in terms of time consumption for data collection. Thus, BPLS might have great potential as a cost-effective data source in forest inventory. Moreover, a final decision about the most profitable source of data for forest inventory should not be based on purely technical considerations, such as reported accuracies. It is of fundamental importance for management that the costs of acquiring the information are balanced against the utility of the information for decision-making. Thus, we recommend that future research focus on this trade-off using for example so-called cost-plus-loss analyses, which may establish a link between errors associated with the inventory and expected losses as a result of future incorrect decisions due to the errors in the data.

5. Conclusions

In this study, we have proposed a novel laser based BPLS method for acquisition of ground references data and compared the method with other laser based systems. The proposed method is a further development of the method presented in Oveland et al. [8]. Novel aspects in the method are how the trees are segmented and how the diameters at breast height are estimated without losing precision due to potential reduced position and orientation accuracy. Most importantly, the trees are directly positioned in a global coordinate system using a GNSS aided inertial navigation system in combination with an iterative closest point approach. The study has compared three different laser based methods to extract the diameter at breast height and tree position within seven different plots. The different methods are BPLS, HLS and TLS. Comparison with manual measurements shows that the TLS method in general had the most consistent positioning of the trees, but is vulnerable to occluded areas. The HLS method has difficulties detecting smaller trees. The fastest and most accurate method in this study is the BPLS, where the diameter at breast height has a mean difference of 0.1 cm, root mean square error of 2.2 cm and the largest amount of detected trees with 87.5%. The BPLS has however the highest number of false trees and the tree positions are slightly degraded, but the position accuracy should be acceptable for many forestry inventory purposes. Thus, the BPLS seems to be promising and further development should be focused on the possibility to go from a GNSS aided inertial navigation system to a GNSS and laser odometry aided inertial navigation system in combination with simultaneous localization and mapping. Cost-plus-loss analyses of the final forest inventory results assessing required accuracy of ground reference data should also be subject to further research.

Supplementary Materials: The following are available online at http://www.mdpi.com/2072-4292/10/4/538/s1, Video 20170703_backpack_scanner.mp4: Data collection with the backpack laser scanner system.

Acknowledgments: The study was partly funded by the Research Council of Norway through the project "Sustainable Utilization of Forest Resources in Norway" (grant #225329/E40).

Author Contributions: Ivar Oveland wrote the paper, performed the BPLS fieldwork, conducted the hardware installation, method development, and processed the data. Marius Hauglin co-authored the paper, performed the TLS fieldwork, the caliper fieldwork and processed the data. Francesca Giannetti performed the HLS fieldwork and processed the data, performed the caliper fieldwork and revised the paper. Narve Schipper Kjørsvik provided the GNSS/IMU processing tool, supported the pose processing and revised the paper. Terje Gobakken supervised the study and revised the paper.

Conflicts of Interest: Narve Schipper Kjørsvik works at Terratec AS which is a GNSS/IMU software dealer. The authors declare no conflict of interest.

References

1. Vauhkonen, J.; Maltamo, M.; McRoberts, R.E.; Næsset, E. Introduction to forestry applications of airborne laser scanning. In *Forestry Applications of Airborne Laser Scanning*; Springer: Berlin, Germany, 2014; pp. 1–16.
2. Næsset, E. Practical large-scale forest stand inventory using a small-footprint airborne scanning laser. *Scand. J. For. Res.* **2004**, *19*, 164–179. [CrossRef]
3. Gjertsen, A.K. Accuracy of forest mapping based on Landsat TM data and a kNN-based method. *Remote Sens. Environ.* **2007**, *110*, 420–430. [CrossRef]
4. Breidenbach, J.; Næsset, E.; Lien, V.; Gobakken, T.; Solberg, S. Prediction of species specific forest inventory attributes using a nonparametric semi-individual tree crown approach based on fused airborne laser scanning and multispectral data. *Remote Sens. Environ.* **2010**, *114*, 911–924. [CrossRef]
5. Liang, X.; Kankare, V.; Hyyppä, J.; Wang, Y.; Kukko, A.; Haggrén, H.; Yu, X.; Kaartinen, H.; Jaakkola, A.; Guan, F.; et al. Terrestrial laser scanning in forest inventories. *ISPRS J. Photogramm. Remote Sens.* **2016**, *115*, 63–77. [CrossRef]

6. Liang, X.; Litkey, P.; Hyyppa, J.; Kaartinen, H.; Vastaranta, M.; Holopainen, M. Automatic Stem Mapping Using Single-Scan Terrestrial Laser Scanning. *IEEE Trans. Geosci. Remote Sens.* **2012**, *50*, 661–670. [CrossRef]
7. Lindberg, E.; Holmgren, J.; Olofsson, K.; Olsson, H. Estimation of stem attributes using a combination of terrestrial and airborne laser scanning. *Eur. J. For. Res.* **2012**, *131*, 1917–1931. [CrossRef]
8. Oveland, I.; Hauglin, M.; Gobakken, T.; Næsset, E.; Maalen-Johansen, I. Automatic Estimation of Tree Position and Stem Diameter Using a Moving Terrestrial Laser Scanner. *Remote Sens.* **2017**, *9*, 350. [CrossRef]
9. Simonse, M.; Aschoff, T.; Spiecker, H.; Thies, M. Automatic Determination of Forest Inventory Parameters Using Terrestrial Laserscanning. Available online: http://www.natscan.uni-freiburg.de/suite/pdf/030916_1642_1.pdf (accessed on 30 March 2018).
10. Strahler, A.H.; Jupp, D.L.B.; Woodcock, C.E.; Schaaf, C.B.; Yao, T.; Zhao, F.; Yang, X.; Lovell, J.; Culvenor, D.; Newnham, G.; et al. Retrieval of forest structural parameters using a ground-based lidar instrument. *Can. J. Remote Sens.* **2008**, *34*, S426–S440. [CrossRef]
11. Yao, T.; Yang, X.; Zhao, F.; Wang, Z.; Zhang, Q.; Jupp, D.; Lovell, J.; Culvenor, D.; Newnham, G.; Ni-Meister, W.; et al. Measuring forest structure and biomass in New England forest stands using Echidna ground-based lidar. *Remote Sens. Environ.* **2011**, *115*, 2965–2974. [CrossRef]
12. Raumonen, P.; Kaasalainen, M.; Åkerblom, M.; Kaasalainen, S.; Kaartinen, H.; Vastaranta, M.; Holopainen, M.; Disney, M.; Lewis, P. Fast Automatic Precision Tree Models from Terrestrial Laser Scanner Data. *Remote Sens.* **2013**, *5*, 491–520. [CrossRef]
13. Dassot, M.; Constant, T.; Fournier, M. The use of terrestrial LiDAR technology in forest science: Application fields, benefits and challenges. *Ann. For. Sci.* **2011**, *68*, 959–974. [CrossRef]
14. Astrup, R.; Ducey, M.J.; Granhus, A.; Ritter, T.; von Lüpke, N. Approaches for estimating stand-level volume using terrestrial laser scanning in a single-scan mode. *Can. J. For. Res.* **2014**, *44*, 666–676. [CrossRef]
15. Bauwens, S.; Bartholomeus, H.; Calders, K.; Lejeune, P. Forest Inventory with Terrestrial LiDAR: A Comparison of Static and Hand-Held Mobile Laser Scanning. *Forests* **2016**, *7*, 127. [CrossRef]
16. Ryding, J.; Williams, E.; Smith, M.; Eichhorn, M. Assessing Handheld Mobile Laser Scanners for Forest Surveys. *Remote Sens.* **2015**, *7*, 1095–1111. [CrossRef]
17. Forsman, M.; Holmgren, J.; Olofsson, K. Tree Stem Diameter Estimation from Mobile Laser Scanning Using Line-Wise Intensity-Based Clustering. *Forests* **2016**, *7*, 206. [CrossRef]
18. Palleja, T.; Tresanchez, M.; Teixido, M.; Sanz, R.; Rosell, J.; Palacin, J. Sensitivity of tree volume measurement to trajectory errors from a terrestrial LIDAR scanner. *Agric. For. Meteorol.* **2010**, *150*, 1420–1427. [CrossRef]
19. Masiero, A.; Fissore, F.; Guarnieri, A.; Piragnolo, M.; Vettore, A. Comparison of low cost photogrammetric survey with TLS and Leica Pegasus Backpack 3D models. *Int. Arch. Photogramm. Remote Sens. Spat. Inf. Sci.* **2017**, *42*.
20. Pierzchała, M.; Giguère, P.; Astrup, R. Mapping forests using an unmanned ground vehicle with 3D LiDAR and graph-SLAM. *Comput. Electron. Agric.* **2018**, *145*, 217–225. [CrossRef]
21. Heinzel, J.; Huber, M.O. Tree Stem Diameter Estimation From Volumetric TLS Image Data. *Remote Sens.* **2017**, *9*, 614. [CrossRef]
22. Liang, X.; Kukko, A.; Kaartinen, H.; Hyyppä, J.; Yu, X.; Jaakkola, A.; Wang, Y. Possibilities of a Personal Laser Scanning System for Forest Mapping and Ecosystem Services. *Sensors* **2014**, *14*, 1228–1248. [CrossRef] [PubMed]
23. Liang, X.; Hyyppä, J. Automatic Stem Mapping by Merging Several Terrestrial Laser Scans at the Feature and Decision Levels. *Sensors* **2013**, *13*, 1614. [CrossRef] [PubMed]
24. Pueschel, P.; Newnham, G.; Rock, G.; Udelhoven, T.; Werner, W.; Hill, J. The influence of scan mode and circle fitting on tree stem detection, stem diameter and volume extraction from terrestrial laser scans. *ISPRS J. Photogramm. Remote Sens.* **2013**, *77*, 44–56. [CrossRef]
25. Andersen, H.-E.; Clarkin, T.; Winterberger, K.; Strunk, J. An accuracy assessment of positions obtained using survey-and recreational-grade global positioning system receivers across a range of forest conditions within the Tanana Valley of interior Alaska. *West. J. Appl. For.* **2009**, *24*, 128–136.
26. Kaartinen, H.; Hyyppä, J.; Vastaranta, M.; Kukko, A.; Jaakkola, A.; Yu, X.; Pyörälä, J.; Liang, X.; Liu, J.; Wang, Y.; et al. Accuracy of Kinematic Positioning Using Global Satellite Navigation Systems under Forest Canopies. *Forests* **2015**, *6*, 3218–3236. [CrossRef]
27. *TerraPos version 2.4.90*; GNSS/INS post processing software; Terratec: Oslo, Norway; Available online: https://www.terratec.no/terrapos (accessed on 16 November 2017).

28. Office National des Forêts. *Computree version 3.0*; A software platform for processing Terrestrial LiDAR data to extract forest information; Office National des Forêts: Paris, France, 2010; Available online: http://computree.onf.fr/?lang=en (accessed on 16 November 2017).
29. Hackenberg, J.; Spiecker, H.; Calders, K.; Disney, M.; Raumonen, P. SimpleTree —An Efficient Open Source Tool to Build Tree Models from TLS Clouds. *Forests* **2015**, *6*, 4245. [CrossRef]
30. Geoslam. *GeoSlam Zeb-1*; Geoslam: Ruddington, Nottinghamshire, UK; Available online: https://geoslam.com/hardware/zeb-1/ (accessed on 16 November 2017).
31. Bosse, M.; Zlot, R.; Flick, P. Zebedee: Design of a spring-mounted 3-d range sensor with application to mobile mapping. *IEEE Trans. Robot.* **2012**, *28*, 1104–1119. [CrossRef]
32. Giannetti, F.; Chirici, G.; Travaglini, D.; Bottalico, F.; Marchi, E.; Cambi, M. Assessment of Soil Disturbance Caused by Forest Operations by Means of Portable Laser Scanner and Soil Physical Parameters. *Soil Sci. Soc. Am. J.* **2017**, *81*, 1577–1585. [CrossRef]
33. Girardeau-Montaut, D. *CloudCompare version 2.8*; Open source 3D point cloud processing software. Available online: http://www.danielgm.net/cc/ (accessed on 16 November 2017).
34. Velodyne Lidar, PUCK, VLP16. Available online: http://velodynelidar.com/vlp-16.html (accessed on 1 October 2017).
35. Anon. *TerraScan User's Guide*; Terrasolid Ltd.: Helsinki, Finland, 2011.
36. Hauglin, M.; Lien, V.; Næsset, E.; Gobakken, T. Geo-referencing forest field plots by co-registration of terrestrial and airborne laser scanning data. *Int. J. Remote Sens.* **2014**, *35*, 3135–3149. [CrossRef]
37. Bienert, A.; Scheller, S.; Keane, E.; Mohan, F.; Nugent, C. Tree Detection and Diameter Estimations by Analysis of Forest Terrestrial Laser Scanner Point Clouds. In Proceedings of the ISPRS Workshop on Laser Scanning 2007 and SilviLaser 2007, Espoo, Finland, 12–14 September 2007; pp. 50–55.

PAPER IV

Laser scanning of buildings, product specification and Level of Accuracy evaluation

Ivar Oveland [1*], Inge Revhaug [1], and Ivar Maalen- Johansen[1]

Ivar Oveland et al. As built laser scanning of existing buildings, product specification and Level of Accuracy evaluation

KART OG PLAN, Vol. 78, pp. xxx–xxx, POB 5003, NO-1432 Ås, ISSN 0047-3278

Laser scanning of existing buildings to extract a building information model has become more common in recent years. The different providers have different instrumentations, methods, technologies and deliver different qualities. When announcing a project for tender, it is important to order a scanning with an unambiguous product specification. This ensures a predictable product and equal competition terms for the providers. Hjelseth et al. presented a framework for product specification at the World Building Congress 2016. This study evaluates the usability of this framework. The framework was tested in a renovation project at the Norwegian University of Life Sciences. A method inherited from the airborne laser industry was used to evaluate the terrestrial scanning. The proposed method is described in the Norwegian standard "Produksjon av basis geodata," but scaled up to work in a three-dimensional environment. Further, the study tested the usability of the Norwegian standard "Geodatakvalitet" to evaluate the statistical significance in relation to the product specification. This article proposes an accuracy evaluation method and proposes an updated product specification framework for building surveys.

Keywords: level of accuracy, AS built, BIM, Laser scanning

[*]*Ivar Oveland,* PhD-Student, Norwegian University of Life Sciences, Faculty of Science and Technology, P.O.B. 5003, NO-1432 Ås. E-mail: ivar.oveland@nmbu.no

1. Introduction

A building information model (BIM) for an existing building has a great potential to ensure efficient facility management (1). There are several different methods to establish a BIM. In general, there are three main steps (2):

1. Point measurement
2. Creating a 3D model
3. Establish building objects enriched with attributes and relations

The cost related to each step varies with the Level of Accuracy (LoA), Level of Development (LoD) and the available instrumentation and methodology. The different methods to establish a BIM have in common that data collection needs to be conducted from

[1]Norwegian University of Life Sciences, Faculty of Science and Technology; ivar.oveland@nmbu.no (I.O); inge.revhaug@nmbu.no(I.R); ivar.maalen@nmbu.no (I.M.J)

different locations inside the building. Different errors occur such as instrument calibration errors and registration errors, Tang et al. (3). Terrestrial laser data from inside a building can be difficult to collect and verify. One of the challenges is to prevent errors to accumulate while the scanner moves through the building. There are two essential standards used to specify the accuracy of a building survey. One from the Deutsches Institut für Normung : DIN18710 Engineering survey(4, 5). In the following referred to as DIN18710. The second from the U. S. Institute of Building Documentation: USIBD Level of accuracy specification guide (6) and will be referred to as USIBD.

DIN18710 specifies survey requirements for construction works and standardizes the quality and verification in accuracy levels. DIN18710 separates between horizontally and vertically directions. Both are divided into five different levels ranging from very low accuracy to very high accuracy. For the horizontal, the levels are named L1 to L5. This standard uses correctness and precision. Correctness or trueness is given by the systematic error between the true value and the average of the measured values. Precision describes the variation of the measurements.

The U.S. Institute of building documentation used the DIN18710 as a model for the USIBD. The main difference compared to DIN18710 is that USIDB has included LoD. In the USIBD, different categories in LoD may have different LoAs. This gives the possibility to set different accuracy demands for different building object categories. The USIDB have five different accuracy levels called LOA10 (low accuracy) to LOA50 (high accuracy). The accuracy limits in DIN18710 correspond with the USIBD limits, but DIN18710 operates with standard deviations while USIDB operates with 95% confidence level. The LoA limits therefore need to be divided by 1.96 to correspond with the accuracy limits in DIN18710 when assuming a normal distribution.

Gross error detection and reliability was commonly used in the Norwegian land surveying community after a project lead by the "Norges teknisk-naturvitenskapelige forskningsråd," where a user guide was published by Espelund et al. (7). The method was implemented in land surveying software like GisLine(8), Powel Gemini Oppmåling (9) and ISY WINMAP landmåling (10). The quality was expressed by internal and external reliability, Teunissen(11) and Revhaug (12). Internal reliability is given by the smallest gross errors that the gross error test is able to detect. Larger gross errors are expected to be removed. Smaller gross errors may remain and influence the result of the computation. External reliability or deformation analyses is given by the largest influence of a remaining small error. In the proposed method all laser measurement is connected to a network of known points. This requires that the network has high accuracy. External reliability is the surveyor's tool to check the accuracy and to evaluate if the result is within a given tolerance. The external reliability can be expressed as point deformation, scale deformation and angle deformation (7, 8, 13, 14), where the different realizations have different characteristics.

Both DIN18710 and the USIDB use the estimated standard deviation. There are different approaches to estimate the standard deviation. One approach is to measure relative distances inside a building. Typically, between different building objects or measured dimensions of a single building object (15). In traditional large-scale mapping projects, it is normal to survey the locations of objects with land surveying or other technics and compare the positions with the delivered map. This approach is described in the standard “Geodatakvalitet” (16), in the following referred to as GeodataQuality. This standard uses a framework based on EN ISO19157:2013 (17).

Instead of using control measurements in the building, it is possible to analyze the deviations in laser point clouds collected from different locations (3, 15, 18), a method commonly used in the large-scale airborne laser mapping industry (19). This deviation method is an effective tool to discover calibration issues for the sensor used for the data capture and to evaluate the position and orientation errors between different data capture locations (15). Other potential errors are mixed pixels due to spatial discontinuity edges, and range errors due to specular reflectance (multipath) (18). The deviation method highlights potential problem areas and looks into deviation patterns (3). This gives a good visualization of the problem areas and has the potential to indicate the source of the problem. The deviation method assumes a proper overlap between the different scan positions. The airborne laser industry uses a method involving cross scan lines and requires that a perpendicular scan line covers a cross-section of all scan lines. This prevents small errors to accumulate between different scan lines. In large buildings with a high number of scan locations, it might be difficult to identify small errors that might have accumulated over a large number of scan locations. These types of error propagation are difficult to handle without additional support or sufficient overlap.

There are different approaches to control a terrestrial laser scanning. Some are based on markers in the field. Typical markers are reflective tape, April tags, checkerboards, natural targets or similar. Common for all is that physical markers need to be placed in the building before scanning. In the airborne laser industry, it is common to use natural targets in the field. The standard "Produksjon av basis geodata” (20) describes a procedure to control an airborne laser project and will in the following be referred to as GeodataProduction. The procedure uses unmarked control surfaces to evaluate the height accuracy. Since they are not marked, it is not necessary to perform any fieldwork before the scanning. This is an arrangement that ensures a flexible control method. The shape of the control surfaces are typical quadratic, and the side length depends on the point density. The method described in GeodataProduction has the capability to control one dimension, typically in height.

This study focused on laser scanning of existing buildings and looked into two different aspects. The first aspect evaluated a framework for a product specification presented by Hjelseth et al. (2). An unambiguous product specification is an important tool to ensure a fair tendering process with clear regulations. It has the potential to increase the product reliability and to decide the criteria for the product evaluation. The second aspect was related to accuracy evaluation of a laser scanning project. We propose to use the control procedures from the airborne laser scanning industry to control an indoor laser scanning. The control procedure described in GeodataProduction section 7, is scaled up to three dimensions. Additionally, GeodataQuality was used as a framework to evaluate the result and the statistical significance of the findings. The result was used to update the framework for product specification presented by Hjelseth et al. (2).

2. Materials and Methods

2.1. Product specification presented at the World Building Congress 2016

In 2017 the Norwegian University of Life Sciences started the renovation of the main building at the Faculty of Science and Technology. A full terrestrial laser scanning of the building was performed to support the renovation. The tendering process used the product specification presented by Hjelseth et al.(2) at the World Building Congress 2016, but reduce the number of accuracy levels. In the tendering process, the contractor could choose which accuracy level to use. Two out of five contractors specified which accuracy level they would provide and one out of five gave a proper description on how to achieve the result. The final contractor selected accuracy level 1. Table 1 summarizes the optional accuracy levels.

Table 1. Accuracy Levels

Accuracy level	Level 1	Level 2
Relative accuracy	0.003 m	0.010 m
Maximum average deviation	0.010 m	0.040 m

Calculated on a 0.2 m x 0.2 m control area.

Flat surfaces in the point cloud should have an average offset distance smaller than the "Maximum average deviation" compared to the true coordinate realized in the reference frame EUREF89, map projection NTM, zone 10 and height system NN2000.

2.2. Accuracy levels interpreted into the evaluation framework

The selected evaluation framework GeodataQuality is based on standard deviation, systematic deviation, and gross errors. Compared to the accuracy level presented in Table 1, two accuracy indicators were missing. These were the standard deviation and gross errors. To be able to use the GeodataQuality, an interpretation was needed. The accuracy level in Table 1 consists of relative accuracy and maximum average deviation. The maximum average deviation corresponds to the systematic deviation in GeodataQuality. Using a 99.7% confidence interval, the standard deviation demand was found by dividing the maximum average deviation by a factor of three. This gave a standard deviation demand of 0.003 m. The relative accuracy parameter in Table 1 was interpreted to be the variation along a perpendicular axis within a 0.2m x 0.2 m surface, realized as a standard deviation. The variation can be described as the point cloud thickness. If the laser point cloud has a high noise level, a flat surface will appear as a thick carpet in the point cloud. This results in poor relative accuracy. Another situation with large point cloud thickness is typically when a flat surface appears as multiple surfaces. This situation can occur where the same surface is measured from different scan locations, and the position or orientation of the scanner is poor. This situation is an example that gives a poor relative accuracy. This accuracy indicator is not a part of the framework described in GeodataQuality but was added to the evaluation proposal. The gross error was defined as a large error that clearly deviated with the expected error distribution, typically a weak position and orientation estimate of a scan position.

2.3. Establishment of the known points

2.3.1. Locations of the known points

A network surrounding the building was established. The network points are referred to as known points. The main purpose of the known points was to establish a local reference frame and to establish a connection to a global reference frame. Finally, the know points are used to control the terrestrial laser measurements. All laser measurements should be realized in the local reference frame defined by the known points. In total, eight known points were established and surveyed with high accuracy. Figure 1 shows the location of the known points.

Figure 1. The project building with the surrounding network of known points.

It can be challenging to find good locations for the known points. They should be close to the building and have good sky visibility to optimize the GNSS condition. Three of the points had good sky visibility. The rest of the points had obstacles blocking part of the sky. Table 2 shows the angle above the horizon for the highest obstacles at each of the known points. This gives an overview of the sky visibilities.

Table 2. Sky visibility expressed as the highest obstacles above the horizon in degrees

Point ID	Highest obstacles, angle above horizon
100	27°
N9	23°
102	45°
103	44°
N7	33°
104	42°
VEI	61°
N8	78°

(**a**) (**b**)

Figure 2. (a) shows the sky visibility at point VEI and (b) shows the sky visibility at point N8. The blue line has an elevation of 23° above the horizon.

Figure 2 shows examples of typical bad visibility situations. The known points coordinates were measured using three different methods:

- Real-Time Kinematic (RTK) GNSS
- Static GNSS,
- Closed traverse measured with a total station.

2.3.2. RTK GNSS

The RTK GNSS measurements were done with a Topcon Hiper SR using the CPOS services (21) from The Norwegian Mapping Authority. The expected standard deviation under optimal conditions is 0.008 m in the horizontal direction and 0.020 m in height according to The Norwegian Mapping Authority (22). All points were measured three times with approximately 20 minutes between the first and second round and 7 hours between the first and third round. The repetition ensured measurements with different satellite constellations to increase the independence between measurements. The final RTK GNSS result was found by averaging the result from each round.

2.3.3. Static GNSS

All static GNSS measurements were performed with Topcon Legant 2 antennas and Topcon GB-3 receivers as individual baselines. Each point was measured up to three times with individual alignment of tripod and antenna. The number of measurements and total observation time varied between each point due to different GNSS observation conditions and sky visibility. The measurement method has the potential to achieve a standard deviation of 0.003 m with short baselines(23).

For each known point, a GNSS vector was measured to a point called AASC, in the national grid with a permanent GNSS station. The maximal vector distance was 700 m. The national grid is managed by the Norwegian Mapping Authorities who claims the coordinate standard deviation to be 0.005 m. All GNSS processing were performed with the software Terrapos, v 2.3.99b3 from Terratec (24) and the result was exported as a point observation with covariance.

2.3.4. Closed traverses, total station

The closed traverses were performed with the total station Topcon ES 103 and Sokkia AP11 prism with a target plate. All observations were performed in both faces and measured in two independent closed traverses, except point 103 which only was included in one closed traverse.

2.4. Terrestrial laser scanning

The terrestrial laser scanning was performed by Astacus AB in June 2016. The survey was performed with instruments from Zoller Fröhlich called IMAGER 5010 3D laser scanner (25). In total 1189 different scan positions were made. A combination of reflecting targets and circle checkerboards was used to support the alignment of the different scans. Eight of the reflecting targets had known positions. The point cloud processing was done with Leica Cyclone (26). In the end, the point cloud was translated and rotated to the known points described in section 2.3.1 with a best-fit approach.

2.5. Control measurements

The GeodataProduction standard use control surfaces to evaluate the height accuracy in airborne laser projects. A typical control surface is a square grid of surveyed control points. The size of the control surface and the number of control points may vary based on the laser point density. The smallest control surface described in GeodataProduction is 4 m^2 containing 13 control point and is used in airborne laser projects with a point density from 3 points per m^2. This point density will provide more than 12 laser points within the control surfaces. To correspond, we assumed that 12 laser points or more located within each control surface were sufficient and the size of the control area was set to 0.2 m x 0.2 m. Since terrestrial laser scanning has high point density, it was assumed that control surfaces containing one control point were sufficient. Three perpendicular axes were selected and aligned with the building. The building used in this study is aligned in a west to east direction, and special alignment of the axes was not necessary. Several control areas aligned perpendicular to the selected axes were found, and control points were surveyed in reflector less mode with the total station Topcon ES103. The angle between the surface normal and the measuring beam was tried minimized. According to the instrument manual, the distance accuracy without prism was 0.003 m with additional 2 parts per million. A simplified error budget for the control points survey is listed in Table 3.

Table 3. Summarizes a simplified error budget for the control point measurements.

Error	St. deviation (m)
Centering of prism	0.002
Error of pointing	0.002
Distance measurement	0.003

We assumed that each element was independent and used the propagation of error to summarize the standard deviations, as shown in Equation 1:

$$\sigma = \sqrt{(0.002)^2 + (0.002)^2 + (0.003)^2} = 0.004\ m \tag{1}$$

Some measurements were done from the outside through open windows. Other measurements were performed inside the building while performing a closed traverse through the building. In the closed traverse, a combination of reflecting targets and unmarked control points were used. Altogether 159 control points were measured. Figure 3 shows the location of the control points and the measurement method.

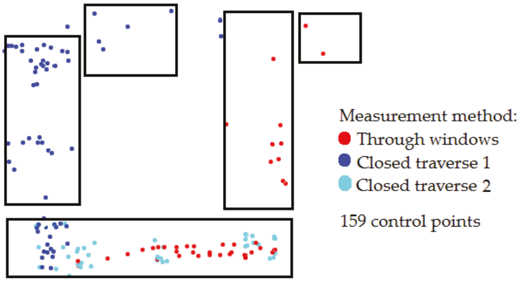

Figure 3. The location of the measured control points

2.6. Deviation

Vosselman and Maas (27) section 7, divides point-wise comparison into three different classes. These are "point to point", "point to surface" and "surface to surface". The comparison method used in this study was "point to surface", where the control measurements were the points, and the terrestrial laser measurements were the surfaces. The systematic deviation between the control points and the delivered laser point cloud was measured manually in Tscan v. 17.001 from Terrasolid (28). This was performed by plotting a 0.2 m wide vertical profile that showed the laser points and the control point. The deviation is the distance from the center of the laser points within the control area to the control point shown in Figure 4. The deviation was measured along a line perpendicular to the surface described by the laser points within the 0.2 m x 0.2 m control area.

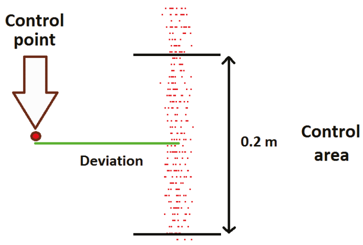

Figure 4. The control points were used to measured potential deviations in the laser point cloud.

Walls facing north was used to measure deviations in the north direction. Walls facing east was used to measure deviations in the east direction, and floors and ceiling were used to measure deviations in the height direction.

2.7. GeodataQuality as a framework to evaluate the result

In general, the framework presented in GeodataQuality can be described in six steps:

1. Find the total number of objects as defined in GeodataQuality
2. Decide the minimum number of control points
3. Calculate the systematic deviation, a_{offset}
4. Calculate the standard deviation σ_{offset} for the systematic deviation
5. Calculate the standard deviation for the measured control points, $\sigma_{control}$
6. Estimate the rejection values

The first step was to decide the number of objects. Based on the laser scanners specification (25) we assumed that one terrestrial laser scanning realized in a local coordinate frame was very accurate and down to a sub-millimeter level . The consequence of the assumption was that the internal accuracy within a limited sized room was consider to be high. Fitting errors may occur when multiple scans from different rooms were merged into a common point cloud. Based on this assumption it was assumed that one object was the same as one room. Step 2 was found in a lookup table in GeodataQuality (16). The systematic deviations in step 3 were found by averaging the deviation in each of the three directions. The standard deviation in step 4 was found based on the measurement used in step 3. The standard deviation for the control measurements in step 5 was found with Equation 1 and Table 4. In step 6 the rejection values were estimated. This was calculated for both the standard deviation σ_{offset} and the systematic deviation, a_{offset}. The calculation was based on statistical hypotheses testing described in (11, 16, 29) .

The H_0 hypothesis was that the standard deviation for the laser points called σ_{laser} was equal or better than the demanded standard deviation, σ_{demand}. We assumed that the error was normally distributed. The H_0 and the alternative hypothesis H_1 were:

$$H_0: \sigma_{laser} \leq \sigma_{demand}$$

$$H_1: \sigma_{laser} > \sigma_{demand}$$

We also assumed that the control point measurements and the laser measurements were independent. Based on this assumption Equation 2 express the σ_{laser} as:

$$\sigma_{laser}{}^2 = \sigma_{offset}{}^2 - \sigma_{control}{}^2 \tag{2}$$

The estimated standard deviations for the measurements deviations were evaluated with a Fisher test with a significance level, $\alpha = 0.05$. Equation 3 was used to estimate the rejection limit. H_0 was rejected if the Rejection limit $> \sigma_{demand}$.

$$Rejection\ limit = \frac{\sqrt{\sigma_{offset}{}^2 - \sigma_{control}{}^2}}{\sqrt{F_{0.05,n-1,\infty}}} \tag{3}$$

Similar statistical hypothesis was present for the systematic deviation called a_{offset}. The a_{offset} was computes as the average of all measured offsets between the laser point cloud and the control points. The Maximum average deviation demand a_{demand} was collected from Table 1. The standard deviation for the a_{offset} was found by dividing the σ_{offset} by the square root of the number of observations and was built into Equation 4.

$$H_0: a_{offset} \leq a_{demand}$$

$$H_1: a_{offset} > a_{demand}$$

Equation 4 was used to estimate the lower limit. A double-sided student t- distribution with a significance level, $\alpha = 0.05$ was used. H_0 and the laser point cloud was rejected if the $Rejection\ limit$ was larger than the deviation demand a_{demand} .

$$Rejection\ limit = |a_{offset}| - \frac{\sigma_{offset}}{\sqrt{n}} * t_{0.025,n-1} \tag{4}$$

3. Results

3.1. Establishment of known points

The known points were surveyed with three different methods, all with different characteristics. The RTK GNSS solution was fast to establish. The static GNSS had a high accuracy in a global coordinate frame, and the total station had a high accuracy in a local coordinate frame. To benefit from the different methods the measurements were imported into a network adjustment. It was found that the RTK GNSS measurements had large deviations compared to the rest of the measurements and were rejected. Figure 5 shows the deviations between the RTK GNSS and the final result from the network adjustments and shows that the position accuracies would not have been achieved with RTK GNSS alone. However, the achieved accuracy was within the expectation of the CPOS services (22). The rejection was accordingly to NS3580:2015 (13) saying that RTK GNSS methods are not recommended in these levels of accuracy demands.

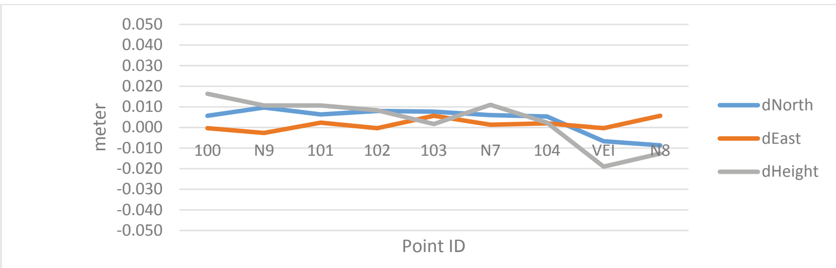

Figure 5. The deviation between the Real-Time Kinematic GNSS measurement and the final result.

The network adjustment was performed with GISLine Landmåling v 6.0 from Norkart (8, 30). The covariance for the GNSS point observations from *Terrapos* was scaled to balance the GNSS variance with the closed traverses variance. This was done accordingly to recommendations in NS3580:2015 (13). The observation test recommended rejecting GNSS observations from point 102, 103, N8 and VEI. In total 8 of 20 GNSS observations were rejected based on the observation test. All of these points had obstacles in the sky view stretching from 44° *above the horizon, which result in degraded GNSS conditions.* The external reliability expressed as point deformations were estimated in the reference network described by the known points. The adjustment ended up with point deformation of 0.003 m and a standard deviation of 0.001 m.

3.2. Statistical significance

The main question in the second aspect was to verify the laser point cloud and to decide if the building survey was significant inside or outside the specifications. This was performed using the framework presented in GeodataQuality. The framework consists of six main steps described in chapter 2.6, where the first step decide the number of objects. The current building had approximately 320 rooms which give the same amount of objects. The second step was to use the number of objects and GeodataQuality section 7.4 (table 4) to find the minimum amount of control points. We found that 20 control points were needed in every selected axis. The systematic deviation a_{offset} was found in the third step, by averaging the measured deviation. The standard deviation σ_{offset} in step four were calculated using the measured deviation. Step five calculated the standard deviation of the control points. Table 4 summarizes the different standard deviation for each measuring stage.

Table 4. The table summarizes standard deviation for each stage.

Error	St. deviation (m)
National grid, AASC	0.005
GNSS	0.003
Estimated for known points	0.001
Assumed for control points	0.004

We assumed that each element was independent and used the propagation of error to summarize the standard deviations $\sigma_{control}$ to be 0.007 m. The last step was to find the rejecting limit using statistic tests. The estimated standard deviations for the measurements offset were evaluated with a Fisher test. Table 5 summarizes the evaluation of the estimated standard deviation. The rejecting limits showed that the standard deviation was within the demand in the north direction and outside the demand in the east and height direction.

Table 5. Evaluation of standard deviation

Direction	Average offset, a_{offset} (m)	St.dev, σ_{offset} (m)	Number of observations	St.dev, σ_{control} (m)	$F_{0.05,n-1,\infty}$	Rejecting limit (m) (approved if ≤ 0.003m)
North	0.000	0.006	44	0.007	1.379	0.000
East	0.011	0.009	48	0.007	1.362	0.005
Height	0.067	0.027	41	0.007	1.394	0.022

The systematic deviations were evaluated with a student t- distribution. Table 6 summarizes the evaluation of the systematic deviation. The rejecting limits show that the systematic deviation was within the demand in the east and north direction and outside the demand in height direction.

Table 6. Evaluation of systematic deviation

Direction	Average offset, a_{offset} (m)	St.dev, σ_{offset} (m)	Number of observations	St.dev, σ_{control} (m)	$t_{0.975,n-1}$	Rejecting limit (m) (approved if ≤ 0.01m)
North	0.000	0.006	44	0.007	2.017	0.000
East	0.011	0.009	48	0.007	2.012	0.010
Height	0.067	0.027	41	0.007	2.021	0.058

3.3. Product specification update

Based on the experiences from this project the accuracy demands from Hjelseth et al. (2) were extended to include all accuracy indicators presented in the GeodataQuality. This is summarized in Table 7.

Table 7. Description of different accuracy levels.

Accuracy level	Level 1	Level 2	Level 3
Number of gross error	0	0	0
Max. Point cloud thickness	0.018 m	0.060 m	0.240 m
Standard deviation *	0.003 m	0.010 m	0.040 m
Maximum average deviation *	0.010 m	0.030 m	0.120 m

* Calculated on a 0.2 m x 0.2 m surfaces separately in three orthogonal directions.

Additional specifications are summarized in the following:

- The accuracy demand should be given in a local reference frame realized with a minimum of four known points surrounding the building.
- The local reference frame should have a tolerance at the same level as the maximum average deviation in the selected accuracy level. The achieved accuracy should be documented accordingly to NS3580:2015 (13).
- The local reference frame should be connected to a global reference frame with a 6.0 cm coordinate tolerance, which opens up for using RTK GNSS according to NS3580:2015 (13).
- A gross error is present where the maximum point cloud thickness is exceeded.
- It is reasonable to require a certain delivery format with maximum file size.
- The laser point density should be stated and realized as the maximum allowed laser point distance.

4. Discussion

The proposed control method required that flat hard surfaces were present perpendicular to all of the axes in the selected local coordinate system. Normally this requirement will be fulfilled since most buildings are build up by squares. If not it might be necessary to use targets. Another requirement is that the building needs to be stable in-between the terrestrial laser scanning and the survey of the control points. A tall building tends to deform accordingly to the weather conditions. Lower buildings are not affected at the same level and can in most cases be considered as a fixed construction if the ground is stable.

The deviations between the laser points and control points were measured manually. In situations where the laser point cloud had good accuracy, the visual approach was easy to achieve. Where the scan position and orientation had a low accuracy, and a false double wall situation occurred, it was difficult to find the center point visually. This is illustrated in Figure 6. In this example, the ceiling seemed to be three ceilings when it actually was the same single ceiling. The point cloud thickness was 0.036 m, and it was difficult to manually set the center point of the point cloud. In such a situation it would be beneficial to have a tool to calculate the center point automatically.

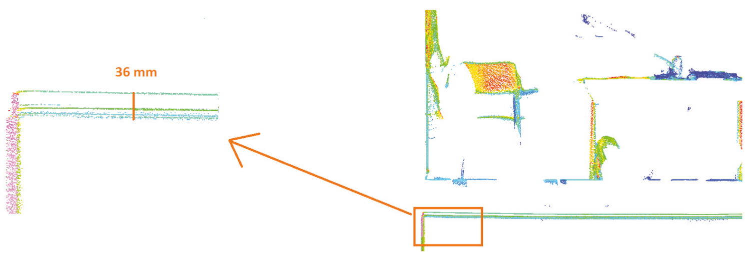

Figure 6. The different scan positions had a low position and orientation accuracy that gave a situation where the ceiling measured from different scan position ends up at different locations and gives a large point cloud thickness.

The standard NS 3580:2015 (13) provides a detailed recommendation for the establishment of a local reference frame for construction and building sites. Most of the demands have been followed in this study. The most important deviation is regarding the number of connections to the national grid. The demand is that the site grid should be connected to a minimum of three points in the national grid. In this study, the local reference frame was only connected to one point in the national grid of permanent GNSS stations. The permanent GNSS stations and national grid points had a different realization of the EUREF89 at the time of the data capture. This could have introduced a small amount of force into the local network frame. The control measurements and laser point cloud were connected to the same known points. Any potential offsets and rotation to the actual global coordinate frame would have been the same for control measurements and the laser point cloud and would not have an effect on the observed laser point cloud deviations.

The standard NS 3580:2015 (Table 1 and 2) (13) has strict demands regarding survey instrumentations and tolerances. The list can be used to select the approved survey method. The main problem with this approach is that technologies can be blocked. There is an opening to deviate from the list, but this requires a special agreement with the project owner. Based on the development of the survey technology NS 3580:2015 (13) should be updated to get the full potential of the latest developments.

The standard Grunnlagsnett (14), NS 3580:2015 (13) and "Kommunalt Fastmerkenett" (7) use scale deformation and angle deformation as criteria to document the network accuracy. The test is able to detect scale variation internally in the network, but are not able to detect a potential scale error in the entire network. A scale error in the entire network would have been a critical error in this study and would have affected the deviation result. This means that a scale deformation test would not have revealed all potential problem with scale in our network of known points. An angle deformation test is able to detect angle deformation internally in the network, but are not able to detect any rotation of the entire network. This is not a problem in a local frame, but it might be critical in a global frame. The angle and scale deformation analyses are therefore not able to provide a full analysis of the achieved accuracy in the site grid network. A point deformation analyses demand is missing in the current version of Grunnlagsnett (14) and should be clarified in the next version. External reliability realized as point deformation, scale deformation, and angle deformation are built into land survey software like GisLine (8) and Isy landmåling (10).

The product specification used in this study demands that the point cloud should be delivered in a global reference frame and that the accuracy demand should be related to the same frame. This required a time consuming high accuracy survey. GeodataQuality requires that the accuracy should be 1/3 of the standard deviation demand to be treated as a true value. To ensure such accuracy the standard deviation for the known points should be around 0.003 m. This accuracy level was not fulfilled in the global coordinate frame. To achieve this level in a global reference frame is challenging, time-consuming and is difficult to achieve with GNSS due to the degraded sky visibility close to buildings. In most cases, it is not necessary to achieve this accuracy level in a global frame. A tolerance of 0.060 m, in the global frame, might be sufficient in most cases and is easy to achieve with RTK GNSS measurements. Even this accuracy level might have a positive effect on the multiple purposes of the end product. High accuracy in a local coordinate frame is essential and practically achievable.

An easy method to control the homogeneity of the point cloud was to evaluate the point cloud thickness. This was performed using vertical profiles perpendicular to the walls, floors, and ceilings. In situations where the point cloud thickness was small, the point cloud had a good local homogeneity and indicated an accurate point cloud. If the point cloud thickness was large, the point clouds from different scan position did not fit well. The reason for such a situation can be laser calibration or measurement accuracy. The largest contributor will normally be the scanners position and orientation. In an indoor environment, the point cloud thickness can be a good indication of a position and orientation accuracy.

5. Conclusions

We propose a method to control a laser scanning project of an existing building. The method demands a network of known points and that the laser point cloud is fitted to these known points. To be able to control the result, the study proposes that the coordinate tolerance for the known is equal or better than the maximum average deviation described in the product specification. In this study, the accuracy demand was set in a global reference frame. To achieve sufficient accuracy in the global reference frame, it was necessary to perform a combination of static GNSS and closed traverse using a total station. This is a costly and time-consuming operation. In most cases, it would be sufficient to specify the tolerance in a local coordinate frame. This would have a big influence on the time consumption. The main reason is that you do not need the accuracy of the Static GNSS. Instead, the measurement can be performed with a combination of RTK GNSS and closed traverse with a total station.

It is important to document and control the accuracy of the building survey. This is important to increase the product trust and the possible purposes of the product. This is a fundamental step to achieve a multi-purpose BIM (2). A control method described in GeodataProduction, used in airborne laser data projects, was scaled up to three dimensions. This made it possible to control the laser point cloud anywhere in the building without performing any preparations before the laser scanning. The biggest advantage was that the control measurements could be executed in a different way than the laser points have been collected. Where the laser scan traverse might end up in a dead end, the control measurements can go directly through openings in the building like doors and windows. The statistical significance was evaluated using the framework described in Geodata Quality (16). This standard uses the following parameters: gross error, standard deviation, and systematic deviation. The proposed product specification matched these accuracy indicators. Additional demands were given such as point thickness and maximum point distance in the laser point cloud.

In general, it is more expensive to deliver a high accuracy product than a low accuracy product. The same issue is present regarding point density. It is important that the customer specifies demand that directly influences the data capture cost to ensure a fair and reliable competition situation. A product specification is an important tool to achieve a predictable product. This is achieved when each contractor has an unambiguous understanding of the project. With a common understanding of the product specification, the contractors have the possibility to provide a price estimate on equal products that fulfill the specification while using the most suitable technology. An effect with an unambiguous product specification is that the contractor can select the best-suited technology for the job. If the accuracy described by the customer is low, the contractor can select a technology that is faster than a traditional static terrestrial laser scanning.

The analyze of the tendering process in this study showed that most of the contractors did not respond to the requested product specification and the final product did not fulfill the requested accuracy. Further work should investigate if this is a common problem. The first step is to evaluate how the contractors respond to the product specification. The second step is to evaluate if they are able to deliver within the requested demand. The third step is to continue to develop the product specification to improve the communication between the contractor and the customer.

Acknowledgments: The laser scanning was paid by the property department at the University of Life Sciences. The studies have not received any external funding.

References

1. Azhar S. Building information modeling (BIM): Trends, benefits, risks, and challenges for the AEC industry. Leadership and management in engineering. 2011;11(3).
2. Hjelseth E, Oveland I, Maalen-Johansen I. Framework for enabling scan to BIM services for multiple purposes - Purpose BIM. 20th World Building Congress; 2016; Tampere (Finland). Tampere (Finland): Tampere University of Technology; 2016.
3. Tang P, Anil EB, Akinci B, Huber D. Efficient and effective quality assessment of as-is building information models and 3D laser-scanned data. Computing in Civil Engineering (2011)2011.
4. DIN18710-1:2010-09. Engineering survey. Part 1: General requirements,. Beuth Verlag GmbH, 10772 Berlin, Germany: Deutsches Institut für Normung; 2010.
5. DIN18710-2:2010-09. Engineering survey. Part 2: Site surveying, . Beuth Verlag GmbH, 10772 Berlin, Germany: Deutsches Institut für Normung; 2010.
6. USIBD. USIBD Level of Accuracy (LOA) Specification Guide. Document C120 - C320, Version 20: U.S. Institute of Building Documentation; 2016.
7. Espelund T, Solgaard EJ, Mathisen O. Kommunalt fastmerkenett : planlegging, måling og beregning i gamle og nye nett: Norges teknisk-naturvitenskapelige forskningsråd 1996.
8. Norkart. Geografiske informasjonssystemer, GISLINE [Product description]. Available from: https://www.norkart.no/produkter/gisline/.
9. Powel. Gemini Oppmåling [Available from: https://www.powel.com/no/produkter/.
10. Norconsult. ISY WINMAP Landmåling [Available from: https://www.nois.no/produkter/gis/isy-winmap/#Landm%C3%A5ling.
11. Teunissen P. Testing theory: VSSD; 2006.
12. Revhaug I. Feillære og utjevningsregning, Elementutjevning, feilsøking og pålitelighet. Landbruksbokhandelen; 1993.

13. Standard_Norge. NS 3580:2015 Site grids for constrution, Distribution of responsibility, quality acceptance requirements and methods. 2015.
14. Kartverket. Grunnlagsnett: The Norwegian Mapping Authority; 2009 [Available from: https://www.kartverket.no/geodataarbeid/Standarder/Standarder-for-geografisk-informasjon/.
15. Anil EB, Tang P, Akinci B, Huber D. Deviation analysis method for the assessment of the quality of the as-is Building Information Models generated from point cloud data. Automation in Construction. 2013;35.
16. Kartverket. Geodatakvalitet, version 1.0: The Norwegian Mapping Authority 2015 [updated 01.01.2015. Available from: https://kartverket.no/geodataarbeid/Standarder/Standarder-for-geografisk-informasjon/.
17. EN-ISO19157. geographic information-Data quality. International Standards Organisation; 2013.
18. Anil EB, Tang P, Akinci B, Huber D, editors. Assessment of the quality of as-is building information models generated from point clouds using deviation analysis. Three-Dimensional Imaging, Interaction, and Measurement; 2011.
19. Klang D, Burman H, editors. Airborne Laser Scanning, an Efficient Revision Procedure for the Swedish Digital Elevation Model. Proceedings of the 7th Conference on Optical, 10; 2005.
20. Kartverket. Produksjon av basis geodata, version 1.0: The Norwegian Mapping Authority 2015 [updated 01.03.2015. Available from: https://kartverket.no/geodataarbeid/Standarder/Standarder-for-geografisk-informasjon/.
21. Kartverket. CPOS Positioning: The Norwegian Mapping Authority; 2017 [Available from: https://www.kartverket.no/en/Positioning/.
22. kartverket. CPOS - Kvalitet: The Norwegian Mapping Authority; 2018 [Available from: https://www.kartverket.no/posisjonstjenester/cpos/.
23. kartverket. Satellittbasert posisjonsbestemmelse, Versjon 2.1, December 2009 [Available from: https://www.kartverket.no/globalassets/standard/bransjestandarder-utover-sosi/satbaspossystemer.pdf.
24. Terratec. GNSS/INS post processing software [cited 2018 10. January]. Available from: https://www.terratec.no/terrapos.
25. Zoller+Fröhlich. Z+F IMAGER® 5010, 3D Laser scanner [Available from: https://www.zf-laser.com/Z-F-IMAGER-R-5010.3d_laserscanner0.0.html?&L=1.
26. Leica. Leica Cyclone REGISTER [Available from: https://leica-geosystems.com/products/laser-scanners/software/leica-cyclone/leica-cyclone-register.
27. Vosselman G, Maas H-G. Airborne and terrestrial laser scanning: CRC; 2010.
28. Soininen A. TerraScan User's Guide. For the 32-bit version of TerraScan: Terrasolid Ltd.; 2016.
29. Løvås GG. Statistikk for universiteter og høgskoler: Universitetsforlaget; 2013.
30. Norkart. NO 934 161 181 [Available from: https://www.norkart.no/.

PAPER V

Article

Evaluation of product specification for terrestrial laser scanning to extract a building information model

Ivar Oveland [1]

[1] Faculty of Science and Technology, Norwegian University of Life Sciences, 1432 Ås, Norway

* Correspondence: ivar.oveland@nmbu.no; Tel.: +47-40220711

Academic Editor: name
Received: date; Accepted: date; Published: date

Abstract:

In 2017 Ullensaker municipality in Norway arranged a framework agreement competition. The goal was to find competent producers to provide terrestrial laser scanning, surveying, and extraction of building information model of existing buildings. Ten different companies participated. Each company performed a terrestrial laser scanning and building information model extraction of the same selected area at the town hall of Ullensaker municipality. This study used the competition to test the usability of a product specification and a framework for quality evaluation based on open access standards. The result showed that the product specification and quality framework was able to identify the data quality and projects characteristics. Each of the companies was given a binary score based on 12 criteria described in the product specification. The results were used to update the product specification to improve the communication between the involved parties.

Keywords: product specification, building information model, terrestrial laser scanning

---

1. Introduction

Ullensaker municipality in Norway arranged a framework agreement competition in 2017. The goal was to get an agreement for terrestrial laser scanning, surveying, and extraction of Building information model (BIM) of existing buildings. Due to a purchase agreement between the municipalities in the area, the framework agreement became valid for five additional municipalities. The laser points clouds and BIM will be used for operation, facility management, and potential renovation. The winner of the agreement was paid accordingly to the client's offer. The second and third place were paid a compensation of 5000 NOK. In total ten different companies participate in the competition. The offered price was weighted at 30% while quality was weighted 70%. The quality criteria were based on the result of the test case, understanding of task, skills, knowledge, and capacity.

A group divided into three teams performed the evaluations and were given different responsibility areas:

1. Legal demand and price, Ullensaker municipality, Norway
2. Data accusation and accuracy, Norwegian university of life sciences, Norway
3. Building information model. Areo, Norway

The product specification was constructed to follow a simple form of transaction pattern between two parties. This transaction pattern is described by Dietz [1], and shown in Figure 1. The pattern is divided into four main steps. The first step is the customer's "request" for the product. The producer responds to this request in the second step with a "promise". In the third step the producer "state" that the promised result is realized. The final step is the "accept" of the result performed by the customer.

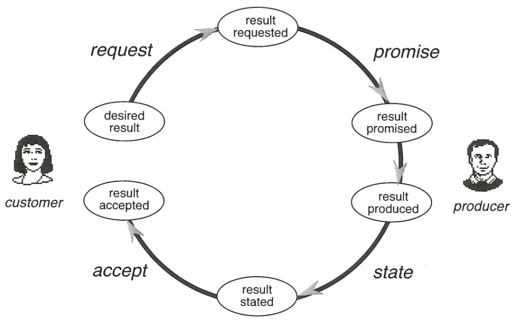

Figure 1. Transaction pattern from Dietz [1]

The main focus of this study is the customer's action steps called "request" and "accept". The first goal was to use the product specification to define the customer "request", to improve the communications between the customer and producer. The second goal was to evaluate the achieved result accordingly to the product specification. This is the final step in the transaction pattern. The transaction is successful where the request corresponds to the accepted result. The product specification was designed to ensure that all of the desired requested could be verified in the acceptation step. In total 12 different criteria were defined in the product specification. These criteria were given a binary score that forms the proposed evaluation matrix.

There are two main standards that cover different aspects of the customer's "request", regarding the establishment of a BIM for an existing building. The first is a standard made by the "Deutsches Institut für Normung" and is called "DIN18710 Engineering survey" [2, 3]. In the following referred to as DIN18710. The topics are requirements for surveying activities at constructions sites and look at the quality verification of the result. The standard divide accuracy requirements into five different levels of accuracies (LoA). The lower accuracy is called L1, and the high accuracy demand is called L5. The second standard is made by the U.S. Institute of building documentation and is called "USIBD Level of accuracy specification guide" [4]. The standard will in the following be referred to as USIBD. When they developed the standard, they used DIN18710 as an inspiration and inherited the accuracy levels from DIN18710. They used the same numbers, but DIN18710 is referring to a standard deviation while USIBD is referring to a 95% confidence level. Another difference is that USIBD allows the user to set different LoA for different building objects. Additional different Level of Development (LoD) could be set to the different building objects. This makes the standard very flexible and makes it possible to have different demand for building objects like doors, windows, walls, etc.

The result from the producer, shown in Figure 1 is approved in an acceptation process. The goal is to verify if the request corresponds to the delivered product. An important part of such an evaluation is to analyze the accuracy. This can be done by evaluating the internal relative accuracy. For a laser point cloud, this can be done by evaluating potential deviations between data captured from different locations, that covers the same area [5]. The deviation in the overlapping area is an expression of the relative accuracy in the data set. A deviation is normally caused by an error in the instruments position and orientation [6], mixed pixels due to spatial discontinuity edges, laser shots with multiple reflections (multipath) and instrument calibration [7]. The relative accuracy can also be evaluated by measure relative distances between the building objects or relative distances within a building object. Another approach analyzes absolute accuracy. This involves a certain level of surveying and use of targets like reflective tape, april tags or checkerboards. Common for all is that targets need to be placed in the field before the data capture. To be more flexible it is possible to use natural targets. This is a normal procedure in the airborne laser industry and is described in the Norwegian standard "Produksjon av basis geodata"[8]. The standard will in the following be referred to as GeodataProduction and provide a framework to perform deviation analyses in one dimension. Oveland et al.[9] proposed a method to scale this up to work in a tree-dimensional environment. The same study found that the Norwegian standard "Geodatakvalitet" [10] was suitable to test the statistical significance of the achieved accuracy. The standard will in the following be referred to as GeodataQuality and describes a method to estimate and evaluate the standard deviation, systematic deviation, and gross errors.

This study analyzes the data accusation and accuracy of terrestrial laser scanning. This is done by analyzing the test cases, based on the criteria in the product specification. In 2016 Hjelseth et al. [11] proposed a framework for product specification for data capture and BIM extraction of existing buildings. The proposal was tested in a real project and was presented by Oveland et al. [9]. The study was based on five different tenders and one delivered laser scan. The criteria in this study were inspired by the result of Oveland et al. [9] and Hjelseth et al. [11]. The main resource question in this study was the evaluation of the product specification with the corresponding quality evaluation framework. Based on the findings an updated product specification was proposed. Oveland et al. [9] showed that only two out of five tenders specified which accuracy demand they would fulfill and did not responded fully to the customer request. This showed that the communication between the involved parties could be a challenge. In the end, the delivered result did not respond to the customer request. The second research question in this study was to investigate if this is a common situation.

2. Materials and Methods

2.1. Customer request

The customer request in this framework agreement competition was a terrestrial laser scanning and extraction of a BIM. The work should be executed on a section of the town hall in Ullensaker municipality shown in Figure 2.

Figure 2. The blue shaded area shows the location of the test area.

All ten participant should perform the data accusation accordingly to the required product specification. The product specification consisted of the following parameters and defined the customer request:

- Accuracy in the delivered point cloud should be stated accordingly to Table 1.
- The survey should be realized in EUREF89 NTM10 and height system NN2000. All used coordinate and height system should be described.
- A network of known points should be established in the surroundings of the building. The coordinate accuracy should have a standard deviation of 0.003 m both in the local and global coordinate frame.
- Laser point cloud density realized as maximum point distance should not exceed 0.004 m.

Table 1. Accuracy Levels

Accuracy level	Level 1	Level 2	Level 3
Number of gross error	0	0	0
Max. Point cloud thickness	0.02 m	0.06 m	0.24 m
Standard deviation *	0.003 m	0.01 m	0.04 m
Maximum average deviation *	0.01 m	0.03 m	0.12 m

* Calculated on a 0.2 m x 0.2 m surface.

2.1. Customer "accept"

The requested scan area was located on the top floor, and nine limited areas, called rooms were selected to be a part of the project. It was important to stretch the test area over a long distance to better test the quality of the position and orientation calculation for the scan locations. Figure 3 shows the selected areas.

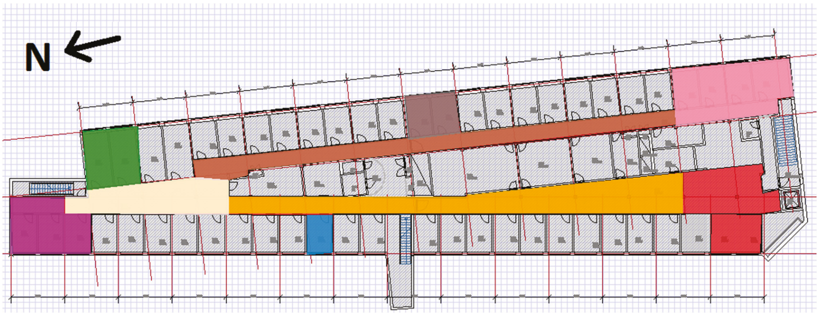

Figure 3. The colored areas show the area to be measured and modeled.

The control method from GeodataProduction was scaled up to three dimensions. Due to the high point density, it was assumed that one measurement was sufficient to represent a control surface [9]. In the further description, the surveyed points representing a control surface is called a control point. A set of control points were established in three perpendicular directions that corresponded with the axis in the local network described by the known points. The standard GeodataQuality was used to decide the number of control points needed to verify the findings. It was assumed that one room represented one object, which gave a total of nine objects. From a lockup table in GeodataQuality, it was found that five objects in each perpendicular direction needed to be controlled.

The first step in the customer "accept" actions was to survey the coordinates for the known points. In total five known points where established by one of the participants. Figure 4 shows the locations of the known points.

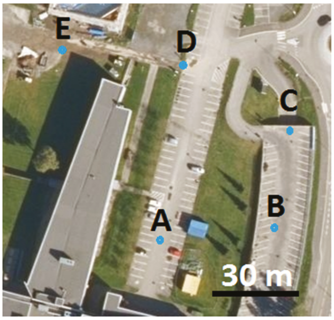

Figure 4. The location of the known points.

The locations of the known points were not optimal for its purpose due to blocking vegetation and light poles. A better position would have ensured a clear view of the targets of interest. For example, if point E had been moved 0.5 m, it would have not been in conflict with a light pole that blocked the clear view to point C. Additionally, it would have ensured no conflict with vegetation towards the building. Point B was placed behind trees so that all areas of interests were blocked. Despite this, it was possible to ensure sufficient measurement of the known points network and control points inside the building.

The known points B, C, D, and E were measured with static differential GNSS. The GNSS reference station was operated by the Norwegian Mapping Authority, which claims the coordinate standard deviation to be 0.005 m. The station was located 17 km apart and is called ARNC. The observation time was 1 hour, and the GNSS post-processing was done in Terrapos v 2.5.90 [12]. "Satelittbasert posisjonstjeneste" [13] claim that a differential GNSS measurement between two stations has the potential to achieve 5mm + 1ppm at a 2σ level or a standard deviation of 0.011 in our case. Additional to the GNSS measurements, a traverse network was measured with the total station Topcon ES 103 and Sokkia AP11 prism with a target plate. The GNSS results were imported as point observation together with the observation from the total station into “GISLine Landmåling” v 6.0 from Norkart [14]. The final coordinates were estimated in a bundle adjustment. The maximum estimated standard deviation was 0.002 m for all known points and the external reliability realized as point deformation was estimated to maximum 0.007 m.

The control points were measured with a reflectorless total station, the same used for the traverse network. The total station was mounted on a tripod at each of the known points, and possible walls, floors, and ceilings inside the areas of interests were surveyed. Oveland et al. [9] assumed that the control point measurements had a standard deviation of 0.004 m. The control points were located on hard flat surfaces with a minimum size of 0.2 m x 0.2 m. The measurements were performed through open windows. The measurements were done during the winter period that gave a temperature difference of 30 degrees between the indoor and outdoor environment. An error budget was made to give an estimate of the standard deviation for the control points realized in the global coordinate frame and is shown in Table 2. The assumed standard deviation for the control points measurements was adapted from Oveland et al. [9].

Table 2. The table summarizes the standard deviations.

	St. deviation (m)
National grid, ARNC	0.005
Differential GNSS	0.011
Estimated for known points	0.002
Control points measurements	0.004

Each element in the error budget was assumed to be independent, and the propagation of error was used to summarize the standard deviations $\sigma_{control}$ to be 0.013 m. For each of the control points, the perpendicular distance to a surface described by the laser points within a control area of 0.2 m x 0.2 m was measured. The distance is called deviation and is shown in Figure 5.

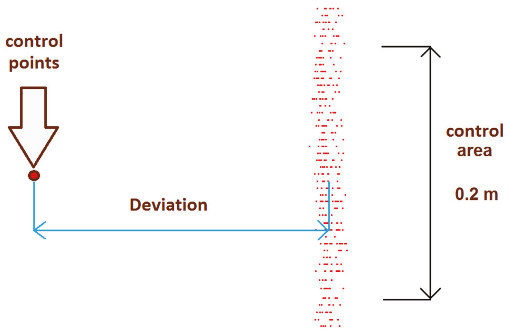

Figure 5. The deviation measurements.

The measured deviations, x_i were used to calculate the average deviation $\bar{x}$, and were done separately for each axis. The standard deviation $\sigma_{deviation}$ were calculated based on Equation 1, where n was the number of observations.

$$\sigma_{deviation} = \sqrt{\frac{\sum_{i=1}^{n}(x_i - \bar{x})}{n-1}} \quad (1)$$

GeodataQuality was used to evaluate the estimated average deviation and standard deviation. The standard deviation was tested with an F-test. The first step was to evaluate the control points measurements. The correspond F-value for was found based on the number of observations, and a 95% confidence level. If the threshold in Equation 2 was below the standard deviation demand described in the product specification, the estimated standard deviation was accepted.

$$Threshold\ st.dev = \sqrt{\frac{\sigma_{deviation}^2 - \sigma_{control}^2}{F_{0.05,n-1}}} \quad (2)$$

The average deviation $\bar{x}$ was tested using a T-test (two-tails) at a 95% confidence level with n observations. The threshold for rejection was defined by Equation 3. If the threshold deviation was larger than the selected maximum average deviation, the average deviation was rejected.

$$Threshold\ deviation = |\bar{x}| - \frac{\sigma_{deviation}^2\, t_{0.975,n-1}}{\sqrt{n}} \quad (3)$$

The laser point cloud density was evaluated by measuring the maximum distance between two neighbor points inside the project area. Occluded areas and surfaces with difficult reflectance were not counted. The point thickness measurements were performed on laser points within a 0.2 m x 0.2 m area and were measured manually. The measurements were carried out at the location of the control points but could have been performed at random locations. In locations where the point cloud thickness was small the relative position and orientation of the different scanner locations were good. Figure 6 shows a situation where the laser scans had degraded position and orientation that gave a 0.006 m point cloud thickness.

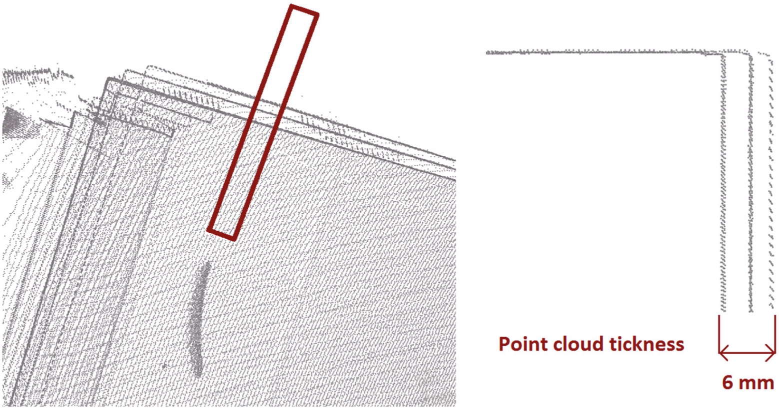

(**a**) (**b**)

Figure 6. Point cloud thickness, (a) shows a top view of the laser point cloud, and the red rectangle shows the location of the vertical profile shown in (b).

3. Result

3.1. customer accept

The maximum laser point distance demand was 0.004 m, and the result from the point distance analyses is shown in Figure 7.

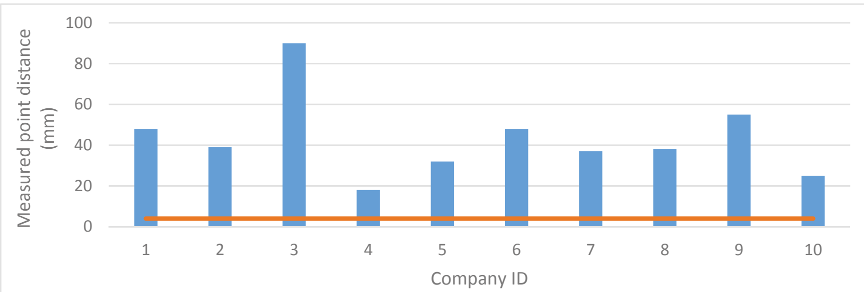

Figure 7. The measured maximum laser point distance. The orange line shows the maximum point distance demand.

The maximum point cloud thickness was measured manually at each of the control points locations, and shown in Figure 8. The maximum point cloud thickness for accuracy level 1 was 20 mm.

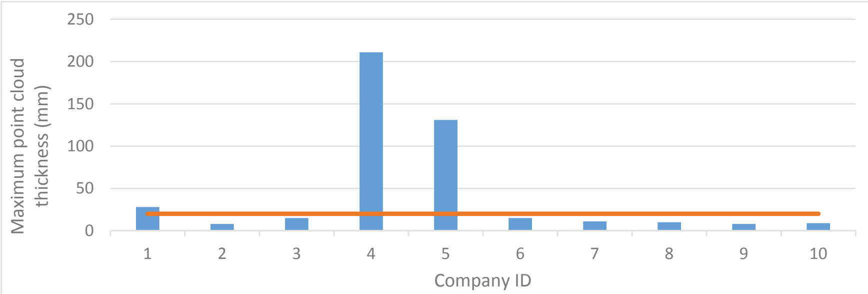

Figure 8. The measured point cloud thickness. The orange line shows the maximum allowed point cloud thickness.

The average deviation is shown in Figure 9, and the estimated standard deviation for the measured deviation between the control points and point cloud is shown in Figure 10.

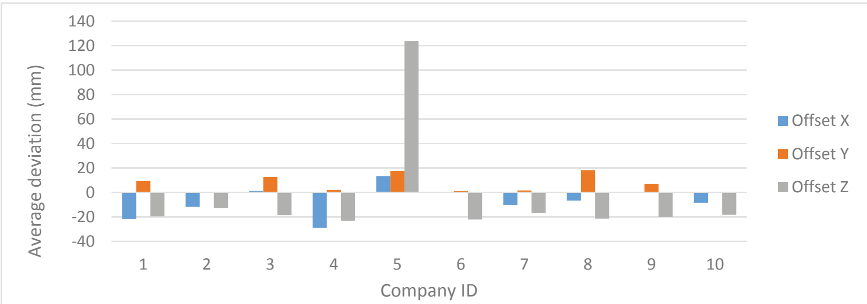

Figure 9. The average deviations

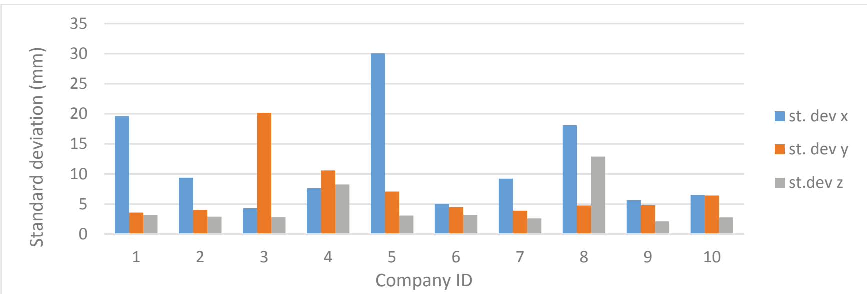

Figure 10. The standard deviation for the measured deviation.

All requirements from the product specification were given a binary score. If the result was within each respective threshold the category was given the score of 1 and if the result where outside the demand the score 0 was given. The product specification was divided into 12 different categories. The result from the evaluation during the customer accept process is summarized in the proposed evaluation matrix shown in Table 3.

Table 3. Proposed evaluation matrix, summarize the score from each category in the product specification

Company ID	Stated accuracy level	Description of used coordinate and height system	Quality control, known point	Density	Point cloud thickness	Gross error	St. dev			Offset			Total score (max 12)
							x	y	z	x	y	z	
1	0	0	0	0	0	1	0	1	1	0	1	0	**4**
2	0	0	1	0	1	1	1	1	1	1	1	0	**8**
3	1	1	0	0	1	1	1	0	1	1	1	0	**8**
4	0	1	0	0	0	0	1	1	1	0	1	0	**5**
5	0	0	0	0	0	1	0	1	1	1	0	0	**4**
6	0	1	1	0	1	1	1	1	1	1	1	0	**9**
7	0	0	0	0	1	1	1	1	1	1	1	0	**7**
8	0	0	0	0	1	1	0	1	1	1	0	0	**5**
9	0	1	1	0	1	1	1	1	1	1	1	0	**9**
10	0	0	0	0	1	1	1	1	1	1	1	0	**7**

3.2. The updated customer request

The result of the study was used to update the product specification. The update had two main goals. The first was to improve the communication between the involved parties and the second was to synchronize the demands with international standards.

Demand inherited from Oveland et al.[9] :

- The accuracy demands should be given in a local reference frame realized with a minimum of four known points surrounding the building.
- The local reference frame should have a tolerance at the same level as the maximum average deviation in the selected accuracy level. The achieved accuracy should be documented accordingly to NS3580:2015 [15].
- The local reference frame should be connected to a global reference frame with a 6.0 cm coordinate tolerance, which opens up for using Real-Time Kinematic (RTK) GNSS according to NS3580:2015 [15].
- It is reasonable to require a certain delivery format with maximum file size.

Additional demands from the evaluation process in this study:

- A project report should be delivered following the demands for geodetic mapping described in GeodataProduction. All demands should be documented in a project report, and all used coordinate and height system should be described.
- Accuracy should be stated accordingly to Table 4.
- Density demand, the maximum distance between two neighbor laser points should be stated as a fixed distance. Typical distance is between 0.002-0.010 m.
- A gross error is present when a group of laser points exceeds the accuracy demands. Errors due to multi-reflection and noise points from surfaces with difficult reflectance are not considered as gross errors.

New accuracy levels where the standard deviation is inherited from DIN18710 is shown in Table 4.

Table 4. Accuracy Levels

Accuracy level	Level 1	Level 2	Level 3	Level 4	Level 5
Number of gross errors	0	0	0	0	0
Max. Point cloud thickness *	6x** m	0.300 m	0.090 m	0.030 m	0.006 m
Standard deviation *	x** m	0.050 m	0.015 m	0.005 m	0.001 m
Maximum average deviation *	3x** m	0.150 m	0.045 m	0.015 m	0.003 m

* Calculated based on a 0.2 m x 0.2 m surface. ** x: custom standard deviation

An updated binary evaluation matrix is proposed in Table 5 with a maximum score of 13 points.

Table 5. The updated binary evaluation matrix

Report	Stated accuracy level	Description of used coordinate and height system	Quality control, known point	Density	Point cloud thickness	Gross error	St. dev			Offset			Total score (max 13)
							x	y	z	x	y	z	
x	x	x	x	x	x	x	x	x	x	x	x	x	0-13

4. Discussion

The result from Oveland et al. [9] showed that the known points did not need to be realized in a global coordinate frame with high accuracy. In most cases, it is sufficient to have high accuracy in a local coordinate frame. This was originally intended in this study but was omitted in the final version of the tender request. In the end, this seemed to simplify the evaluation due to the lack of metadata. The study showed that 60% of the participants did not describe which coordinate frame they have used. It was therefore assumed that the producers delivered the result in the requested global coordinate frame. The evaluation was performed in the global frame.

There were some misunderstandings during data accusation regarding the known points. It was stated in the product specification that the supplier was responsible for establishing and to measure the known points. The physical marking of the known points was done by one of the participants. The same participant measured the coordinates with an RTK GNSS system using the real-time correction system called CPOS [16] provided by the Norwegian mapping authority [17]. This coordinate list was delivered to the participants so that they did not need to establish new physical points in the field. The coordinate list was important to find the physical marks in the field. If every participant should physical marked their own points, it would have been over 30 points in the surroundings of the building. This would have made the evaluation quite confusing and create an unnecessary impact on the infrastructure surrounding the building. 70% of the participants used the coordinates on the list without further consideration. All participants should have measured the know points to ensure that the standard deviation demand was fulfilled. When we look back, the coordinates list should have been manipulated in such way that the participants were able to find the physical marks, but not able to use them in the processing without discovering large deviations.

The accuracy levels in the product specification were divided into three levels inherited from Hjelseth et al. [11]. To reduce the possibilities for mixing different demand, it was decided to change the standard deviation demand to a command standard. It was decided to use the DIN18710. This standard use a set of standard deviation interval ranging from high accuracy level to low accuracy level. Each interval is given in a lower and upper limit. It was decided to inherit the upper-level limits from DIN18710 and use this in a set of new accuracy levels. To avoid misunderstandings, it was decided to also inherit the accuracy level numbering. The different accuracy level is shown in Table 4. Each of the levels demands different equipment and data capture procedure to be fulfilled. The highest accuracy level 5 can be fulfilled with equipment from typically manufacture industry. Level 2 and 3 is typically achievable with a tripod mounted terrestrial scanners. Level 1 should be achievable with a human carried laser scanner system.

The result showed that few of the participants delivered sufficient metadata. A description of the different coordinate and height systems, and expected accuracy level accordingly to Table 1 were often missing. Relevant information regarding the point cloud could play a key role when the owner evaluate which purposes the result can fulfill. Based on the lack of metadata it is natural to address further demand in the product specification regarding metadata documentation. In the updated version it is therefore added a demand saying that all projects should include a project report with all necessary metadata. The report should be based on the demand for geodetic mapping described in GeodataProduction.

In the evaluation process, the archived results were analyzed and tested towards the requirements in the product specification. The total score varied from 3 to 9 points out of 12 points. There are two categories where all companies have failed. This was point density and offsets in height. The offset in height is caused by the different GNSS methods used in the projects to connect the local and global coordinate frames.

The ceiling in the selected area had a standard office height, and all companies seemed to have placed the terrestrial scanner closer to the ceiling than the floor. This is normal since the instrument normally is mounted in a comfortable operation height. The laser point density evaluation found that the longest distance between neighbor points was in the ceiling. Important factors for laser point density were the scanner setting, the observed range distance, and the instrument height. The optimal instrument height would have been half of the ceiling height. This would have optimized the point distribution between the floor and ceiling and could have reduced the number of scan position necessary to fulfill the point distance demand. All companies failed to fulfill the laser point density demand. The largest point distance was found in the data from company number 3 with a maximum distance of 90 mm. A slightly larger point distance than the demand will in most cases not make a significant difference to the end product but can be an important factor in the competition situation. A high-density point cloud needs more scan position and is, therefore, more expensive to capture. This will create an unfair competition situation for those companies who fulfill the demand.

In airborne laser projects, the point density demand is evaluated by estimate the average laser point density within each square meter of the project. It is common to claim that 95% of all the subareas fulfill the density demand [18]. A similar demand is difficult to practically implement in terrestrial laser scanning projects. One of the challenges is that the amount of occluded areas, difficult reflectance surfaces, and multipath problems is more significant compared to airborne laser projects. These areas are often excluded from the density analyses. In airborne laser projects, the density analyses are performed in a 2D environment, similar analyses in a terrestrial laser scanning projects must be performed in a 3D environment. This makes the analyses more complicated in an automated process.

The DIN18710 standard separate accuracy in elevation and horizontal level. In this study, we mainly look into terrestrial laser data. A tradition terrestrial laser scanning from a tripod should have the same accuracy in height and horizontal level. The accuracy in the horizontal and vertical direction was therefore not separated. A study performed by Forsman et al. [19] showed that a laser measurement of a column might end up with a positive bias on the diameter estimation of the column. The effect is present where the laser footprint reaches a certain level. The effect can be avoided by selecting a laser scanner with an appropriate beam divergence compared to the requested range. The effect is not present on flat surfaces. Corners might be affected, but this needs further studies to be verified. The USBID standard has built-in functionality to set different accuracy levels on different building objects. In a situation where the column has a lower accuracy than the rest of the point cloud, the USBID standard could be used to handle this effect.

5. Conclusions

This study has analyzed the laser scanning of a building performed by ten different survey companies. They used identical product specification but used their own interpretation of the specification, different scanning procedure, different equipment, and different post process routines. The delivered point clouds were analyzed with an evaluation framework presented by Oveland et al.[9]. The evaluation procedure was constructed to evaluate all the criteria in the product specification. Each criterion was given a binary score and summarized in the proposed evaluation matrix. All companies failed to deliver the requested point density, height accuracy, and important metadata documentation. The companies score varied from 3 to 9 points where 12 was the maximum. The result showed that the acceptance framework was able to discover weaknesses in the delivery and distinguish between the different companies. Based on the findings an updated product specification was made. The main changes were synchronization with international standards and new demands to improve the communication between the involved parties. The study made by Oveland et al.[9] showed that it is difficult to communicate the expectation towards the producer. This was confirmed in this study. The difference between the customer request and the producers stated result shows that the communication between the customer and producer has great potential for improvements.

The main goal of the study is to communicate a clear understanding of the customer's expectation to ensure that the customer request corresponds with the result accepted. This study takes a step towards this goal, and the studies industry impact has the potential to ensure predictable quality on terrestrial laser scanning of existing buildings.

Acknowledgments: A special thanks go to Jürgen Spindler and Ullensaker municipality. I would also like to thank the participants in the framework agreement competition; Geomatikk Survey, Anko AS, Skanska Survey, Exact, Astacus, GeoNord AS, Maskinstyring AS, Pöyry AS, Terratec AS, and Geoplan 3D AS.

References

1. Dietz, J.L., *What is Enterprise Ontology?* 2006: Springer.
2. DIN18710-1:2010-09, *Engineering survey*, in *Part 1: General requirements,*. 2010, Deutsches Institut für Normung: Beuth Verlag GmbH, 10772 Berlin, Germany.
3. DIN18710-2:2010-09, *Engineering survey*, in *Part 2: Site surveying,* . 2010, Deutsches Institut für Normung: Beuth Verlag GmbH, 10772 Berlin, Germany.
4. USIBD, *USIBD Level of Accuracy (LOA) Specification Guide*, in *Document C120 - C320, Version 2.0*. 2016, U.S. Institute of Building Documentation.

5. Anil, E.B., et al., *Deviation analysis method for the assessment of the quality of the as-is Building Information Models generated from point cloud data.* Automation in Construction, 2013. **35**.
6. Tang, P., et al., *Efficient and effective quality assessment of as-is building information models and 3D laser-scanned data*, in *Computing in Civil Engineering (2011)*. 2011.
7. Anil, E.B., et al. *Assessment of the quality of as-is building information models generated from point clouds using deviation analysis*. in *Three-Dimensional Imaging, Interaction, and Measurement*. 2011.
8. Kartverket. *Produksjon av basis geodata, version 1.0*. Standarder Geografisk Informasjon 2015 01.03.2015; Available from: https://kartverket.no/geodataarbeid/Standarder/Standarder-for-geografisk-informasjon/.
9. Oveland, I., I. Revhaug, and I. Maalen- Johansen, *Laser scanning, product specification and Level of Accuracy evaluation.* Kart og Plan, in revision, 2018.
10. Kartverket. *Geodatakvalitet, version 1.0*. Standarder Geografisk Informasjon, 2015 01.01.2015; Available from: https://kartverket.no/geodataarbeid/Standarder/Standarder-for-geografisk-informasjon/.
11. Hjelseth, E., I. Oveland, and I. Maalen-Johansen, *Framework for enabling scan to BIM services for multiple purposes - Purpose BIM*, in *20th World Building Congress*. 2016, Tampere University of Technology: Tampere (Finland).
12. Terratec. *GNSS/INS post processing software*. Terrapos; Available from: https://www.terratec.no/terrapos.
13. kartverket. *Satellittbasert posisjonsbestemmelse, Versjon 2.1, December 2009*. [cited 2019 17. January]; Available from: https://www.kartverket.no/globalassets/standard/bransjestandarder-utover-sosi/satbaspossystemer.pdf.
14. Norkart. *Geografiske informasjonssystemer, GISLINE*. [cited 2018 6th August]; Product description]. Available from: https://www.norkart.no/produkter/gisline/.
15. Standard_Norge, *NS 3580:2015 Site grids for constrution, Distribution of responsibility, quality acceptance requirements and methods*. 2015.
16. kartverket. *CPOS - Kvalitet*. 2018 [cited 2018 23. August]; Available from: https://www.kartverket.no/posisjonstjenester/cpos/.
17. Kartverket. *CPOS Positioning*. 2017 [cited 2017 22. April]; Available from: https://www.kartverket.no/en/Positioning/.
18. Kartverket. *Produktspesifikasjon Nasjonal modell for høydedata fra laserskanning (FKB-Laser)*. FKB-Laser v3.0 2019; Available from: https://register.geonorge.no/data/documents/Produktspesifikasjoner_FKB-Laser_v8_produktspesifikasjon-fkb-laser-3_0_.pdf.
19. Forsman, M., et al., *Bias of cylinder diameter estimation from ground-based laser scanners with different beam widths: A simulation study.* ISPRS Journal of Photogrammetry and Remote Sensing, 2018. **135**.

ISBN: 978-82-575-1589-8
ISSN: 1894-6402

Norwegian University
of Life Sciences

Postboks 5003
NO-1432 Ås, Norway
+47 67 23 00 00
www.nmbu.no

102532 / ANDVORDGRAFISK.NO